Metal – HisTag Coordination for Remote Loading of Biomacromolecules into PLGA Microspheres

by

Jason Albert

A dissertation submitted in the partial fulfillment
of the requirements for the degree of
Doctor of Philosophy
(Pharmaceutical Sciences)
in the University of Michigan
2022

Doctoral Committee:

Professor Steven P. Schwendeman, Chair
Professor David Antonetti
Professor Anna Schwendeman
Professor Peter Tessier

Jason M. Albert

jasonalb@umich.edu

ORCID iD: 0000-0001-6583-5779

Dedication

To my family, my greatest source of strength.

Acknowledgements

From Pre-K onward, I have been lucky to be taught by extraordinary educators. I could list nearly every teacher I've had, but I want to highlight 4th grade Writing with Mrs. Chester, 6th grade Math with Mr. Boyle, middle school Civics and History with Ms. Billig and Mr. Hickey, and high school English, Chemistry, Biology, and Math with Mr. Brown, Mr. Rodriguez, Ms. Russell, and Mrs. Perez, respectively. I was a loud and not often still student, and these teachers nourished and encouraged my academic curiosity and energy. I want to thank undergraduate professors including Drs. Steve Wallace, Gabriel Rosenberg, and David Katz for challenging me and inspiring me to pursue a graduate degree.

In my graduate career, Dr. Steven Schwendeman has helped me become an independent investigator. I appreciate how he has struck the balance between pointing me in the right direction and letting me find that direction for myself. Dr. Schwendeman consistently put me in positions to be successful and try new things. I consider myself fortunate to have been in his lab. I also want to thank the rest of my dissertation committee: Dr. David Antonetti, Dr. Anna Schwendeman, and Dr. Peter Tessier. Their support and scrutiny from a variety of perspectives has greatly improved these projects. I have taken great value in meeting with them formally and speaking with them informally about my research, career, and life.

I am not sure anyone understands just how privileged the Schwendeman Labs are to have Rose Ackerman and Karl Olsen as lab managers. Together and separately, they work to support the lab, allowing students and postdocs to focus on their research. Beyond all the behind-the-scenes work, they have advised me on innumerable protocols and projects. I don't know how the

labs would function without them. Thank you. Similarly, at COP, Patrina Hardy and Antoinette Hopper keep the department and graduate programs running smoothly. Thank you.

In normal times, the Schwendeman lab space and office space were wonderful places to come to work. I am a better scientist and person for the conversations I was able to have with labmates at the bench and cubicle. I sincerely hope that culture can return as we come out of the pandemic. I want to express my gratitude especially to three scientists who mentored me throughout my years in the lab. Besides allowing me to inherit her desk and bench when she graduated, Dr. Morgan Giles also left me invaluable knowledge about how to be the best researcher and scientist I can be. Thank you for your generosity and for your tolerance of my random musings. Dr. Rae Sung Chang led me to this dissertation work and made me a much more complete scientist. Finally, Dr. Jenna Walker was the Platonic ideal of a labmate. Thank you for being selfless to a fault and for always being willing to lend a hand, an ear, or a perspective.

Outside the lab, I enjoyed all kinds of activities with the AAPS student chapter. To Nick Job, Nick Waltz, Emily Morin, Lindsay Scheetz, Ryan Clausen, Brian Thompson, Justin Hong, Minzhi Yu, Phil Rzeczycki, Katie Cavanagh, Jill Coghlan, Jen Diaz-Espinosa, Kristen Hong, Richard Schutzman, Corrine Din, and many more, thank you for being great friends and providing entertaining distractions. Special shoutouts to the IM softball and co-rec flag football teams.

Thank you to Josh Foster and Brett Hanson, two friends of mine who have only recently met but who together have helped fill my days with witticisms, thoughtful perspectives and insights, and dumb jokes.

To my parents, I will never be able to thank you enough for all you have done for me. For my entire life, you have put me in positions to succeed. You have encouraged and supported me, comforted and soothed me. I do not take for granted how you have put Erin and me first, and I hope to one day be close to the kind of parent you both have been.

Above all else, my greatest source of inspiration, motivation, joy, and love has been my fiancée, Jenna. During the toughest days in lab, I was comforted knowing that I'd be coming home to you and Finley; and during the best days, I couldn't wait to come home and tell you about it. Thank you for your patience, for your cheerleading and support, your consoling, and again for your patience. While I am immensely proud of the work described in this document, the best thing I ever did in graduate school was find you. I cannot wait to marry you and start this next part of our lives together.

"Success is not final; failure is not fatal. It is the courage to continue that counts."

- Winston Churchill

- Don Shula

Table of Contents

List of Figures

List of Tables

Abstract

Challenges to discovery and preclinical development of long-acting release systems for protein therapeutics include protein instability and use of organic solvents during encapsulation, specialized equipment and personnel, and high costs. Remote loading self-healing encapsulation has been used to gently and efficiently encapsulate proteins in controlled-release polymers, primarily through protein-specific affinity for a trapping agent. To create a universal remote loading self-healing encapsulation platform, coordination bonds between polyhistidine tags (HisTags) of proteins and divalent transition metal cations (M^{2+}) in self-healing polymers were utilized, similar to immobilized metal affinity chromatography.

Porous, drug-free self-healing poly(lactic-co-glycolic acid) (PLGA) microspheres with high molecular weight dextran sulfate (HDS) and immobilized remotely-loaded M^{2+} ions were placed in the presence of proteins with HisTags to bind in the polymer pores before healing the surface with modest temperature. Using human serum albumin (HSA), insulin-like growth factor 1, and granulocyte-macrophage colony-stimulating factor (GM-CSF), encapsulation efficiencies (EE) of immunoreactive protein increased with the inclusion of HisTags and Zn^{2+}. Immunoreactive protein was continuously released over seven to ten weeks. GM-CSF showed bioactivity >95% relative to immunoreactive protein throughout. Increased EEs were found with other M^{2+} ions, but not with Ca^{2+}. Ethylenediaminetetraacetic acid interfered with this process, reverting EE to Zn^{2+}-free levels.

Following this promising proof-of-concept work, areas of potential improvement were identified: (1) reducing thermal stress, (2) decreasing the complexity and duration of the

protocol, (3) increasing the loading capacity, (4) increasing the penetration depth of protein, and (5) improving the release profile. Directly encapsulating $ZnCO_3$, rather than remotely loading Zn^{2+}, increased the Zn content in the microspheres ~6-fold. Microspheres with directly encapsulated $ZnCO_3$ ($_{DE}ZnCO_3$) more efficiently encapsulated HSA at protein loading solution concentrations ≥ 100 μg/mL than remotely loaded Zn^{2+} ($_{RL}Zn^{2+}$) microspheres. HisTag green fluorescent protein was more deeply encapsulated in $_{DE}ZnCO_3$ microspheres than in $_{RL}Zn^{2+}$ microspheres. Tributyl acetylcitrate was an effective plasticizer in terms of decreasing the glass transition temperature, but also led to a decrease in EE. The loading stage was reducible to 2 hours at 4°C and the healing stage to 6 hours at 37°C while maintaining strong EE for $_{DE}ZnCO_3$ microspheres, which slowly released immunoreactive protein for months, following a substantial burst release. Plasticization decreased the initial burst release.

Next, the effects of various excipients on physiochemical properties of the formulations were studied. HDS was shown to function as a porosigen and encourage water uptake. While HDS did not significantly affect the Zn^{2+} loading of $_{DE}ZnCO_3$ microspheres, it was shown be critical in remote loading of M^{2+} cations. Though the erosion and degradation profiles of the microspheres were not affected by HDS, replacing $MgCO_3$ with $ZnCO_3$ accelerated erosion and degradation significantly, potentially owed to the superior pH-modulation of $MgCO_3$. HDS exhibited a high burst release followed by a plateau and seemingly degradation-dependent release. Zn^{2+} release appeared erosion-driven and was released more quickly from $ZnCO_3$-containing microspheres than from $MgCO_3$-containing microspheres. HisTag HSA release from HDS-free $_{DE}ZnCO_3$ microspheres showed higher burst and faster release than HDS-containing formulations have shown previously.

The self-healing polymer platform described here for remote loading of HisTag proteins could be a valuable asset to drug discovery and early development scientists interested in the controlled release of delicate biologic candidates using very small quantities of the proteins in *in vitro* and pre-clinical *in vivo* studies, providing valuable information to inform further potential development and clinical translation.

Chapter 1: Introduction

1.1. Biologics

1.1.1. History

Before the elucidation of the structure of deoxyribonucleic acid (DNA) by Watson and Crick in 1953,[1] and even for decades after it, the drug discovery industry was dominated by small molecules. Synthetic organic chemistry was necessary and nearly sufficient to discover and optimize novel therapeutics, which were most often "small molecules."[2] There were, though, exceptions to this rule. For example, vaccine antigens and antitoxins, including the diphtheria antitoxin, which was derived from blood serum of horses, were produced with the help of living organisms.[3] In the decades following 1953, molecular biologists set about altering the sequence of DNA, with Paul Berg being the first to do so in 1972, earning him the 1980 Nobel Prize in chemistry.[4] The massive potential of recombinant DNA was understood by the scientific community such that influential scientists met to create self-regulations regarding experimentation with recombinant DNA at the Asilomar Conference of 1975.[5] In 1982, Humulin, recombinant insulin (though identical to endogenous human insulin in sequence of amino acids), became the first FDA-approved therapeutic produced with recombinant DNA.[4] Since then, the biotechnology industry has exploded and biologics accounted for $286-$303 billion in global sales in 2020 and are projected to reach $422-$509 billion by 2026.[6,7] In 2020, 13 of the 53 new molecular entities (NME's) (25%) approved for either a new drug application (NDA) or biologics license application (BLA) by the U.S. Food and Drug Administration (FDA) were biologics.[8]

1.1.2. Uses and advantages

In many disease states, the primary cause of pathogenesis is decreased expression levels or impaired function of a given endogenously expressed protein. In these cases, protein or enzyme replacement therapy by a recombinant version of the molecule is a logical and often effective therapy. In other disease states, it is the overexpression of proteins (i.e., tumor necrosis factor [TNF]-α) that leads to pathology. In these cases, monoclonal antibodies raised specifically to bind to and neutralize these targets have proven to be an effective clinical treatment. Advantages of protein therapeutics include the fact they often lead to fewer and milder off-target effects and toxicity than small molecule drugs, which, unlike proteins, are not endogenous to the body. Further, proteins have evolved naturally (for billions of years, in some cases) to bind to specific targets. Thus, they often bind to a given target with higher specificity and affinity than a small molecule drug competitor can.[9] Indeed, biologics tend to have higher success rates in the FDA authorization process as compared to small molecules, though this is affected by the difference in financial investment needed to bring biologics to market.

Biologics are often much more complicated and expensive to develop and produce, owing to the fact that they are most often expressed via cell lines, have delicate secondary and tertiary structures that must be maintained, and are often prone to aggregation, which can lead to poor efficacy as well as immunogenicity.[10] Another barrier to the development of biologics is their poor oral bioavailability (proteins are degraded and poorly absorbed in the stomach and GI tract), which leads to the need for these products to be injected. This, paired with their relatively short half-lives, necessitates frequent injection, which results in poor patient compliance and outcomes.[11] For these reasons, controlled release products, which are injected less frequently but slowly release drug for days, weeks, or months after injection, have become popular.

1.2. Controlled release of biologics

Controlled release technologies have taken many forms, including micelles, liposomes, nano- and microparticles, hydrogels, *in situ* forming systems, osmotic pumps, thin films, implants, and more, with polymeric systems being especially popular.[12] Besides simply decreasing the frequency of injection, increasing patient convenience and compliance and, therefore, outcomes, controlled release systems can provide myriad other benefits.[13,14] Controlled release can help lead to stabilized plasma concentrations, increasing the amount of time plasma concentrations remain in the therapeutics window, which can increase efficacy and lower toxicity and inefficacy of the treatment. Relatedly, controlled release can result in a smaller mass of the therapeutic being needed, which saves costs. Encapsulating the protein within a controlled release formulation can improve the stability of protein within the body by slowing or preventing degradation, denaturation, and/or aggregation, increasing the half-life of the therapeutic. Controlled release can also be helpful in local delivery of proteins by releasing the protein at or near its site of action, drastically lowering systemic exposure to the protein, which can lower toxicity and costs. Crucially, local controlled release delivery (i.e. include implants, drug-eluting stents, and intravaginal rings) can be accomplished with far fewer applications (i.e. injections) of the drug than would be needed for a standard formulation.[15] Some controlled release formulations are produced using "smart" polymers or other materials than can behave differently depending on environmental stimuli.[16] For example, a vehicle could release the therapeutic upon a change in pH, temperature, force, light, magnetic field, or other stimulus). Today, controlled release formulations of biologics are highly desirable for the reasons described, and such formulations have had commercial success, including Nutropin Depot (human growth hormone)[17], Lupron Depot (leuprolide)[18] and Bydureon (exenatide)[19].

1.3. Poly(lactic-co-glycolic acid)

One of the most popular materials used in biologic controlled release formulations is poly(lactic-*co*-glycolic acid) (PLGA), a synthetic random polyester comprised of both L- and D-enantiomers of lactic acid and glycolic acid (**Figure 1-1**) or lactide and glycolide cyclic dimers. PLGA has been used in at least 19 FDA-approved products and is generally recognized as safe (GRAS) by FDA. PLGA is biocompatible and biodegradable.[20-22] After undergoing water-catalyzed hydrolysis, PLGA breaks down into lactic acid and glycolic acid, which are metabolized and excreted, respectively. One reason the use of PLGA has become so common is that the behavior of the polymer in physiological environments can be tuned by adjusting certain physiochemical attributes of the polymer. For example, the ratio of lactic acid to glycolic acid monomers can be adjusted. Glycolic acid is more hydrophilic than lactic acid. Therefore, PLGAs with higher glycolic acid content will degrade more quickly. The terminal group of the polymer chains can also be adjusted between an ester group or a free carboxylic acid, with the free acid leading to faster degradation, and the molecular weight of the polymer chains can be adjusted, with heavier chains requiring more time to degrade, leading to slower gross erosion.

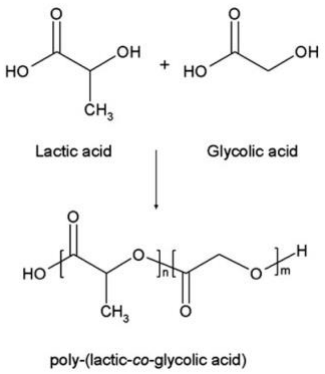

Figure 1-1*. Chemical structure of PLGA. Lactic acid and glycolic acid monomers are joined via ester linkages. Adapted from Danhier, et al.*[23]

PLGA can be formed into a variety of drug-encapsulating geometries, including thin films, micro- and nanospheres, and implants. It is a versatile polymer and has been used to encapsulate and slowly release small molecules, hormones, peptides, proteins, and antibodies for

weeks-to-months. For example, PLGA microspheres have been used to deliver leuprolide acetate for 1, 3, 4, and 6 months with just a single injection in Lupron Depot.[24]

1.3.1. PLGA microsphere formulation

PLGA microspheres can be formed using several different processes, including single emulsion or double emulsion and solvent evaporation, spray drying, and coacervation (or phase separation), and newer, less developed methods including electrospraying and membrane emuslsification.[21,25]

1.3.1.1. Emulsion and solvent evaporation

All microspheres used in the research presented herein were formulated using a water-in-oil-in-water (w/o/w) double emulsion and solvent evaporation method. Other emulsion systems (oil-in-water, solid-in-oil-in-water, e.g.) can also be used, but w/o/w is preferred for water-soluble proteins or similar drug molecules.[21,25] Here, the drug is initially dissolved in the aqueous phase, known as the "inner-water phase" or "disperse phase". This solution is added to an organic solution of PLGA (usually dichloromethane (DCM)) and homogenized to create a w/o primary emulsion. This primary emulsion is then added to another aqueous phase, which often contains an emulsifying agent, like polyvinyl alcohol (PVA), and homogenized, creating a w/o/w double emulsion, with the protein in the inner-water phase, the polymer in the oil phase, and an aqueous bath surrounding.[26] This double emulsion is then stirred in a larger aqueous bath for several hours to allow for the microspheres to harden and for the organic solvent used in the oil phase to evaporate, leaving PLGA microspheres (with inner-water-phase encapsulated) suspended in an aqueous bath (**Figure 1-2**). Microspheres can then be washed with water to remove any PVA or other species in the aqueous bath and sieved to isolate the size fraction of interest. Finally, the washed microspheres can be lyophilized and stored at -20°C for extended periods of time.

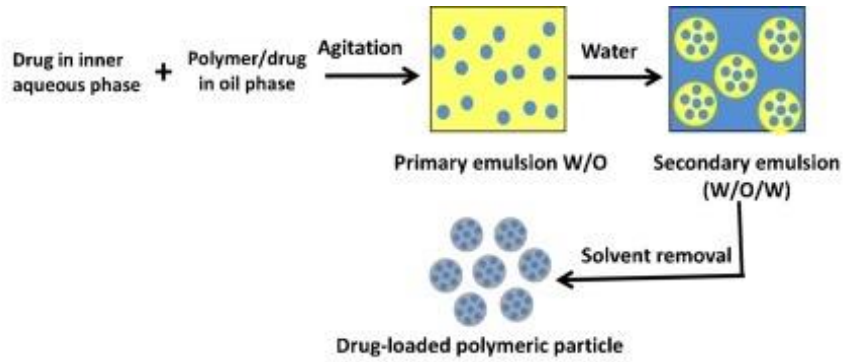

***Figure 1-2**. Schematic cartoon of the double emulsion solvent evaporation method of PLGA microsphere formulation. Adopted from Iqbal et al.*[27]

1.3.1.2. Alternative microsphere formulation techniques

Two other commonly used methods of fabricating PLGA microspheres are coacervation (phase separation) and spray drying. Coacervation involves creating a w/o emulsion using homogenization, similar to the first step of the solvent evaporation technique. The protein is dissolved in the water phase and the polymer is dissolved in the oil phase (usually DCM). Then, a coacervating agent, in which PLGA is much less soluble (often silicone oil) is added. This leads to the creation of droplets of o/w emulsions (i.e., a o/o/w emulsion). This o/o/w emulsion is then added to a bath of a hardening solvent (usually heptane), to allow for the inner organic solvent and coacervating agent to be removed from the microspheres. Excess solvents can then be removed via microsphere washing, and microspheres are sieved and lyophilized.[28,29] Challenges of PLGA microsphere formulation by coacervation include the possibility of aggregation and agglomeration of microspheres before they harden as well as incomplete removal of the coacervating or hardening agents, which can lead to biocompatibility issues.[30]

In spray drying, an emulsion or mixture of the protein and PLGA is atomized in a stream of very hot air creating microspheres. Then, the microspheres are moved into a heated drying chamber, where solvents can be evaporated, usually with the aid of nitrogen gas. The precise parameters of inlet and outlet air pressures and temperatures, atomization energy input, feed rate, and others can have large effects on the process.[28,31] While spray drying removes some of the

stressors present in other microencapsulation techniques, aggregation and denaturation of proteins has been found to occur due to high temperatures and atomization shear stress.[32,33] Low yields can also be a difficulty with spray drying.

1.3.2. Release mechanisms from PLGA microspheres

Drug release from PLGA microspheres is typically controlled by three mechanisms: aqueous diffusion through pores in the polymer (1), diffusion through the polymer matrix (release via this mechanism is often negligible for large molecules like proteins) (2), and release of drug as the polymer matrix erodes around it (3) (**Figure 1-3**). These underlying mechanisms that control the rates of each of these processes are complex and dependent on many factors, including details of the polymer, excipients, and the microsphere formulation process.

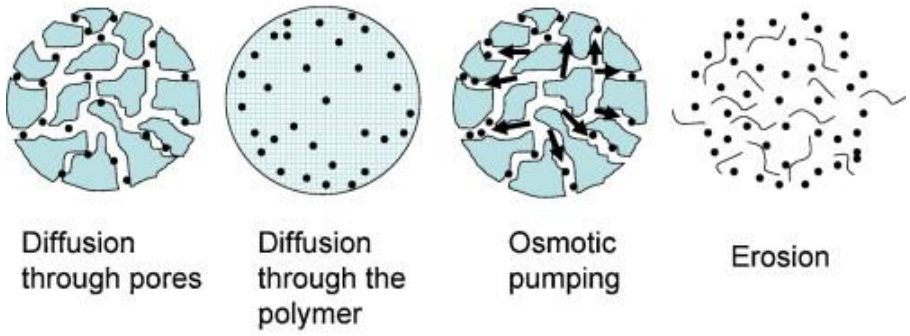

***Figure 1-3**. Drug release mechanisms. Diffusion through water filled pores, diffusion through the polymer, osmotic pumping, and erosion. Adopted from Fredenberg, et al.[34]*

Generally, the drug release from PLGA microspheres can be broken down into three temporal phases: an initial burst phase of quick release (1), a lag phase of minimal or slow release (2), and an erosion phase of increased release (3) (**Figure 1-4**). In the initial burst phase, drug molecules that are at or near the surface of the microspheres and are not bound or trapped by the polymer matrix are able to aqueously diffuse out through pores or cracks in the microspheres. As microspheres are exposed to physiological conditions, polymer chains become mobile and can rearrange, leading to closure of pores, and a reduction in aqueous diffusion out of the microspheres. In the lag phase, polymer erosion and is very slow, and therefore, so is drug

release. In the erosion phase, the microspheres undergo bulk erosion as polymer chains diffuse away, freeing encapsulated cargo, leading to steady release. The competition between these release mechanisms is complex and can give rise to a wide variety of release profiles.

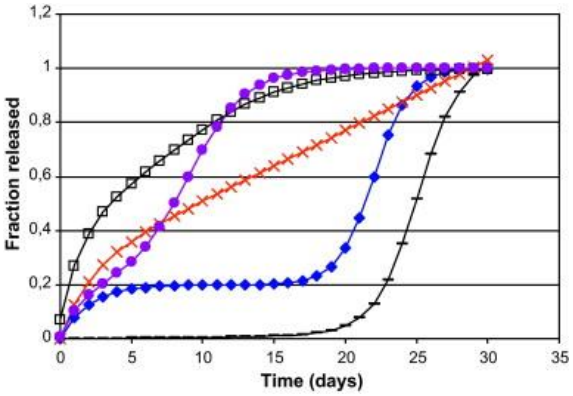

Figure 1-4*. Typical release profiles. Initial burst phase, followed a lag phase where drug may be slowly diffusing out of the polymer matrix, followed by a period of faster release where significant mass loss occurs. Adopted from Fredenberg, et al.*[34]

PLGA microspheres undergo heterogenous degradation and erosion. This is due to the buildup of acidic metabolites within the microsphere. As the ester bonds of PLGA are hydrolyzed, lactic acid and glycolic acid, or PLGA oligomers ending in lactic acid or glycolic acid, are created. Near the surface of the microspheres, these species can diffuse away (if they are of low enough molecular weight), or they can be buffered by the surrounding environment.[35] Deeper within the microspheres, on the other hand, these species are trapped, causing a drop in the pH, which leads to autocatalysis of PLGA chains and increased rates of degradation via a positive feedback loop. Decrease in molecular weight of polymer chains can increase the rate of diffusion of drug molecules through the polymer matrix, though large molecules, like proteins, are not thought to be released significantly through this mechanism. Once chains have been hydrolyzed to monomers or oligomers small enough that they are water-soluble, they can diffuse away from the PLGA formulation.[36] As polymer erodes, encapsulated drug molecules can be freed, or they can diffuse through pores that have been left behind by degraded and/or eroded polymer chains. The degradation rate of PLGAs can be controlled by physical properties of the

polymers, such as the ratio of lactic acid to glycolic acid, the initial molecular weight of the polymer chains, and the blockiness and crystallinity of the polymer.[37]

Water can also catalyze the hydrolysis of the ester bonds. Water content can be affected by the porosity of the microspheres and the osmotic pressure, which is driven by solutes trapped within the microspheres. The porosity and osmotic pressure can be increased by including solutes, especially salts, as excipients during microsphere formulation.[38] These "porosigens" can create porous networks throughout the microspheres, which can impact a variety of behaviors of the microspheres, including remote loading, which is discussed below.

1.3.3. Protein stability issues during encapsulation

Each of the PLGA microsphere fabrication techniques described above, including double emulsion solvent evaporation, requires emulsifying an aqueous solution of protein in an organic polymer-containing phase, which exposes the proteins to a variety of stressors. Proteins are often sensitive molecules whose structure and therefore function can be affected by chemical and physical stresses and modifications. This can be a dangerous combination, as the process of encapsulating proteins for controlled release can cause instability in the protein (**Table 1-1**), resulting in an inefficacious and potentially immunogenic biologic product.

Specifically, the emulsification process can expose proteins to aqueous-organic interfaces and air-liquid interfaces. As proteins are amphiphilic and surface active, they are prone to aggregating at these interfaces, leading to loss of activity. Further, the emulsification process (which can include ultrasonification or mechanical shear due to vortexing or homogenization) can expose proteins to high shear stresses and extreme local temperatures, which can denature proteins, as well.[20,39-46] The lyophilization process, which includes freezing and dehydrating the microspheres, can also be deleterious to proteins, and lyo-protective excipients (often sugars, e.g. trehalose) are included for this reason.[47]

***Table 1-1**. Examples of instability of proteins encapsulated in PLGA delivery systems, with examples occurring during encapsulation highlighted. Adapted from Schwendeman, et al.[40]*

Some Examples of the Instability of Proteins Encapsulated in PLGA Delivery Systems

Protein	Report of instability
Bovine serum albumin	Peptide-bond fragmentation during release
	Noncovalent aggregation during release (with negligible to minor disulfide-bonded component in aggregate)
Hen egg-white lysozyme	Noncovalent aggregation during encapsulation by solvent evaporation
	Covalent dimerization and formation of unknown product during release
Ribonuclease A	Noncovalent aggregation during encapsulation by solvent evaporation
Growth hormone	Soluble aggregation in the absence of zinc acetate and zinc carbonate during release
	Deamidation, oxidation, and aggregation observed at rates similar to those in solution during release
	Aggregation during encapsulation and release
Tetanus toxoid	Incomplete release[a]; losses in immunoreactive antigen during release
Erythropoietin	Covalent aggregation during solvent evaporation; aggregation during release
Insulin-like growth factor-I	Incomplete protein release over 25 days in the absence of zinc carbonate[a]
Vascular endothelial growth factor	Heparin affinity decreased by 13% after 8 days of release
Bone morphogenetic protein	Incomplete protein release; 30% immunoreactive protein recovered after 28 days
Basic fibroblast growth factor	Incomplete protein release; 38% immunoreactive protein recovered after 28 days with heparin stabilizer

1.4. Remote Loading

To avoid the stressors introduced by the encapsulation process, the Schwendeman Lab has developed a technique known as remote loading and self-healing, or self-encapsulation.[42] Here, porous, "blank" drug-free PLGA microspheres are produced via the double emulsion solvent evaporation process previously discussed. A leachable solute is included in the inner-water phase of the double emulsion. This porosigen leaches out of the microspheres during the solvent evaporation process, leaving a porous network behind it. Briefly, the microspheres are subsequently exposed to an aqueous solution of the molecule of interest, which diffuses into the microspheres via the porous network. Then, the temperature is raised above the glass transition temperature (T_g) of the microspheres, leading to polymer chain mobility. This mobility allows the polymers to rearrange into a more thermodynamically favorable orientation, which involves

the closure of pores (**Figure 1-5**).[48,49] Thusly, the molecule of interest becomes encapsulated within the PLGA microspheres without exposing it to harmful conditions discussed above, including air-liquid interfaces, oil-water interfaces, high shear stress, and high temperatures.[26] Remote loading and self-healing has been used to successfully and efficiently encapsulate peptides, proteins, and vaccine antigens while greatly reducing instability and aggregation of encapsulated molecules.[50,51] Previously, protein solutions have been highly concentrated, >> 1 mg/mL.

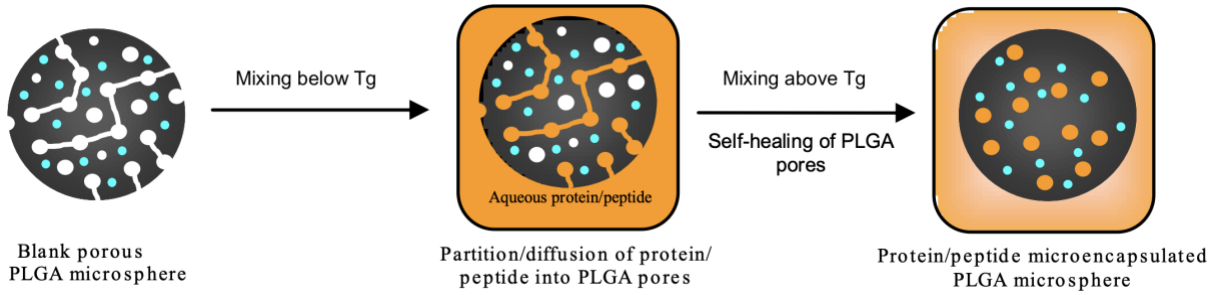

Figure 1-5. *The remote loading and self-healing paradigm. Adapted from Giles.*[26]

Self-healing of polymers is not a novel concept and is not unique to PLGA. Polymers in solution are mobile and intrinsically move to repair damage, moving toward conformations with less interfacial tension. This process has been described in five steps: surface rearrangement, surface approach, wetting, diffusion, and randomization.[52] Our lab has shown that PLGA self-healing follows a similar process.[42]

1.4.1. Passive Remote Loading

When no moiety is included in the "blank" PLGA microspheres for the purpose of attracting and binding the remotely loaded molecule of interest, this is referred to as passive remote loading, which relies mostly on simple diffusion. Model proteins including lysozyme and bovine serum albumin have been remotely loaded and encapsulated this way at 1-10% w/w loading, although encapsulation efficiencies were found to be low, due to the very high concentration of the protein loading solution.[42,50] Cationic peptides have also been passively

remotely loaded. This capitalizes on the charge interaction between the positively charged peptide and negatively charged carboxylic acid end-groups of PLGA, and encapsulation efficiencies have been shown to depend on the number of ionizable moieties on the peptide.[26]

1.4.2. Active Remote Loading

To improve on the low encapsulation efficiencies seen in passive remote loading, biocompatible molecules with affinity for the molecule of interest can be included in the inner water phase of the microspheres during the initial formulation of the microspheres. These "trapping agents" have included aluminum hydroxide gel for vaccine antigens, and biopolymers such as chitosan, dextran sulfate, and hyaluronic acid for a variety of proteins including vascular endothelial growth factor (VEGF) and fibroblast growth factor 20 (FgF-20). Using these active remote loading methods, encapsulation efficiencies above 85% and 70%, respectively, have been achieved.[42,50,53] As stated, the trapping agent is included in the inner water phase. This localizes the trapping agent within the porous network through which the molecule of interest diffuses. Here, the trapping agent and molecule of interest bind, allowing the molecule to be efficiently encapsulated upon self-healing. Further, complexing the proteins has shown to improve their stability in the release process. In all, remote loading, particularly active remote loading, has shown to be an exciting and valuable tool to efficiently encapsulate delicate peptides, proteins, and vaccine antigens without exposing them to many of the harsh conditions needed for traditional direct encapsulation. One major drawback of active remote loading, however, is that it is not a universally applicable method. Specific proteins are only compatible with specific trapping agents.

1.5. Metal – Histidine Coordination Bonding

1.5.1. Histidine Tags

When recombinant proteins are produced via expression hosts, nucleotides coding for several amino acids at the C-terminus or N-terminus end of the protein-coding region are often included in the vector for the purpose of being used to purify the recombinant protein from the result of the cellular media. One such type of "affinity tag" involves adding a series of histidine residues. Specifically, two to 14 histidine residues are added, with six being the most common. This "hexa histidine tag," "6xHis tag," or "His6 tag" was first developed by Roche in 1988, with the original patent having expired in 2003.[54] Often, the histidine tag is preceded or followed by a sequence of amino acids that allows for the tag to be cleaved by an endopeptidase, like the tobacco etch virus Nia protease, after purification, leaving the protein in its native sequence.[55] Sequences of histidine residues interspersed with glutamine residues, asparagine residues, and glycine residues have also been used, though studies have shown that these tags have no practical advantage over exclusively histidine tags.[56] The location of the tag (i.e. N-terminus or C-terminus) and the amino acid immediately following the methionine have been shown to be of more consequence, with certain residues increasing expression.[57] In most cases, including the tag at the N-terminus results in increased expression levels and protein solubility as well as increased stability of the mRNA intermediate, although this can vary between some proteins.[58,59]

Histidine is a very versatile amino acid, and this is owed to its molecular structure.[60] Histidine's side chain contains an imidazole ring, which has a pK_a of 6.5. At neutral charge, this group contains an electron pair, which allows histidine to act as a coordinating ligand with metal cations. At pH below its pK_a, the imidazole ring becomes protonated, and is unable to form the coordination bonds.

1.5.2. Coordination Bonding

Metallic elements are capable of forming a type of bond known as a coordination covalent bond with ions or molecules that contain at least one lone pair of electrons, which is

shared with the metal. These coordination complexes were first accurately described by Alfred Werner in 1893.[61] In these cases, the metal atom is known as the coordination center, and it is typically bound to two, four, or six ligands.[62]

Metal coordination complexes occur naturally in biology, with hemoglobin and chlorophyll containing coordination centers of iron and magnesium, respectively, for examples. Metal coordination bonds are used in medicinal chemistry, with the mechanism of action of the anticancer drug cisplatin involving a platinum coordination center forming coordination covalent bonds with nucleotides within tumor cells.[63] Metal coordination complexes have becomes widely used as industrial catalysts, as well, with many commonly used materials including polypropylene (titanium complex) being manufactured with the aid of metal coordination bonded catalysts.[64] Metal coordination bonds can even be found in a naturally occurring instance of polymer self-healing. The mussel byssus, an acellular tissue that many marine mussel species including *Mytilus* spp. use to attach to hard substrates (most commonly rocks), utilizes coordination bonds between zinc ions and histidine to repair deformations caused by mechanical stress.[65] Coordination complexes can be of neutral charge, or be positively or negatively charged ("complex ions").

1.5.3. Immobilized Metal Affinity Chromatography

In 1975, Jerker Porath discovered that proteins could be separated based on their relative histidine and cysteine content, which correlated with their relative affinity for transition metal cations, like Co^{2+}, Cu^{2+}, Ni^{2+}, and Zn^{2+}.[66] Porath wrote, "A gel loaded with strongly fixed Zn^{2+} and Cu^{2+} ions with excess binding capacity may therefore interact with surface-exposed imidazole and thiol groups of proteins. Consequently, zinc and copper-containing hydrophilic gels might be selective adsorbents for histidine and cysteine-containing peptides and proteins." What Porath described is now known as immobilized metal affinity chromatography (IMAC),

and it is now one of the most popular chromatographic methods of purifying recombinant protein. With the rise of recombinant DNA, scientists no longer had to rely on a protein's innate histidine or cysteine content; polyhistidine tags (HisTag) can now be expressed on the protein, allowing it to be isolated and purified with IMAC. In IMAC, metal ions (usually Ni^{2+}, though other divalent transition metals are used for HisTag proteins and trivalent and tetravalent cations are used for other applications) are rather irreversibly bound to chelating ligands in the stationary phase.[67] Common chelating ligands include iminodiacetic acid (IDA), which binds the metal cation using three of the six coordination sites (although only two are likely available to bind to protein of interest), nitrilotriacetic acid (NTA), which binds the metal cation using four of the six coordination sites, and tris(carboxymethyl) ethylenediamine (TED), which binds the metal cation using five of the six coordination sites.[68] The yield, purity, and amount of metal leaching can be affected by the choice of metal ion and chelating ligand. Once the protein of interest has been bound to the column, it can be eluted and purified using one of two common techniques. The pH of the mobile phase can be decreased from ~8 (where the affinity between the HisTag and the metal cation is strongest) to below 6 (where histidine becomes protonated and the coordination bond is interrupted). Alternatively, a chelating agent, like imidazole or ethylenediaminetetraacetic acid (EDTA), can be added to the mobile phase, displacing the HisTag from the metal cation.[69] The dissociation rate of HisTags from Ni-NTA has been measured to be in the low μM to low tens of nM.[56]

1.6. Motivation and potential use of Metal-HisTag Coordination Remote Loading during drug discovery phase to meet a translational need

This work is in some ways a solution to a solution to a solution to a solution. Specifically, the development of the field of biologics has been a wonderful solution to many untreated or poorly treated diseases. Biologics, however, must be injected quite often. To help solve this

problem, controlled release formulations, with PLGA microspheres being a favorite, have been developed. Unfortunately, the process of encapsulating biomacromolecules within PLGA microspheres is harsh and can cause instability in the molecules. To address this, our lab has pioneered remote leading and self-encapsulation, which removes the biomacromolecule from the traditional encapsulation process. Penultimately, a shortcoming of current active remote loading technologies is that they are not universal, but rely on some specific binding affinity of the molecule. Finally, the goal of this work is to create a remote loading controlled release platform that (1) is virtually universal for any recombinant peptide or protein, (2) is highly efficient, (3) uses very small quantities of the protein or peptide, (4) slowly and continuously releases active protein, and (5) can be performed by scientists without training in microencapsulation and without specialized mixing or drying equipment.

Meeting these goals would make this platform attractive during the discovery and early development of biologics, when producing and using large amounts of the molecules of interest could be very costly or infeasible. This platform would be most useful for local delivery of potent proteins, such as growth factors, due to the relatively small amounts of protein encapsulated, although it is not limited to these applications. To date, due partly to lack of involvement of drug delivery and formulation scientists early in the drug discovery and development process, a common cause of failure in clinical trials has been inaccurate preclinical pharmacokinetic data.[70] Thus, allowing non-formulation scientists to easily and cost-effectively test early stage drug candidates with a controlled release formulation in *in vitro* and *in vivo* pre-clinical studies could allow for much better translation from the bench to the patient.[71] This would help inform decisions regarding whether or not to pursue further development of a potential clinical controlled release formulation. We offer this platform as a potential solution to

this critical translational need. Due to the immunogenicity of HisTags, this platform does not lend itself to clinical use.

1.7. Proteins Used

In the experiments described herein, a variety of proteins were used as molecules of interest in an effort to prove universality and usefulness. To begin, two growth factors, for both of which recombinant protein biologics are marketed, were used: granulocyte-macrophage colony-stimulating factor (GM-CSF) and insulin-like growth factor 1 (IGF-1). Each of these proteins has utility for local controlled release applications.[72-79] GM-CSF is a hematopoietic cytokine that is endogenously secreted by blood cells to induce to proliferation and maturation of certain types of white blood cells.[80] It has a molecular weight of 14.5 kDa (when non-glycosylated) and an isoelectric point (pI) of 5.21, though this can be lower depending on glycosylation. Recombinant GM-CSF has been marketed as both sargramostim and molgramostim. IGF-1 is an anabolic growth hormone that is most abundant in the body during puberty.[81] It has a molecular weight of 7.7 kDa and a pI of 9.78. A recombinant form of IGF1 is marketed as mecasermin. Human serum albumin (HSA) was used as an inexpensive model protein. It is the most abundant protein in human plasma and acts as a carrier protein and osmotic.[82] It has a molecular weight of 67.3 kDa and a pI of 4.7. HSA has also been shown to have affinity for Zn^{2+}.[83] Finally, green fluorescent protein (GFP) was used for its fluorescent properties. It was first discovered in jellyfish and is used commonly in molecular biology as a reporter gene, due to the convenient fact that it fluoresces at 509 nm when excited at 395 nm.[84] It has a molecular weight of 32.7 kDa and a pI of 5.7.[85]

***Table 1-2**. Information regarding proteins used as molecules of interest.*

Protein	**MW (kDa)**	**pI**	**Recombinant product**
GM-CSF	14.5	5.21	sargramostim, molgramostim
IGF-1	7.7	9.78	mecasermin
HSA	67.3	4.7	N/A
GFP	32.7	5.7	N/A

1.8. Dissertation Scope Overview

With the goals discussed in mind, this dissertation moves through the discovery and development of a novel and universal PLGA microsphere aqueous remote loading platform that requires very small quantities of protein: Metal-HisTag Coordination Remote Loading (MHCRL). In building a new platform, there are many considerations to weigh including ease of use, release profile, versatility, protein stability, encapsulation efficiency, polymer erosion and degradation, and more. Using a variety of proteins, these aspects of various MHCRL formulations are examined, with the intention of developing a tested, optimized, and characterized platform. Hopefully, this platform, or one that builds off its development, can be used in preclinical biologic discovery and early development to help advance candidates into later stages of development. This dissertation is comprised of five chapters, beginning with this introduction.

The second chapter is focused on proof-of-concept. Here, metal-HisTag coordination is utilized as a remote loading trapping mechanism for the first time. Using three proteins, the effects of the inclusion of Zn^{2+} and/or HisTags on encapsulation efficiency are measured and the release profile of the Zn^{2+}- and HisTag-containing formulations are examined. Several experiments are also conducted with the aim of determining whether or not metal-HisTag coordination is the mechanism driving the encapsulation. This work is separately produced in a peer-reviewed publication in the journal *Bioengineering and Translational Medicine*.

The third chapter is aimed at optimizing MHCRL. A change in Zn source, the inclusion of plasticizers, a range of pH's of loading solutions, and various temperatures and durations of loading and healing stages are tried in an effort to improve upon a series of areas of focus. These changes are meant not just to improve the performance of the platform (in terms of encapsulation efficiency, protein stability, and release profile), but also to make the platform a more practical and helpful tool for the eventual user. This work is being submitted for publication to the *International Journal of Pharmaceutics*.

In the fourth chapter, mechanisms of release of drug and excipients and the effect of various excipients and release conditions on the erosion and degradation of the formulation are explored. The formulation proposed here is rather complex as compared to a standard double-emulsion PLGA microsphere. A robust characterization of the microspheres and the factors affecting their breakdown and release of payload is valuable information in the pursuit of further development of this or similar platforms.

The fifth chapter discusses the major conclusions drawn from the second, third, and fourth chapters, and proposed future directions to probe deeper and beyond the findings of this work.

In all, this dissertation provides a ground-up perspective of Metal-HisTag Coordination Remote Loading, a novel PLGA microsphere platform which has demonstrated potential to be a useful tool in the discovery and development of delicate and/or costly biologic candidates. Remote loading has proven to be a valuable technique in the controlled release formulation of proteins and peptides, and it is the goal of this platform to extend this technique to virtually any recombinant protein while requiring very small quantities of that protein.

1.9. References

1. Strauss BS. Why Is DNA Double Stranded? The Discovery of DNA Excision Repair Mechanisms. *Genetics*. Jun 2018;209(2):357-366. doi:10.1534/genetics.118.300958
2. Lowe D. Rise of the biologics. *Medchemcomm*. Jan 2018;9(1):10-11. doi:10.1039/c7md90046e
3. Bren L. The Road to the Biotech Revolution - Highlights of 100 Years of Biologics Regulation. *FDA Consumer magazine*. 2006;Centennial Edition
4. Pavlou AK, Reichert JM. Recombinant protein therapeutics--success rates, market trends and values to 2010. *Nat Biotechnol*. Dec 2004;22(12):1513-9. doi:10.1038/nbt1204-1513
5. Berg P, Baltimore D, Brenner S, Roblin RO, Singer MF. Summary statement of the Asilomar conference on recombinant DNA molecules. *Proc Natl Acad Sci U S A*. Jun 1975;72(6):1981-4. doi:10.1073/pnas.72.6.1981
6. Staff BP. *Biologic Therapeutic Drugs: Technologies and Global Markets*. 2021. BIO079D. April 2021.
7. Intelligence M. *Biologics Market- Growth, Trends, COVID-19 Impact, and Forecasts (2021 - 2026)*. 2020.
8. Arnum PV. New Drug Approvals in 2020: Which Drugs Made the Mark? DCAT Value Chain Insights. Updated January 20, 2021.
9. Craik DJ, Fairlie DP, Liras S, Price D. The future of peptide-based drugs. *Chem Biol Drug Des*. Jan 2013;81(1):136-47. doi:10.1111/cbdd.12055
10. Wang W, Singh SK, Li N, Toler MR, King KR, Nema S. Immunogenicity of protein aggregates--concerns and realities. *Int J Pharm*. Jul 15 2012;431(1-2):1-11. doi:10.1016/j.ijpharm.2012.04.040
11. Schwendeman SP, Shah RB, Bailey BA, Schwendeman AS. Injectable controlled release depots for large molecules. *Journal of Controlled Release*. 2014-09-01 2014;190:240-253. doi:10.1016/j.jconrel.2014.05.057
12. Kamaly N, Yameen B, Wu J, Farokhzad OC. Degradable Controlled-Release Polymers and Polymeric Nanoparticles: Mechanisms of Controlling Drug Release. *Chem Rev*. Feb 24 2016;116(4):2602-63. doi:10.1021/acs.chemrev.5b00346
13. Tibbitt MW, Dahlman JE, Langer R. Emerging Frontiers in Drug Delivery. *J Am Chem Soc*. Jan 27 2016;138(3):704-17. doi:10.1021/jacs.5b09974
14. Vaishya R, Khurana V, Patel S, Mitra AK. Long-term delivery of protein therapeutics. *Expert Opin Drug Deliv*. Mar 2015;12(3):415-40. doi:10.1517/17425247.2015.961420
15. Weiser JR, Saltzman WM. Controlled release for local delivery of drugs: barriers and models. *J Control Release*. Sep 28 2014;190:664-73. doi:10.1016/j.jconrel.2014.04.048
16. Priya James H, John R, Alex A, Anoop KR. Smart polymers for the controlled delivery of drugs - a concise overview. *Acta Pharm Sin B*. Apr 2014;4(2):120-7. doi:10.1016/j.apsb.2014.02.005
17. Cawley P, Wilkinson I, Ross RJ. Developing long-acting growth hormone formulations. *Clin Endocrinol (Oxf)*. Sep 2013;79(3):305-9. doi:10.1111/cen.12240
18. Zhou J, Hirota K, Ackermann R, et al. Reverse Engineering the 1-Month Lupron Depot®. *AAPS J*. 10 2018;20(6):105. doi:10.1208/s12248-018-0253-2
19. Ballav C, Gough S. Bydureon: long-acting exenatide for once-weekly injection. *Prescriber*. 2012-01-01 2012;23(1-2):30-33. doi:10.1002/psb.852

20. Han FY, Thurecht KJ, Whittaker AK, Smith MT. Bioerodable PLGA-Based Microparticles for Producing Sustained-Release Drug Formulations and Strategies for Improving Drug Loading. *Front Pharmacol*. 2016;7:185. doi:10.3389/fphar.2016.00185
21. Qi F, Wu J, Li H, Ma G. Recent research and development of PLGA/PLA microspheres/nanoparticles: A review in scientific and industrial aspects.
22. Park K, Skidmore S, Hadar J, et al. Injectable, long-acting PLGA formulations: Analyzing PLGA and understanding microparticle formation. *J Control Release*. 06 2019;304:125-134. doi:10.1016/j.jconrel.2019.05.003
23. Danhier F, Ansorena E, Silva JM, Coco R, Le Breton A, Preat V. PLGA-based nanoparticles: an overview of biomedical applications. *J Control Release*. Jul 20 2012;161(2):505-22. doi:10.1016/j.jconrel.2012.01.043
24. Ochi M, Wan B, Bao Q, Burgess DJ. Influence of PLGA molecular weight distribution on leuprolide release from microspheres. *Int J Pharm*. Apr 15 2021;599:120450. doi:10.1016/j.ijpharm.2021.120450
25. Jain RA. The manufacturing techniques of various drug loaded biodegradable poly(lactide-co-glycolide) (PLGA) devices. *Biomaterials*. Dec 2000;21(23):2475-90. doi:10.1016/s0142-9612(00)00115-0
26. Giles M. *Aqueous Remote Loading of Peptides in PLGA Microspheres*. University of Michigan; 2017. hdl.handle.net/2027.42/144200
27. Iqbal M, Zafar N, Fessi H, Elaissari A. Double emulsion solvent evaporation techniques used for drug encapsulation. *Int J Pharm*. Dec 30 2015;496(2):173-90. doi:10.1016/j.ijpharm.2015.10.057
28. Butreddy A, Gaddam RP, Kommineni N, Dudhipala N, Voshavar C. PLGA/PLA-Based Long-Acting Injectable Depot Microspheres in Clinical Use: Production and Characterization Overview for Protein/Peptide Delivery. *Int J Mol Sci*. Aug 18 2021;22(16)doi:10.3390/ijms22168884
29. NIHANT N, STASSEN S, GRANDFILS C, JEROME R, TEYSSIE P. MICROENCAPSULATION BY COACERVATION OF POLY(LACTIDE-CO-GLYCOLIDE) .2. ENCAPSULATION OF A DISPERSED AQUEOUS-PHASE. Article. *Polymer International*. 1993 1993;32(2):171-176. doi:10.1002/pi.4990320210
30. Thomasin C, Ho NT, Merkle HP, Gander B. Drug microencapsulation by PLA/PLGA coacervation in the light of thermodynamics. 1. Overview and theoretical considerations. *J Pharm Sci*. Mar 1998;87(3):259-68. doi:10.1021/js970047r
31. Baldinger A, Clerdent L, Rantanen J, Yang M, Grohganz H. Quality by design approach in the optimization of the spray-drying process. *Pharm Dev Technol*. Jul-Aug 2012;17(4):389-97. doi:10.3109/10837450.2010.550623
32. Mumenthaler M, Hsu CC, Pearlman R. Feasibility study on spray-drying protein pharmaceuticals: recombinant human growth hormone and tissue-type plasminogen activator. *Pharm Res*. Jan 1994;11(1):12-20. doi:10.1023/a:1018929224005
33. Wan F, Yang M. Design of PLGA-based depot delivery systems for biopharmaceuticals prepared by spray drying. *Int J Pharm*. Feb 10 2016;498(1-2):82-95. doi:10.1016/j.ijpharm.2015.12.025
34. Fredenberg S, Wahlgren M, Reslow M, Axelsson A. The mechanisms of drug release in poly(lactic-co-glycolic acid)-based drug delivery systems--a review. *Int J Pharm*. Aug 30 2011;415(1-2):34-52. doi:10.1016/j.ijpharm.2011.05.049

35. Li S, McCarthy S. Further investigations on the hydrolytic degradation of poly (DL-lactide). *Biomaterials*. Jan 1999;20(1):35-44. doi:10.1016/s0142-9612(97)00226-3
36. Husmann M, Schenderlein S, Luck M, Lindner H, Kleinebudde P. Polymer erosion in PLGA microparticles produced by phase separation method. *Int J Pharm*. Aug 21 2002;242(1-2):277-80. doi:10.1016/s0378-5173(02)00187-4
37. Wu XS, Wang N. Synthesis, characterization, biodegradation, and drug delivery application of biodegradable lactic/glycolic acid polymers. Part II: biodegradation. *J Biomater Sci Polym Ed*. 2001;12(1):21-34. doi:10.1163/156856201744425
38. Crotts G, Park T. Preparation of porous and nonporous biodegradable polymeric hollow microspheres. Article. *Journal of Controlled Release*. AUG 1995 1995;35(2-3):91-105. doi:10.1016/0168-3659(95)00010-6
39. Wu F, Jin T. Polymer-based sustained-release dosage forms for protein drugs, challenges, and recent advances. *AAPS PharmSciTech*. 2008;9(4):1218-29. doi:10.1208/s12249-008-9148-3
40. Schwendeman SP. Recent advances in the stabilization of proteins encapsulated in injectable PLGA delivery systems. *Crit Rev Ther Drug Carrier Syst*. 2002;19(1):73-98. doi:10.1615/critrevtherdrugcarriersyst.v19.i1.20
41. van de Weert M, Hoechstetter J, Hennink WE, Crommelin DJ. The effect of a water/organic solvent interface on the structural stability of lysozyme. *J Control Release*. Sep 2000;68(3):351-9. doi:10.1016/s0168-3659(00)00277-7
42. Reinhold SE, Desai KG, Zhang L, Olsen KF, Schwendeman SP. Self-healing microencapsulation of biomacromolecules without organic solvents. *Angew Chem Int Ed Engl*. Oct 2012;51(43):10800-3. doi:10.1002/anie.201206387
43. Cohen S, Bernstein H. *Microparticulate systems for the delivery of proteins and vaccines*. Drugs and the pharmaceutical sciences,. Marcel Dekker; 1996:ix, 525 p.
44. Ando S, Putnam D, Pack DW, Langer R. PLGA microspheres containing plasmid DNA: preservation of supercoiled DNA via cryopreparation and carbohydrate stabilization. *J Pharm Sci*. Jan 1999;88(1):126-30. doi:10.1021/js9801687
45. Giovagnoli S, Blasi P, Ricci M, Rossi C. Biodegradable microspheres as carriers for native superoxide dismutase and catalase delivery. *AAPS PharmSciTech*. Oct 2004;5(4):e51. doi:10.1208/pt050451
46. Manning MC, Chou DK, Murphy BM, Payne RW, Katayama DS. Stability of protein pharmaceuticals: an update. *Pharm Res*. Apr 2010;27(4):544-75. doi:10.1007/s11095-009-0045-6
47. Pikal MJ, Rigsbee D, Roy ML. Solid state stability of proteins III: calorimetric (DSC) and spectroscopic (FTIR) characterization of thermal denaturation in freeze dried human growth hormone (hGH). *J Pharm Sci*. Dec 2008;97(12):5122-31. doi:10.1002/jps.21386
48. Mazzara JM, Balagna MA, Thouless MD, Schwendeman SP. Healing kinetics of microneedle-formed pores in PLGA films. *J Control Release*. Oct 2013;171(2):172-7. doi:10.1016/j.jconrel.2013.06.035
49. Huang J, Mazzara JM, Schwendeman SP, Thouless MD. Self-healing of pores in PLGAs. *J Control Release*. May 2015;206:20-9. doi:10.1016/j.jconrel.2015.02.025
50. Desai KG, Schwendeman SP. Active self-healing encapsulation of vaccine antigens in PLGA microspheres. *J Control Release*. Jan 2013;165(1):62-74. doi:10.1016/j.jconrel.2012.10.012

51. Mazzara JM, Ochyl LJ, Hong JKY, Moon JJ, Prausnitz MR, Schwendeman SP. Self-healing encapsulation and controlled release of vaccine antigens from PLGA microparticles delivered by microneedle patches. *Bioeng Transl Med*. Jan 2019;4(1):116-128. doi:10.1002/btm2.10103
52. Wool RP. Self-healing materials: a review. *Soft Matter*. Feb 21 2008;4(3):400-418. doi:10.1039/b711716g
53. Shah RB, Schwendeman SP. A biomimetic approach to active self-microencapsulation of proteins in PLGA. *J Control Release*. Dec 2014;196:60-70. doi:10.1016/j.jconrel.2014.08.029
54. Hochuli E. Purification of recombinant proteins with metal chelate adsorbent. *Genet Eng (N Y)*. 1990;12:87-98. doi:10.1007/978-1-4613-0641-2_6
55. Puhl AC, Giacomini C, Irazoqui G, Batista-Viera F, Villarino A, Terenzi H. Covalent immobilization of tobacco-etch-virus NIa protease: a useful tool for cleavage of the histidine tag of recombinant proteins. *Biotechnol Appl Biochem*. May 29 2009;53(Pt 3):165-74. doi:10.1042/BA20080063
56. Knecht S, Ricklin D, Eberle AN, Ernst B. Oligohis-tags: mechanisms of binding to Ni2+-NTA surfaces. *J Mol Recognit*. Jul-Aug 2009;22(4):270-9. doi:10.1002/jmr.941
57. Dalboge H, Bayne S, Pedersen J. In vivo processing of N-terminal methionine in E. coli. *FEBS Lett*. Jun 18 1990;266(1-2):1-3. doi:10.1016/0014-5793(90)90001-b
58. Cebe R, Geiser M. Rapid and easy thermodynamic optimization of the 5'-end of mRNA dramatically increases the level of wild type protein expression in Escherichia coli. *Protein Expr Purif*. Feb 2006;45(2):374-80. doi:10.1016/j.pep.2005.07.007
59. Woestenenk EA, Hammarstrom M, van den Berg S, Hard T, Berglund H. His tag effect on solubility of human proteins produced in Escherichia coli: a comparison between four expression vectors. *J Struct Funct Genomics*. 2004;5(3):217-29. doi:10.1023/b:jsfg.0000031965.37625.0e
60. Liao SM, Du QS, Meng JZ, Pang ZW, Huang RB. The multiple roles of histidine in protein interactions. *Chem Cent J*. Mar 2013;7(1):44. doi:10.1186/1752-153X-7-44
61. Diercks CS, Kalmutzki MJ, Diercks NJ, Yaghi OM. Conceptual Advances from Werner Complexes to Metal-Organic Frameworks. *ACS Cent Sci*. Nov 28 2018;4(11):1457-1464. doi:10.1021/acscentsci.8b00677
62. Lawrance GA. *Introduction to Coordination Chemistry*. Wiley.
63. Saad JS, Benedetti M, Natile G, Marzilli LG. Basic coordination chemistry relevant to DNA adducts formed by the cisplatin anticancer drug. NMR studies on compounds with sterically crowded chiral ligands. *Inorg Chem*. Jun 21 2010;49(12):5573-83. doi:10.1021/ic100494f
64. Malinowski J, Zych D, Jacewicz D, Gawdzik B, Drzezdzon J. Application of Coordination Compounds with Transition Metal Ions in the Chemical Industry-A Review. *Int J Mol Sci*. Jul 30 2020;21(15)doi:10.3390/ijms21155443
65. Zechel S, Hager MD, Priemel T, Harrington MJ. Healing through Histidine: Bioinspired Pathways to Self-Healing Polymers via Imidazole–Metal Coordination. *Biomimetics (Basel)*. Feb 2019;4(1)doi:10.3390/biomimetics4010020
66. Porath J, Carlsson J, Olsson I, Belfrage G. Metal chelate affinity chromatography, a new approach to protein fractionation. *Nature*. Dec 1975;258(5536):598-9. doi:10.1038/258598a0

67. Burgess RR, Deutscher MP. *Guide to protein purification*. 2nd ed. Academic Press; 2009:1 online resource (915 p.).
68. Yip TT, Hutchens TW. Immobilized metal ion affinity chromatography. *Methods Mol Biol*. 1992;11:17-31. doi:10.1385/0-89603-213-2:17
69. Giacometti J, Josic D. Protein and Peptide Separations. *Liquid Chromatography: Applications*. Elsevier Inc.; 2013:149-175:chap 3.
70. Tan T, Watts SW, Davis RP. Drug Delivery: Enabling Technology for Drug Discovery and Development. iPRECIO Micro Infusion Pump: Programmable, Refillable, and Implantable. *Front Pharmacol*. 2011;2:44. doi:10.3389/fphar.2011.00044
71. Kwong E, Higgins J, Templeton AC. Strategies for bringing drug delivery tools into discovery. *Int J Pharm*. Jun 2011;412(1-2):1-7. doi:10.1016/j.ijpharm.2011.03.024
72. Reali E, Canter D, Zeytin H, Schlom J, Greiner JW. Comparative studies of Avipox-GM-CSF versus recombinant GM-CSF protein as immune adjuvants with different vaccine platforms. *Vaccine*. Apr 22 2005;23(22):2909-21. doi:10.1016/j.vaccine.2004.11.060
73. Choi KJ, Kim JH, Lee YS, et al. Concurrent delivery of GM-CSF and B7-1 using an oncolytic adenovirus elicits potent antitumor effect. *Gene Ther*. Jul 2006;13(13):1010-20. doi:10.1038/sj.gt.3302759
74. Steinwede K, Tempelhof O, Bolte K, et al. Local Delivery of GM-CSF Protects Mice from Lethal Pneumococcal Pneumonia. *The Journal of Immunology*. 2011-11-15 2011;187(10):5346-5356. doi:10.4049/jimmunol.1101413
75. Pan S, Qi Z, Li Q, et al. Graphene oxide-PLGA hybrid nanofibres for the local delivery of IGF-1 and BDNF in spinal cord repair. *Artificial Cells, Nanomedicine, and Biotechnology*. 2019-12-04 2019;47(1):650-663. doi:10.1080/21691401.2019.1575843
76. Tokunou T, Miller R, Patwari P, et al. Engineering insulin-like growth factor-1 for local delivery. *The FASEB Journal*. 2008-06-01 2008;22(6):1886-1893. doi:10.1096/fj.07-100925
77. Park J, Yan G, Kwon KC, et al. Oral delivery of novel human IGF-1 bioencapsulated in lettuce cells promotes musculoskeletal cell proliferation, differentiation and diabetic fracture healing. *Biomaterials*. 03 2020;233:119591. doi:10.1016/j.biomaterials.2019.119591
78. Davis ME, Hsieh PCH, Takahashi T, et al. Local myocardial insulin-like growth factor 1 (IGF-1) delivery with biotinylated peptide nanofibers improves cell therapy for myocardial infarction. *Proceedings of the National Academy of Sciences*. 2006-05-23 2006;103(21):8155-8160. doi:10.1073/pnas.0602877103
79. Zhang X, Xing H, Qi F, Liu H, Gao L, Wang X. Local delivery of insulin/IGF-1 for bone regeneration: carriers, strategies, and effects. *Nanotheranostics*. 2020;4(4):242-255. doi:10.7150/ntno.46408
80. Hamilton JA. GM-CSF in inflammation. *J Exp Med*. Jan 6 2020;217(1)doi:10.1084/jem.20190945
81. Laron Z. Insulin-like growth factor 1 (IGF-1): a growth hormone. *Mol Pathol*. Oct 2001;54(5):311-6. doi:10.1136/mp.54.5.311
82. Fanali G, di Masi A, Trezza V, Marino M, Fasano M, Ascenzi P. Human serum albumin: from bench to bedside. *Mol Aspects Med*. Jun 2012;33(3):209-90. doi:10.1016/j.mam.2011.12.002

83. Stewart AJ, Blindauer CA, Berezenko S, Sleep D, Sadler PJ. Interdomain zinc site on human albumin. *Proc Natl Acad Sci U S A*. Apr 1 2003;100(7):3701-6. doi:10.1073/pnas.0436576100
84. Chalfie M. Green fluorescent protein. *Photochem Photobiol*. Oct 1995;62(4):651-6. doi:10.1111/j.1751-1097.1995.tb08712.x
85. Nakatani T, Yasui N, Tamura I, Yamashita A. Specific modification at the C-terminal lysine residue of the green fluorescent protein variant, GFPuv, expressed in Escherichia coli. *Sci Rep*. Mar 18 2019;9(1):4722. doi:10.1038/s41598-019-41309-8

Chapter 2: Proof-of-Concept of Metal-HisTag Remote Loading of Very Small Quantities of Biomacromolecules into PLGA Microspheres

2.1. Abstract

Challenges to discovery and preclinical development of long-acting release (LAR) systems for protein therapeutics include protein instability, use of organic solvents during encapsulation, specialized equipment and personnel, and high costs of proteins. We sought to overcome these issues by combining remote-loading self-healing encapsulation with binding HisTag protein to transition metal ions. Porous, drug-free self-healing microspheres of copolymers of lactic and glycolic acids (PLGAs) with high molecular weight dextran sulfate (HDS) and immobilized divalent transition metal (M^{2+}) ions were placed in the presence of proteins with or without HisTags to bind the protein in the pores of the polymer before healing the surface pores with modest temperature. Using human serum albumin (HSA), insulin-like growth factor 1 (IGF-1), and granulocyte-macrophage colony-stimulating factor (GM-CSF), encapsulated efficiencies of immunoreactive protein relative to non-encapsulation protein solutions increased from ~41%, ~23%, and ~9%, respectively, without Zn^{2+} and HisTags to ~100%, ~83%, and ~75% with Zn^{2+} and HisTags. These three proteins were continuously released in immunoreactive form over seven to ten weeks to 73-100% complete release, and GM-CSF showed bioactivity >95% relative to immunoreactive protein throughout the release interval. Increased encapsulation efficiencies were also found with other divalent transition metals ions (Co^{2+}, Cu^{2+}, Ni^{2+}, and Zn^{2+}, but not with Ca^{2+}. Ethylenediaminetetraacetic acid (EDTA) was found to interfere with this process, reverting encapsulation efficiency back to

Zn^{2+}-free levels. These results indicate that M^{2+}-immobilized self-healing microspheres can be prepared for simple and efficient encapsulation by simple mixing in aqueous solutions. These formulations provide slow and continuous release of immunoreactive proteins of diverse types by using a fraction of protein (e.g., <10 μg), which may be highly useful in the discovery and early pre-clinical development phase of new protein active pharmaceutical ingredients, allowing for improved translation to further development of potent proteins for local delivery.

2.2. Introduction

Over the last several decades, the landscape of pharmaceutical drug products has been transformed from a near monolith of small molecules to a diverse space with biologics gaining more and more dominance. In 1982, the first genetically engineered form of insulin was approved.[1] By 2017, half of the top ten best-selling drug products over the previous 15 years were biologics.[2] Recombinant proteins, fusion proteins, antibodies, and others biologics have led to therapeutic breakthroughs in a number of treatment areas. They are also costlier and often more complicated to discover, develop, formulate, and manufacture. Another challenge of biologics is that they must be injected, rather than taken orally like most small molecule drug products, which is a significant impediment to patient compliance.[3] To reduce the number of injections and increase patient compliance, controlled release formulations have been developed, which require weekly, biweekly, or monthly injections rather than daily injections for non-controlled release formulations. Particularly useful for proteins, controlled release can also be helpful for local delivery to hard-to-reach areas, like the brain,[4,5] joints,[6,7] and posterior segment of the eye.[8,9] One difficulty, however, in the evaluation and development of new protein APIs, which require slow release to evaluate drug efficacy, is that large quantities of the biomacromolecule are required during formulation of controlled release dosage forms. Moreover, common encapsulation procedures require trained personnel with the use of organic

solvent-based unit operations.[3] These combined factors can significantly impede the early drug development process when producing and using large amounts of the proteins of interest can be financially infeasible.[10] Here, we aim to address these cases by creating a simple, general, and low-cost paradigm for preparation of local controlled-release dosage forms for protein drug discovery that could be simple enough for most any bench scientist to use.

Copolymers of lactic (or lactide) and glycolic (or glycolide) acids (PLGAs) have become a desired delivery vehicle for a wide variety of therapeutics, including peptides, proteins, antibodies, vaccine antigens, and nucleic acids. Advantages of PLGA microspheres include biocompatibility and biodegradability, injectability of PLGA microspheres through a syringe needle with minimal discomfort, and tunable and long-term complete release of the therapeutics, including peptides and proteins.[11-15] PLGA is used in at least 19 FDA-approved controlled-release products on the market in the US,[3,16,17] and therefore usually is the first biodegradable polymer considered for such applications.

While many hurdles of PLGA drug product formulation have been overcome, one long-standing issue is protein stability during encapsulation.[18] Traditional methods of encapsulation in PLGA microspheres require exposing biomacromolecules to micronization, organic/aqueous interfaces, air/water interfaces, high shear stress, organic solvents, and high temperatures, all of which can result in instability or aggregation of the biomacromolecule and low encapsulation efficiencies.[16,19-25]

To avoid these stressors and the resulting damage to protein and low encapsulation efficiency, our group previously devised organic solvent-free self-healing microencapsulation, in which porous PLGA microspheres are mixed with an aqueous solution of biomacromolecule.[22] The temperature is then raised above the glass transition temperature (T_g), causing the pores in

the surface of the microspheres to heal, encapsulating the biomacromolecule within the microspheres.[26,27] In active remote loading, a trapping agent is contained in the drug-free self-healing microspheres before exposure to the biomacromolecule to dramatically increase encapsulation efficiency.[18,28] The charge interaction between cationic peptides and the negatively charged carboxylic end-group of PLGA chains has also been targeted as an active remote loading strategy for smaller net cationic peptides that do not require preservation of tertiary structure.[29] Using active remote loading, encapsulation efficiencies greater than 95% have been achieved with elevated drug loading (>7% w/w).[18,28] Examples of trapping agents include aluminum- and calcium-based adjuvants[22,30-33] for vaccines and glycosaminoglycan-like biopolymers[18] that often bind growth factors. One drawback of these methods is that the trapping agent must be paired with specific biomacromolecules that have binding affinity for said trapping agent, and therefore, the methods are not universal. Here, we aim to take advantage of the coordination binding between divalent transition metals and poly-histidine tags (HisTags) to create an active remote loading method that is more universal to a broader spectrum of recombinant proteins.

Immobilized metal affinity chromatography (IMAC) was first developed in 1975 as a method of separating and purifying proteins based on their cysteine and histidine content.[34] These amino acids form coordination bonds with transition metals like Ni^{2+}, Cu^{2+} and Zn^{2+}.[35] Thus, proteins rich in cysteine and histidine can be purified by flowing them through a column with immobilized divalent transition metals. As the capability to express recombinant proteins expanded, so did strategies for IMAC. Today, HisTags (typically His_6 or His_{10}) can be expressed at the C- or N-terminus end of peptides and proteins, allowing them to be easily purified via IMAC.[36] To elute purified proteins or peptides of interest from the column, the pH can be lowered to protonate the histidine, interrupting the coordination bond, or imidazole, glycine, or a

chelating agent like ethylenediaminetetraacetic acid (EDTA) can be added to the column buffer solution, displacing the molecule of interest.[37]

In the active remote loading and self-encapsulation platform described in **Figure 2-1**, our approach is to directly encapsulate high molecular weight dextran sulfate (HDS), a negatively charged branched polysaccharide,[18] in drug-free and porous PLGA microspheres to serve as a metal-immobilizing scaffold. A divalent metal cation is then bound to the HDS to serve as a trapping agent for HisTag proteins before self-healing encapsulation. Our goal is to create a remote-loading controlled-release platform that (1) is virtually universal for any recombinant peptide or protein, (2) is highly efficient, (3) uses very small quantities of the protein or peptide, (4) slowly and continuously releases active protein, and (5) can be performed by scientists without training in microencapsulation and without specialized mixing or drying equipment. Meeting these goals would make this platform attractive during the discovery and early development of biologics, when producing and using large amounts of the molecules of interest could be very costly or infeasible and controlled release efficacy data is desired. Due to the low quantities encapsulated here, local delivery of potent proteins is the targeted application of this platform. For example, a single injection of only 0.01% protein-loaded PLGA implants for controlled release of basic fibroblast growth factor was sufficient to rescue limbs and restore perfusion in a murine hindlimb ischemic model.[38]

For decades, unpredictable or inadequate pharmacokinetics, resulting in undesirable toxicology and poor efficacy, has plagued drug candidates in clinical trials.[39] To combat this, drug delivery and formulation scientists have been introduced earlier in the development process. Allowing drug researchers with or without formulation expertise to easily and cost-effectively test early stage drug candidates with a controlled release formulation *in vivo* could allow for

much better translation from the bench to the patient.[40] We offer this platform as a potential solution to this critical translational need.

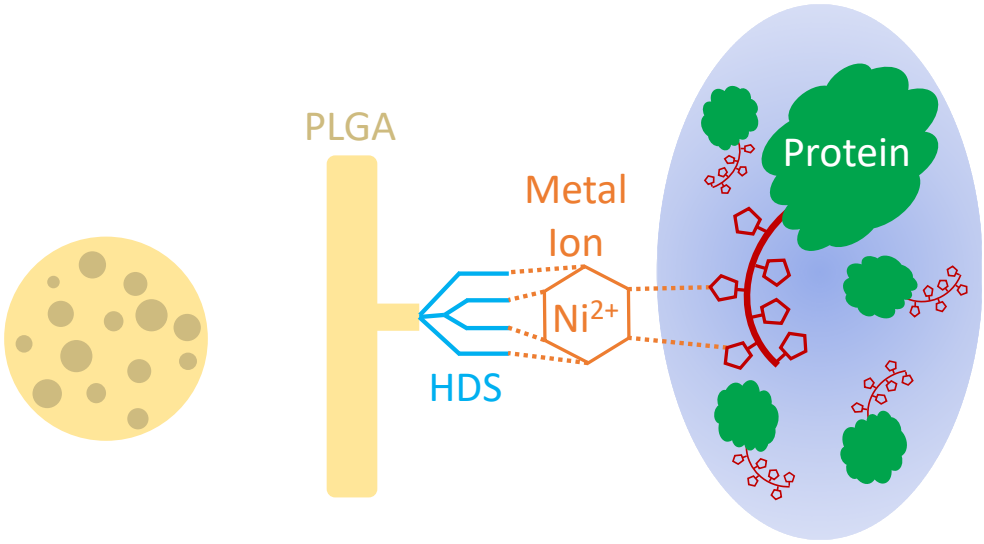

***Figure 2-1**. Schematic of remote loading mechanism into porous PLGA microspheres as related to Immobilized Metal Affinity Chromatography (IMAC). PLGA acts as the support structure. HDS acts as the chelating agent, immobilizing the metal ion, which binds a HisTag protein out of the loading solution through the porous network within the microsphere.*

2.3. Experimental Methods

2.3.1. Materials

Resomer RG 504 PLGA (50:50, ester-terminated, molecular weight 38,000-54,000 Da), magnesium carbonate, trehalose, 88% hydrolyzed poly(vinyl alcohol) (PVA), and high molecular weight (>500,000 Da) dextran sulfate (HDS) were purchased from Sigma Aldrich. Zinc, copper, cobalt, nickel, and calcium acetate salts were purchased from Sigma Aldrich. Poly-histidine tagged (HisTag) Human Serum Albumin (HSA) was purchased from Arco Biosystems and untagged (NoTag) HSA was purchased from Raybiotech. HisTag and NoTag granulocyte macrophage colony stimulating factor (GM-CSF) was purchased from Sino Biological. HisTag and NoTag insulin-like growth factor 1 (IGF-1) was purchased from Signalway Antibodies. All HisTag proteins contained tags of six histidine residues. Tags were at the N-terminus for GM-CSF and IGF-1. Tags were at the C-terminus for HSA. Ethylenediaminetetraacetic acid (EDTA)

and bovine serum albumin (BSA) were purchased from Sigma Aldrich. Blocker casein in PBS was purchased from ThermoFisher. All other common reagents and solvents were purchased from Sigma Aldrich, except where otherwise specified.

2.3.2. Preparation of microspheres

Porous PLGA microspheres with HDS as a metal immobilizer, $MgCO_3$ as a pH-modulator and porosigen,[18,19] and trehalose as a porosigen were prepared by double water-oil-water (w/o/w) emulsion and solvent evaporation. The first emulsion was created by homogenizing a suspension of 1 mL of 250 mg/mL dissolved PLGA and 6% w/w fine particulate $MgCO_3$ in methylene chloride with an inner water phase of 200 μL of 4% w/v HDS and 3% w/v trehalose in a glass cell culture tube at 18,000 rpm for 60 s over an ice bath, using the Tempest IQ^2. The second emulsion was created by adding 2 mL of 5% PVA to the primary emulsion and vortexing for 60 s. The w/o/w double emulsion was added to 100 mL of 0.5% PVA and stirred for 3 h at room temperature in a 150 mL beaker to allow for hardening and evaporation of methylene chloride. The 20-63 μm fraction of microspheres was collected using sieves and the microspheres were washed with excess double-distilled water and lyophilized.

2.3.3. Assessment of microsphere morphology by scanning electron microscopy

The surface morphology of microspheres was examined via a Tescan MIRA3 FEG electron microscope (SEM). Microspheres were mounted onto a brass stub via double-sided adhesive tape and sputtered with gold for 60 s at 40 W under vacuum. Images were taken at an excitation voltage of 5 kV. Prior to imaging, microspheres were incubated in protein-free loading solution for the specified duration at the specified temperature rotating at 30 rpm, then washed with double-distilled water and lyophilized.

2.3.4. Remote loading and encapsulation of metals and proteins

2.3.4.1. Standard Procedure

Metals were remotely loaded into the PLGA microspheres by incubating the microspheres in at least 1 mL of 500 mM metal acetate salt solution (or water as a control) per 1 mg of microspheres for 24 h rotating at 30 rpm at room temperature. Microspheres were washed with double-distilled water under vacuum on a 0.2 μm nylon filter and lyophilized. Remote loading HisTag and NoTag protein solutions were prepared by buffer exchange with Amicon ultra centrifugal filter units (for HSA and 10 μg/mL GM-CSF) or by diluting lyophilized powders in loading solution. Proteins were remotely loaded into the metal-loaded microspheres by incubating 1 mg of microspheres in 100 μL of 50 μg/mL protein (HisTag or NoTag), unless otherwise specified at 10 μg/mL GM-CSF in one case, in 50 mM sodium acetate, 300 mM sodium chloride, pH 8.0 solution (loading solution) for 48 h at room temperature rotating at 30 rpm followed by 42 h at 43 ºC rotating at 30 rpm to induce healing and pore-closure.

2.3.4.2. Inhibition of remote loading with EDTA

The effect of EDTA on the capacity of Zn-loaded microspheres to remotely load HisTag HSA was determined by incubating Zn-loaded microspheres (or water-incubated microspheres as a control) in 50% saturated EDTA solution (or water as a control) for 24 h rotating at 30 rpm at room temperature. Microspheres then underwent HSA loading as described above and loading and encapsulation were determined using Coomassie Plus protein assay as described below.

2.3.4.3. Effect of divalent metal cation on remote loading

To examine the effect of different divalent metal cations on the remote loading and encapsulation of HisTag IGF-1, zinc acetate, copper acetate, cobalt acetate, nickel acetate, or calcium acetate were used in the metal loading step as described above. Metal loading percentage and IGF-1 encapsulation efficiency were quantified as described below.

2.3.4.4. Determination of divalent metal cation loaded

The amount of divalent metal cation remotely loaded into microspheres was determined by dissolving several mg of microspheres in acetone, centrifuging for 5 min at 8,000 rpm, and removing the supernatant for three cycles. The pellet was then reconstituted in water and analyzed using a Perkin-Elmer Nexion 2000 ICP-MS using appropriate standards and scandium as an internal standard. Metal cation loading percentage was calculated as (mass of metal cation in microspheres / total mass of microspheres) x 100.

2.3.4.5. Determination of immunoreactive protein by ELISA

HSA and IGF-1 ELISA kits were purchased from Raybiotech and performed according to kit instructions to determine immunoreactive protein concentrations. GM-CSF ELISA kits were purchased from Raybiotech and PeproTech and were similarly applied. In all ELISAs, NoTag and HisTag proteins used for remote loading encapsulation were also included as reference standards.

2.3.4.6. Determination of total protein by Coomassie Plus protein assay

Total protein content for No Tag and HisTag HSA in loading solutions was measured by Coomassie Plus protein assay using a 1:1 sample-to-reagent ratio. BSA standards were used, with the HSA proteins included as reference standards, and absorbance was read at 595 nm in accordance with the protocol.

2.3.4.7. Estimation of protein loading and encapsulation efficiency

Protein loading (l) in microspheres was estimated by ELISA and Coomassie Plus protein assay by comparing the final concentrations of protein in the loading solution to a control loading solution, which underwent the same conditions without microspheres as follows:

$$l = V(C_C - C_{MS})$$

Where V (= 0.1 mL), C_C, and C_{MS} are the volume of loading solution, concentration of protein in control loading solution, and the concentration of protein in the loading solution with microspheres, respectively.

Encapsulation efficiency of the available active protein (i.e., relative to unencapsulation control) was calculated as:

$$EE_{avail} = \frac{C_C - C_{MS}}{C_C} \times 100\%$$

Where C_C and C_{MS} are the concentration of protein in control loading solution and the concentration of protein in the loading solution with microspheres quantified by ELISA, respectively. Encapsulation efficiency of available total protein was calculated similarly with concentrations of protein quantified by Coomassie Plus protein assay used in place of those measured by ELISA.

Actual active encapsulation efficiency of active protein was calculated as:

$$EE_{actual} = \frac{C_C - C_{MS}}{C_i} \times 100\%$$

Where C_C, C_{MS}, and C_i are the concentration of protein in control loading solution, concentration of protein in the loading solution with microspheres, and the original concentration of protein in the loading solution quantified by ELISA, respectively. Actual total encapsulation efficiency was calculated similarly with concentrations of protein quantified by Coomassie Plus protein assay used in place of those measured by ELISA.

2.3.4.8. Evaluation of release kinetics

HSA release was conducted by incubating 1 mg microspheres in 1 mL phosphate buffered saline (PBS) + 0.02% Tween 80 + 1% casein, pH 7.4. IGF-1 release was conducted from 1 mg microspheres in 1 mL PBS + 0.02% Tween 80 + 1% BSA, pH 7.4. GM-CSF release

was conducted from 1 mg microspheres in 1 mL PBS + 0.02% Tween 80 + 1% BSA, pH 7.4 or 1 mL 0.1M HEPES buffer + 1% BSA, pH 7.4. Media was completely replaced at each timepoint. All samples were incubated at 37 ºC with shaking. Casein was used as a blocking agent in place of BSA for HSA release to avoid interference in the HSA ELISA. HEPES was used in place of PBS in one instance in an effort to measure Zn^{2+} release, as phosphate salts are known to co-precipitate Zn.[41]

2.3.4.9. GM-CSF activity assay

The activity of HisTag GM-CSF released from Zn-loaded microspheres was determined using the PathHunter® Sargramostim Bioassay Kit from Eurofins DiscoverX. HisTag GM-CSF was included as a reference standard.

2.3.5. Statistics

All significance testing was conducted using one-tailed Student's t-tests. Statistical significance was considered $p < 0.5$.

2.4. Results and Discussion

To test our approach, high-molecular weight dextran sulfate (HDS) and $MgCO_3$ were co-encapsulated in the porous PLGA 50/50 microspheres, as described previously.[18] These microspheres were originally designed to microencapsulate growth factors that are known to bind to extracellular matrix. In these formulations, HDS binds the growth factor and $MgCO_3$ is present to both inhibit acid drop caused by PLGA hydrolysis and provide continuous release by production of salt when reacting to low-molecular weight degradation products.[18,42] We demonstrated high loading and encapsulation efficiency, and slow release of vascular endothelial growth factor without significant loss of immunoreactivity or heparin-binding affinity for weeks during slow and continuous release. Basic proteins, bFGF20 and lysozyme, were similarly encapsulated.[18]

2.4.1. Remote Zn^{2+} Loading

To expand the capability of these microspheres to deliver a wider spectrum of proteins, we bound Zn^{2+} and other divalent metal cations to HDS/PLGA microspheres by incubating 1 mL of acetate salt solution of the cation in the presence of a modest 1 mg of microspheres at room temperature for 24 h before loading the protein. ICP-MS showed that Zn^{2+} was significantly loaded into the microspheres after Zn-acetate exposure at a level of 0.42 ± 0.12% w/w%.

2.4.2. Encapsulation and Release of GM-CSF

After metal-ion uptake in HDS/PLGA microspheres, exchanging the solution to a 100 μL solution of 1 μg of HisTag granulocyte-macrophage colony-stimulating factor (HisTag GM-CSF), which has local delivery applications,[43-45] and raising the temp for 42 h at 43 ºC resulted in an estimated self-healing microencapsulation of ~75% protein available in the loading solution (**Figure 2-2a**, **Table 2-1**). If the Zn^{2+} was not added before loading, the encapsulation efficiency (EE) dropped to ~14%. If GM-CSF was added without a HisTag, the encapsulation efficiency was ~28% for Zn^{2+}/HDS/PLGA and ~9% for HDS/PLGA. The release kinetics of the resulting HisTag GM-CSF in the self-healed Zn^{2+}/HDS/PLGA microspheres is shown in **Figure 2-2b**. After a modest initial burst release, a continuous release of protein was recorded by ELISA over 70 days. Because of the focus on protein drug discovery, we did not seek to further stabilize the encapsulated protein and/or examine the immunoreactivity of any protein remaining in the polymer after the release incubation. Scanning electron micrographs also confirmed that open surface pores were maintained until the final heated self-healing step (Error! Reference source n ot found.). Hence this proof-of-principle experiment shows that a protein that does not seem to bind well to HDS can be encapsulated on a very small scale with Zn^{2+}/HDS/PLGA microspheres when using the HisTag version and then slowly release immunoreactive protein under physiological conditions for months. Note that the SEM images were acquired after washing and

drying the microspheres. Therefore, the polymer loses the swollen state that exists during incubation and the drying creates an altered morphology under the electron microscope. However, the number and size of the pores on the dry microsphere surface in the micrographs when evaluated at each stage of the aqueous encapsulation procedure is useful to confirm the healing of the polymer, as we have demonstrated in previous studies.[18,22,26,27]

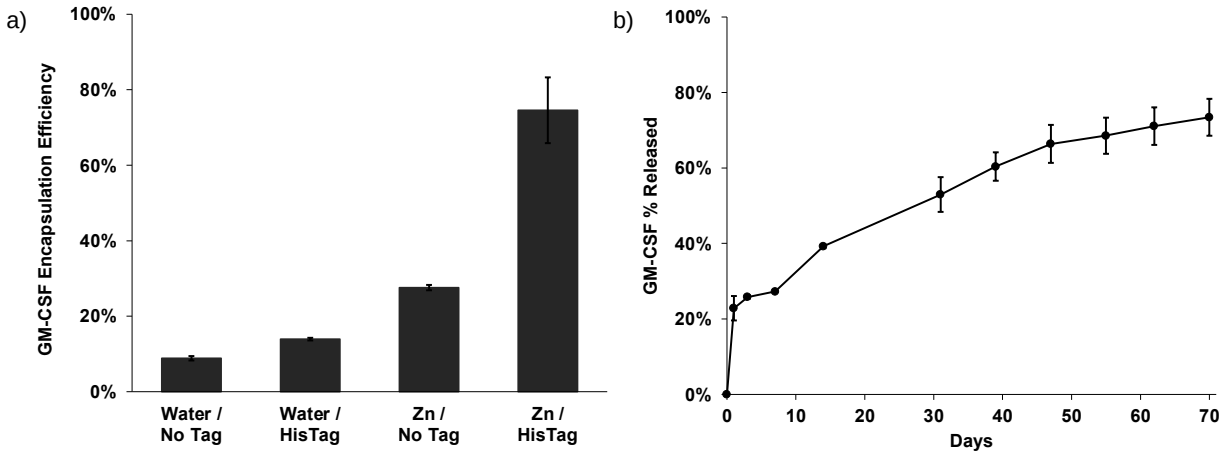

***Figure 2-2**. HisTag GM-CSF is efficiently encapsulated in Zn^{2+}-immobilized PLGA microspheres by remote loading and slowly released. a) Active available protein encapsulation efficiency of NoTag and HisTag GM-CSF into Zn^{2+}-free and Zn^{2+}-immobilized PLGA microspheres from ~10μg/mL protein loading solution. b) Release of immunoreactive HisTag GM-CSF from Zn^{2+}-immobilized PLGA microspheres in 1 mL PBS + 0.02% Tween 80 + 1% BSA, pH 7.4 at 37 °C. One μg protein and 1 mg of microspheres in 100 μL loading solution for self-healing encapsulation. Zn / HisTag EE_{avail} significantly greater than each control; $p < 0.05$*

***Table 2-1**. Summary of remote self-healing encapsulation by Zn^{2+}-HisTag protein binding (EE = Encapsulation Efficiency).*

Protein	Active Protein Loaded (μg)	Total Protein Loaded (μg)	Active Available EE	Total Available EE	Actual Active EE	Actual Total EE
GM-CSF (~10μg/mL)	0.21 ± 0.03	--	75 ± 9%	--	37 ± 4%	--
GM-CSF (50 μg/mL)	1.9 ± 0.3	2.3 ± 0.2	55 ± 7%	49 ± 1%	37 ± 6%	46 ± 3%
IGF-1 (50 μg/mL)	2.4 ± 0.9	--	81 ± 23%	--	48 ± 17%	--
HSA (50 μg/mL)	3.5 ± 0.2	4.6 ± 0.4	100 ± 3%	97 ± 2%	70 ± 2%	92 ± 6%

2.4.3. Increased Encapsulation and Release of GM-CSF

Although promising, the above remote loading example used a very low concentration of protein and only 49.5 ± 1% of protein remained immunoreactive in the control solution. Proteins

at this low concentrations commonly bind to vessel walls even if coated with low-protein-binding materials.[46] We then increased the protein concentration in the loading media to 50 μg/mL HisTag GM-CSF. In this case the loading efficiency decreased slightly to ~55%, and the differential advantage relative to the Zn^{2+}-free/HisTag or Zn^{2+}/NoTag controls also decreased slightly (**Figure 2-3a**). Moreover, encapsulation of active and total protein by employing ELISA (55 ± 7%) and Coomassie Plus protein assay (49 ± 1%), respectively, were performed and shown to yield consistent values. Here, 68 ± 6% of the protein in the control loading solution remained immunoreactive after incubation at loading conditions, which is much higher than at the lower concentration. Once again, we observed slow and continuous release of immunoreactive HisTag GM-CSF for 49 days (**Figure 2-3b**) The bioactivity of the protein was also monitored according to a CSF2RA-CSF2RB dimerization cell-based assay (**Figure 2-3c**). As seen in the figure, there was no noticeable loss in bioactivity over the entire release interval.

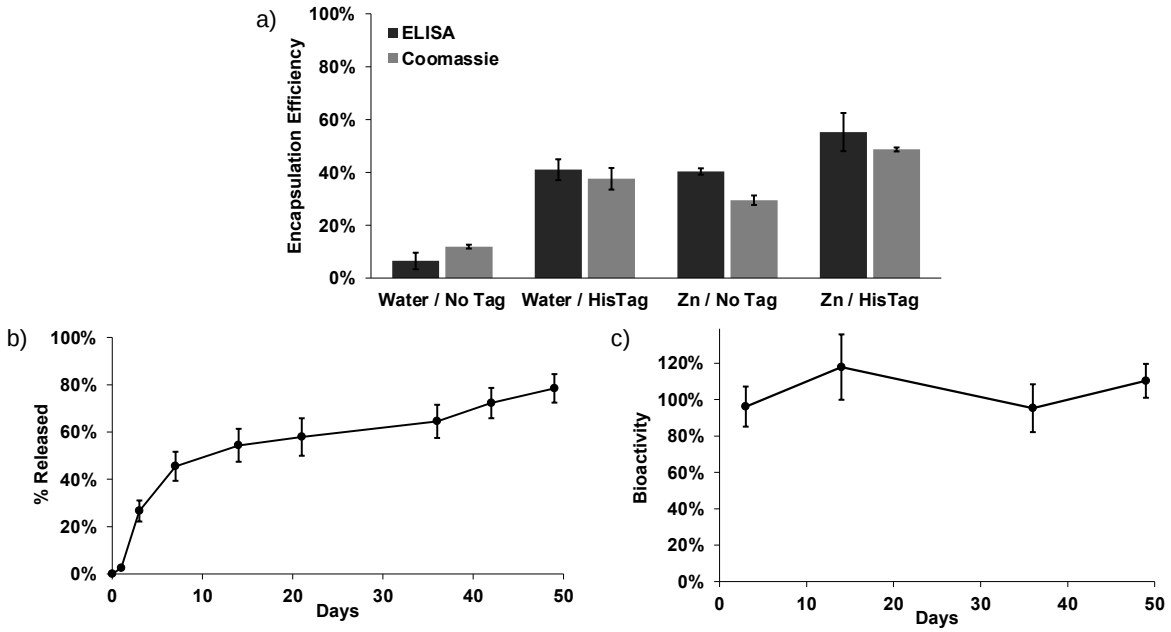

Figure 2-3*. HisTag GM-CSF is efficiently encapsulated in Zn^{2+}-immobilized PLGA microspheres by remote loading and slowly released while maintaining bioactivity. a) Active and total available protein encapsulation efficiency of NoTag and HisTag GM-CSF into Zn^{2+}-free and Zn^{2+}-immobilized PLGA microspheres from 50 μg/mL protein loading solution. b) Release of immunoreactive HisTag GM-CSF from Zn^{2+}-immobilized PLGA microspheres in 0.1 M HEPES + 1% BSA, pH 7.4 at 37 °C. c) Bioactivity of released GM-CSF relative to immunoreactive protein. Five μg protein and 1 mg of microspheres in 100 μL loading solution was used for self-healing encapsulation. Zn / HisTag EE_{avail} by ELISA and total protein assay significantly greater than each control; $p < 0.05$.*

2.4.4. IGF-1 Encapsulation and Release

While promising for GM-CSF, we further tested our approach with a second protein, insulin-like growth factor-1 (IGF-1), which also has local delivery utility,[47-51] at the higher 50 μg/mL level. As expected, the HisTag IGF-1 was loaded in the self-healing Zn^{2+}/HDS/PLGA microspheres at about 80% efficiency, as measured by ELISA (**Figure 2-4a**). All other controls displayed encapsulation efficiencies of ~20% or less. Here, 59 ± 13% of the protein in the control loading solution remained immunoreactive after incubation at loading conditions. Release of the protein was again continuous and nearly complete over 56 days, although with a larger burst release than for GM-CSF (**Figure 2-4b**).

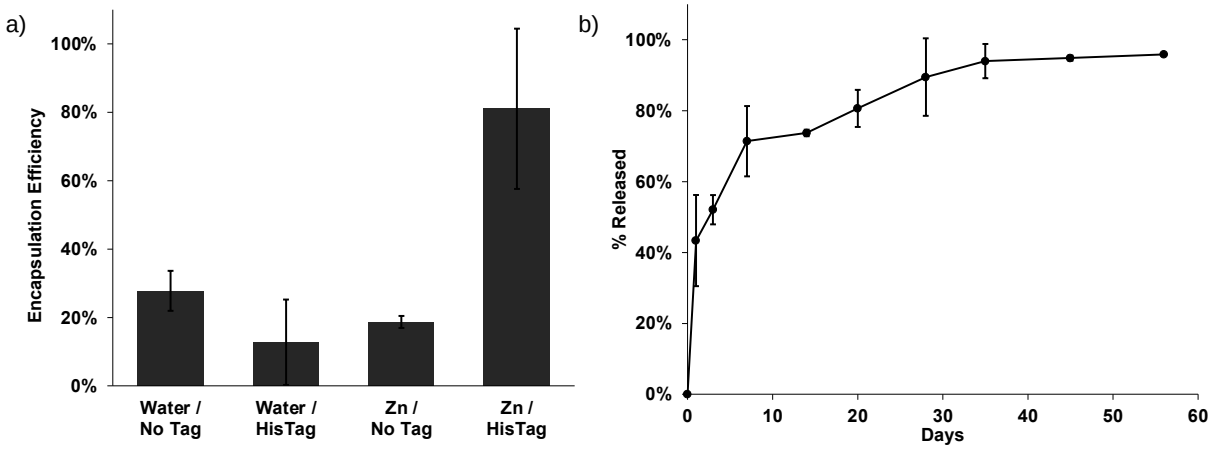

Figure 2-4*. HisTag IGF-1 is efficiently encapsulated in Zn^{2+}-immobilized PLGA microspheres by remote loading and slowly released. a) Active available encapsulation efficiency of NoTag and HisTag IGF-1 into Zn^{2+}-free and Zn^{2+}-immobilized PLGA microspheres from 50μg/mL protein loading solution. b) Release of immunoreactive HisTag IGF-1 from Zn^{2+}-immobilized PLGA microspheres in 1 mL PBS + 0.02% Tween 80 + 1% BSA, pH 7.4 at 37 °C. Zn / HisTag EE_{avail} by ELISA significantly greater than each control; $p < 0.05$.*

2.4.5. Effect of divalent metal cation on remote loading

To examine the effect of the divalent cation on our approach, self-healing HDS/PLGA microspheres were exposed to acetate salts of transition metals (Co^{2+}, Cu^{2+}, Ni^{2+}, and Zn^{2+}), an alkaline earth metal (Ca^{2+}), or no salt control. Compared to the no salt control, HisTag IGF-1 was encapsulated with higher efficiency in the microspheres exposed to divalent transition metals. Accounting for the amount of metal loaded into the microspheres (**Figure S2-9**) and the

amount of protein encapsulated in the metal-free microspheres, the encapsulated protein above control per mole of metal ion followed $Cu^{2+} > Zn^{2+} > Ni^{2+} \approx Co^{2+} >>> Ca^{2+}$, as expected by the relative affinity of these cations for HisTag (**Figure 2-5**).[34] Microspheres exposed to Ca^{2+} showed no substantial difference in encapsulation efficiency as compared to the no salt control, as Ca^{2+} is known to possess much less affinity than transition metals for HisTags. Hence, these data further strongly support the HisTag-to-transition metal binding occurring during loading of the HisTag protein before self-healing encapsulation.

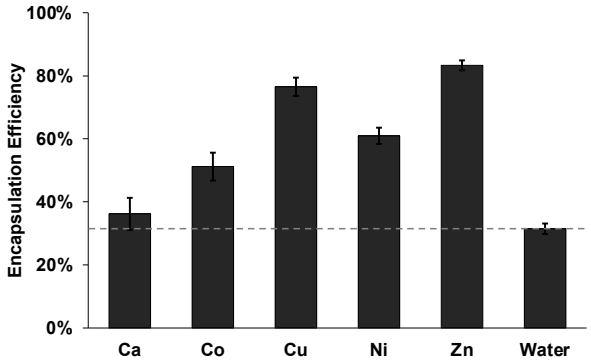

Figure 2-5*. The immobilization of divalent transition metals improves the total protein encapsulation efficiency of HisTag IGF-1 into PLGA microspheres. Encapsulation efficiency of HisTag IGF-1 into Ca^{2+}-, Co^{2+}-, Cu^{2+}-, Ni^{2+}-, and Zn^{2+}-immobilized, and M^{2+}-free PLGA microspheres. Ca^{2+} EE_{avail} by total protein assay not significantly greater than water control; $p > 0.05$. All transition metal EE_{avail} by total protein assay significantly greater than water and Ca^{2+} controls; $p < 0.05$.*

2.4.6. Encapsulation and Release of HSA

We then applied a third protein, human serum albumin (HSA), as a model protein to examine various phenomena at lower cost and to further support the generality of the approach. As shown in **Figure 2-6a**, again the HisTag HSA bound preferentially to the Zn^{2+}/HDS/PLGA microspheres, with an encapsulation efficiency of >95%. Controls without HisTag, without Zn^{2+}, and without HisTag and Zn^{2+} were higher for HSA than for the previously studied proteins, but nonetheless all below ~41% as measured by ELISA. Here, 70 ± 1% of the protein in the control loading solution remained immunoreactive after incubation at loading conditions. HisTag HSA release from the standard formulation was complete, and slow and continuous after a modest initial burst by ELISA (**Figure 2-6b**).

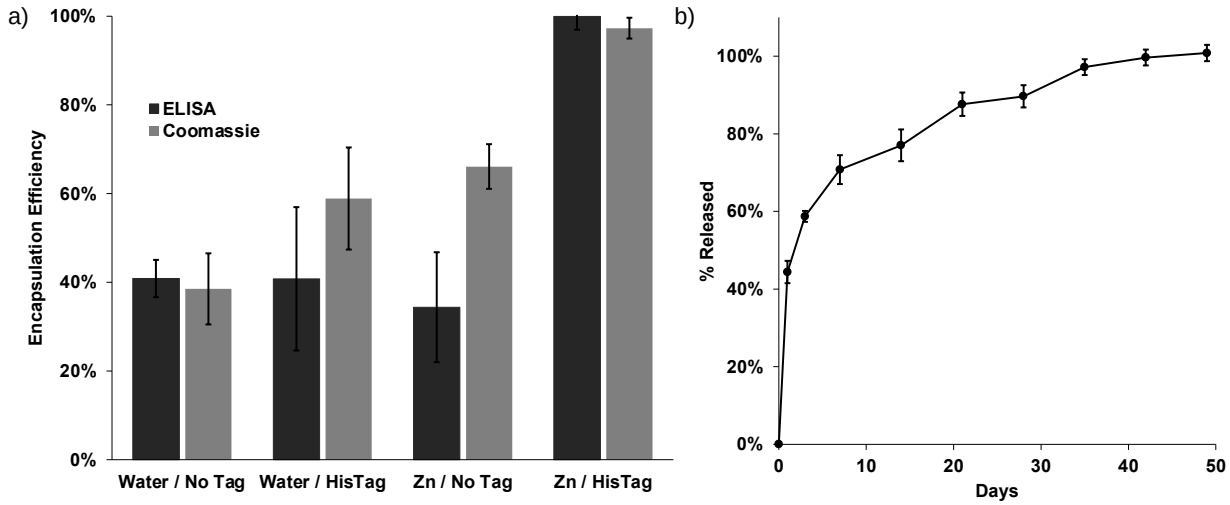

***Figure 2-6**. HisTag HSA is efficiently encapsulated in Zn-immobilized PLGA microspheres by remote loading and slowly released. a) Active and total protein encapsulation efficiency of NoTag and HisTag HSA into Zn^{2+}-free and Zn^{2+}-immobilized PLGA microspheres from 50µg/mL protein loading solution. b) Release of immunoreactive HisTag HSA from Zn^{2+}-immobilized PLGA microspheres in 1 mL PBS + 0.02% Tween 80 + 1% casein, pH 7.4 at 37 °C. Zn / HisTag EE_{avail} by ELISA and total protein assay significantly greater than each control; $p < 0.05$.*

2.4.7. EDTA blockade of HSA Encapsulation

To further probe the Zn^{2+}-HisTag coordination, we tested whether EDTA, a strong chelating agent often used to elute HisTag proteins of IMAC columns, interfered with the encapsulation of HisTag proteins. To do this, after exposing HDS/PLGA microspheres to Zn^{2+} but before exposing the microspheres to HisTag HSA, we exposed the microspheres to EDTA. The EDTA/Zn^{2+}/HDS/PLGA microspheres showed nearly the same encapsulation efficiency as microspheres that had been exposed to neither Zn^{2+} nor EDTA, and far lower efficiency than the standard formulation (**Figure 2-7**). These data again support the HisTag-to-transition metal binding and are consistent with EDTA entirely inhibiting the coordination.

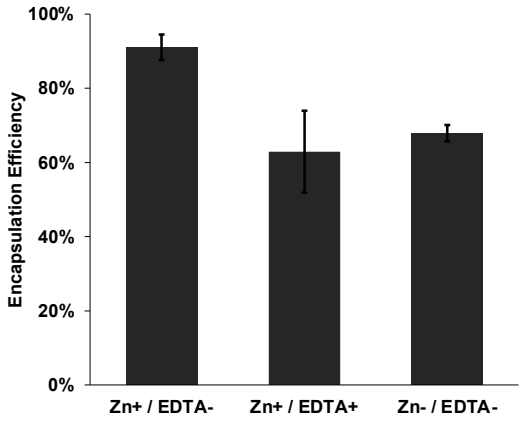

Figure 2-7*. EDTA interferes with the ability of Zn-immobilized PLGA microspheres to efficiently encapsulate HisTag HSA. Encapsulation efficiency of HisTag HSA into Zn^{2+}-immobilized PLGA microspheres without and with incubation with EDTA and into Zn^{2+}-free PLGA microspheres without incubation with EDTA from 50μg/mL loading solution as determined by mass loss from loading solution compared to control loading solution, measured by Coomassie assay. Zn+/EDTA- EE_{avail} by total protein assay significantly greater than other treatments; $p < 0.05$.*

2.4.8. Protein stability considerations

As previously discussed, the stability of proteins is a major obstacle in controlled release formulations. Our data strongly support the stable, immunoreactive, and bioactive encapsulation and release of a wide variety of HisTag proteins via Zn^{2+}/HDS/PLGA microspheres. This formulation evolved from multiple improvements in protein stabilization during encapsulation and release. The poorly soluble base, $MgCO_3$, has been shown capable of helping to obviate pH-induced protein damage from aliphatic ester-capped PLGA 50/50 under specific formulation conditions.[52] The common damage to protein during organic solvent exposure and excess mixing was averted by making use of passive polymer healing to allow encapsulation under aqueous conditions with gentle agitation.[22] Finally, when combining a protein-binding excipient that largely remains in the polymer during loading such as HDS, we found that both high efficiency loading of protein drugs and further stabilization during release was observed.[18]

While this encapsulation method avoids many of the harsh stressors of direct double emulsion and solvent evaporation encapsulation, it is not free of potential damage to the protein. The relatively high pH (8) of the loading solution buffer needed to optimize the interaction

between the metal cations and the HisTag proteins can be deleterious to proteins, particularly at elevated temperature.[53,54] The slightly high temperature (43 °C) used to heal the microspheres can cause unfolding and/or aggregation of some proteins. Indeed, we did see decreases in immunoreactivity of proteins after exposure to loading conditions (**Table 2-1**).

2.5. Conclusion

During biologic drug discovery and early development, the slow and continuous release of immunoreactive and bioactive protein is crucial so that protein candidates can be studied *in vivo* in hard-to-reach areas like the brain, eye, and joints, where repeated injection may not be feasible, or in tissue engineering applications where local growth factor support is also desired.[55] Aside from PLGA formulations, osmotic pumps are another option, but these can be cumbersome and difficult to apply in certain cases.[39] For traditional PLGA formulations, though, depending on the desired protein loading, typically more than 1-100 mg of protein is often used (with the lower level often accompanying a second bulk protein excipient such as albumin[38,52]) to formulate microspheres using traditional direct encapsulation batch methods depending on the target loading, and there is no specific binding mechanism used to help stabilize the protein. For these reasons, studying candidates in the proper formulation and pharmacokinetic settings is difficult, leading to costly failures or missed opportunities.[56,57] Using the method described here, immunoreactive and bioactive protein can be encapsulated and slowly released using just 1-5 μg of protein (in a 100 μL loading solution and 1 mg of microspheres). Others have developed micro- and nanoparticle encapsulation methods for biologics that require very small quantities of drug, for example with poly(ethylene-co-vinyl acetate),[58] or with PLGA.[38,52] However, these methods require organic solvent, are not generalizable, and require specialized equipment and training to perform encapsulation. It is noted that the current goal here is to develop a more universal formulation for simple and low-cost remote loading of proteins in the drug discovery

phase and not to identify a final formulation for development. This represents a drug delivery solution to a drug discovery problem, with the aim of improving translation from discovery to pre-clinical studies and, eventually, to the clinic.

2.6. References

1. Lowe D. Rise of the biologics. *Medchemcomm*. Jan 2018;9(1):10-11. doi:10.1039/c7md90046e
2. Midlam C. Status of Biologic Drugs in Modern Therapeutics-Targeted Therapies vs. Small Molecule Drugs. In: Ramzan I, ed. *Biologics, Biosimilars, and Biobetters: An Introductions for Pharmacists, Physicians, and Other Health Practictioners*. John Wiley & Sons, Inc.; 2021:chap 3.
3. Qi F, Wu J, Li H, Ma G. Recent research and development of PLGA/PLA microspheres/nanoparticles: A review in scientific and industrial aspects.
4. Torres-Ortega PV, Saludas L, Hanafy AS, Garbayo E, Blanco-Prieto MJ. Micro- and nanotechnology approaches to improve Parkinson's disease therapy. *J Control Release*. 02 2019;295:201-213. doi:10.1016/j.jconrel.2018.12.036
5. Panagiotou T, Fisher RJ. Enhanced Transport Capabilities via Nanotechnologies: Impacting Bioefficacy, Controlled Release Strategies, and Novel Chaperones. *J Drug Deliv*. 2011;2011:902403. doi:10.1155/2011/902403
6. Zeng Y, Hoque J, Varghese S. Biomaterial-assisted local and systemic delivery of bioactive agents for bone repair. *Acta Biomater*. 07 2019;93:152-168. doi:10.1016/j.actbio.2019.01.060
7. Chen H, Sun T, Yan Y, et al. Cartilage matrix-inspired biomimetic superlubricated nanospheres for treatment of osteoarthritis. *Biomaterials*. Feb 2020;242:119931. doi:10.1016/j.biomaterials.2020.119931
8. Honda M, Asai T, Oku N, Araki Y, Tanaka M, Ebihara N. Liposomes and nanotechnology in drug development: focus on ocular targets. *Int J Nanomedicine*. 2013;8:495-503. doi:10.2147/IJN.S30725
9. Chen M, Li X, Liu J, Han Y, Cheng L. Safety and pharmacodynamics of suprachoroidal injection of triamcinolone acetonide as a controlled ocular drug release model. *J Control Release*. Apr 2015;203:109-17. doi:10.1016/j.jconrel.2015.02.021
10. Strohl WR, Knight DM. Discovery and development of biopharmaceuticals: current issues. *Curr Opin Biotechnol*. Dec 2009;20(6):668-72. doi:10.1016/j.copbio.2009.10.012
11. Tomic I, Vidis-Millward A, Mueller-Zsigmondy M, Cardot JM. Setting accelerated dissolution test for PLGA microspheres containing peptide, investigation of critical parameters affecting drug release rate and mechanism. *Int J Pharm*. May 2016;505(1-2):42-51. doi:10.1016/j.ijpharm.2016.03.048
12. Jiang W, Gupta RK, Deshpande MC, Schwendeman SP. Biodegradable poly(lactic-co-glycolic acid) microparticles for injectable delivery of vaccine antigens. *Adv Drug Deliv Rev*. Jan 2005;57(3):391-410. doi:10.1016/j.addr.2004.09.003
13. Alonso MJ, Gupta RK, Min C, Siber GR, Langer R. Biodegradable microspheres as controlled-release tetanus toxoid delivery systems. *Vaccine*. Mar 1994;12(4):299-306. doi:10.1016/0264-410x(94)90092-2

14. Aguado MT, Lambert PH. Controlled-release vaccines--biodegradable polylactide/polyglycolide (PL/PG) microspheres as antigen vehicles. *Immunobiology*. Feb 1992;184(2-3):113-25. doi:10.1016/S0171-2985(11)80470-5
15. Waeckerle-Men Y, Gander B, Groettrup M. Delivery of tumor antigens to dendritic cells using biodegradable microspheres. *Methods Mol Med*. 2005;109:35-46. doi:10.1385/1-59259-862-5:035
16. Han FY, Thurecht KJ, Whittaker AK, Smith MT. Bioerodable PLGA-Based Microparticles for Producing Sustained-Release Drug Formulations and Strategies for Improving Drug Loading. *Front Pharmacol*. 2016;7:185. doi:10.3389/fphar.2016.00185
17. Park K, Skidmore S, Hadar J, et al. Injectable, long-acting PLGA formulations: Analyzing PLGA and understanding microparticle formation. *J Control Release*. 06 2019;304:125-134. doi:10.1016/j.jconrel.2019.05.003
18. Shah RB, Schwendeman SP. A biomimetic approach to active self-microencapsulation of proteins in PLGA. *J Control Release*. Dec 2014;196:60-70. doi:10.1016/j.jconrel.2014.08.029
19. Wu F, Jin T. Polymer-based sustained-release dosage forms for protein drugs, challenges, and recent advances. *AAPS PharmSciTech*. 2008;9(4):1218-29. doi:10.1208/s12249-008-9148-3
20. Schwendeman SP. Recent advances in the stabilization of proteins encapsulated in injectable PLGA delivery systems. *Crit Rev Ther Drug Carrier Syst*. 2002;19(1):73-98. doi:10.1615/critrevtherdrugcarriersyst.v19.i1.20
21. van de Weert M, Hoechstetter J, Hennink WE, Crommelin DJ. The effect of a water/organic solvent interface on the structural stability of lysozyme. *J Control Release*. Sep 2000;68(3):351-9. doi:10.1016/s0168-3659(00)00277-7
22. Reinhold SE, Desai KG, Zhang L, Olsen KF, Schwendeman SP. Self-healing microencapsulation of biomacromolecules without organic solvents. *Angew Chem Int Ed Engl*. Oct 2012;51(43):10800-3. doi:10.1002/anie.201206387
23. Cohen S, Bernstein H. *Microparticulate systems for the delivery of proteins and vaccines*. Drugs and the pharmaceutical sciences,. Marcel Dekker; 1996:ix, 525 p.
24. Ando S, Putnam D, Pack DW, Langer R. PLGA microspheres containing plasmid DNA: preservation of supercoiled DNA via cryopreparation and carbohydrate stabilization. *J Pharm Sci*. Jan 1999;88(1):126-30. doi:10.1021/js9801687
25. Giovagnoli S, Blasi P, Ricci M, Rossi C. Biodegradable microspheres as carriers for native superoxide dismutase and catalase delivery. *AAPS PharmSciTech*. Oct 2004;5(4):e51. doi:10.1208/pt050451
26. Mazzara JM, Balagna MA, Thouless MD, Schwendeman SP. Healing kinetics of microneedle-formed pores in PLGA films. *J Control Release*. Oct 2013;171(2):172-7. doi:10.1016/j.jconrel.2013.06.035
27. Huang J, Mazzara JM, Schwendeman SP, Thouless MD. Self-healing of pores in PLGAs. *J Control Release*. May 2015;206:20-9. doi:10.1016/j.jconrel.2015.02.025
28. Desai KG, Schwendeman SP. Active self-healing encapsulation of vaccine antigens in PLGA microspheres. *J Control Release*. Jan 2013;165(1):62-74. doi:10.1016/j.jconrel.2012.10.012
29. Giles M. *Aqueous Remote Loading of Peptides in PLGA Microspheres*. University of Michigan; 2017. hdl.handle.net/2027.42/144200

30. Reinhold SE, Schwendeman SP. Effect of polymer porosity on aqueous self-healing encapsulation of proteins in PLGA microspheres. *Macromol Biosci*. Dec 2013;13(12):1700-10. doi:10.1002/mabi.201300323
31. Bailey BA, Desai KH, Ochyl LJ, Ciotti SM, Moon JJ, Schwendeman SP. Self-encapsulating Poly(lactic-co-glycolic acid) (PLGA) Microspheres for Intranasal Vaccine Delivery. *Mol Pharm*. 09 2017;14(9):3228-3237. doi:10.1021/acs.molpharmaceut.7b00586
32. Bailey BA, Ochyl LJ, Schwendeman SP, Moon JJ. Toward a Single-Dose Vaccination Strategy with Self-Encapsulating PLGA Microspheres. *Adv Healthc Mater*. Jun 2017;6(12)doi:10.1002/adhm.201601418
33. Mazzara JM, Ochyl LJ, Hong JKY, Moon JJ, Prausnitz MR, Schwendeman SP. Self-healing encapsulation and controlled release of vaccine antigens from PLGA microparticles delivered by microneedle patches. *Bioeng Transl Med*. Jan 2019;4(1):116-128. doi:10.1002/btm2.10103
34. Porath J, Carlsson J, Olsson I, Belfrage G. Metal chelate affinity chromatography, a new approach to protein fractionation. *Nature*. Dec 1975;258(5536):598-9. doi:10.1038/258598a0
35. Liao SM, Du QS, Meng JZ, Pang ZW, Huang RB. The multiple roles of histidine in protein interactions. *Chem Cent J*. Mar 2013;7(1):44. doi:10.1186/1752-153X-7-44
36. Block H, Maertens B, Spriestersbach A, et al. Immobilized-metal affinity chromatography (IMAC): a review. *Methods Enzymol*. 2009;463:439-73. doi:10.1016/S0076-6879(09)63027-5
37. Giacometti J, Josic D. Protein and Peptide Separations. *Liquid Chromatography: Applications*. Elsevier Inc.; 2013:149-175:chap 3.
38. Zhong Y, Zhang L, Ding AG, et al. Rescue of SCID murine ischemic hindlimbs with pH-modified rhbFGF/poly(DL-lactic-co-glycolic acid) implants. *J Control Release*. Oct 2007;122(3):331-7. doi:10.1016/j.jconrel.2007.05.016
39. Tan T, Watts SW, Davis RP. Drug Delivery: Enabling Technology for Drug Discovery and Development. iPRECIO Micro Infusion Pump: Programmable, Refillable, and Implantable. *Front Pharmacol*. 2011;2:44. doi:10.3389/fphar.2011.00044
40. Kwong E, Higgins J, Templeton AC. Strategies for bringing drug delivery tools into discovery. *Int J Pharm*. Jun 2011;412(1-2):1-7. doi:10.1016/j.ijpharm.2011.03.024
41. Feng Y, Zhang J, Miao Y, et al. Prevention of Zinc Precipitation with Calcium Phosphate by Casein Hydrolysate Improves Zinc Absorption in Mouse Small Intestine ex Vivo via a Nanoparticle-Mediated Mechanism. *Journal of Agricultural and Food Chemistry*. 2020-01-15 2020;68(2):652-659. doi:10.1021/acs.jafc.9b07097
42. Schwendeman SP, Shah RB, Bailey BA, Schwendeman AS. Injectable controlled release depots for large molecules. *Journal of Controlled Release*. 2014-09-01 2014;190:240-253. doi:10.1016/j.jconrel.2014.05.057
43. Reali E, Canter D, Zeytin H, Schlom J, Greiner JW. Comparative studies of Avipox-GM-CSF versus recombinant GM-CSF protein as immune adjuvants with different vaccine platforms. *Vaccine*. Apr 22 2005;23(22):2909-21. doi:10.1016/j.vaccine.2004.11.060
44. Choi KJ, Kim JH, Lee YS, et al. Concurrent delivery of GM-CSF and B7-1 using an oncolytic adenovirus elicits potent antitumor effect. *Gene Ther*. Jul 2006;13(13):1010-20. doi:10.1038/sj.gt.3302759

45. Steinwede K, Tempelhof O, Bolte K, et al. Local Delivery of GM-CSF Protects Mice from Lethal Pneumococcal Pneumonia. *The Journal of Immunology*. 2011-11-15 2011;187(10):5346-5356. doi:10.4049/jimmunol.1101413
46. Steinitz M. Quantitation of the Blocking Effect of Tween 20 and Bovine Serum Albumin in ELISA Microwells. *Analytical Biochemistry*. 2000-07-01 2000;282(2):232-238. doi:10.1006/abio.2000.4602
47. Pan S, Qi Z, Li Q, et al. Graphene oxide-PLGA hybrid nanofibres for the local delivery of IGF-1 and BDNF in spinal cord repair. *Artificial Cells, Nanomedicine, and Biotechnology*. 2019-12-04 2019;47(1):650-663. doi:10.1080/21691401.2019.1575843
48. Tokunou T, Miller R, Patwari P, et al. Engineering insulin-like growth factor-1 for local delivery. *The FASEB Journal*. 2008-06-01 2008;22(6):1886-1893. doi:10.1096/fj.07-100925
49. Park J, Yan G, Kwon KC, et al. Oral delivery of novel human IGF-1 bioencapsulated in lettuce cells promotes musculoskeletal cell proliferation, differentiation and diabetic fracture healing. *Biomaterials*. 03 2020;233:119591. doi:10.1016/j.biomaterials.2019.119591
50. Davis ME, Hsieh PCH, Takahashi T, et al. Local myocardial insulin-like growth factor 1 (IGF-1) delivery with biotinylated peptide nanofibers improves cell therapy for myocardial infarction. *Proceedings of the National Academy of Sciences*. 2006-05-23 2006;103(21):8155-8160. doi:10.1073/pnas.0602877103
51. Zhang X, Xing H, Qi F, Liu H, Gao L, Wang X. Local delivery of insulin/IGF-1 for bone regeneration: carriers, strategies, and effects. *Nanotheranostics*. 2020;4(4):242-255. doi:10.7150/ntno.46408
52. Zhu G, Mallery SR, Schwendeman SP. Stabilization of proteins encapsulated in injectable poly (lactide- co-glycolide). *Nature Biotechnology*. 2000-01-01 2000;18(1):52-57. doi:10.1038/71916
53. Schmitt J, Hess H, Stunnenberg HG. Affinity purification of histidine-tagged proteins. *Molecular Biology Reports*. 1993-10-01 1993;18(3):223-230. doi:10.1007/bf01674434
54. Chi EY, Krishnan S, Randolph TW, Carpenter JF. Physical stability of proteins in aqueous solution: mechanism and driving forces in nonnative protein aggregation. *Pharm Res*. Sep 2003;20(9):1325-36. doi:10.1023/a:1025771421906
55. Mooney DJ, Kaufmann PM, Sano K, et al. Localized delivery of epidermal growth factor improves the survival of transplanted hepatocytes. *Biotechnol Bioeng*. May 1996;50(4):422-9. doi:10.1002/(SICI)1097-0290(19960520)50:4<422::AID-BIT9>3.0.CO;2-N
56. Neervannan S. Preclinical formulations for discovery and toxicology: physicochemical challenges. *Expert Opin Drug Metab Toxicol*. Oct 2006;2(5):715-31. doi:10.1517/17425255.2.5.715
57. Rosen H, Abribat T. The rise and rise of drug delivery. *Nature Reviews Drug Discovery*. 2005-05-01 2005;4(5):381-385. doi:10.1038/nrd1721
58. Murray J, Brown L, Langer R. Controlled release of microquantities of macromolecules. *Cancer Drug Deliv*. 1984;1(2):119-23. doi:10.1089/cdd.1984.1.119

2.7. Supplementary Information

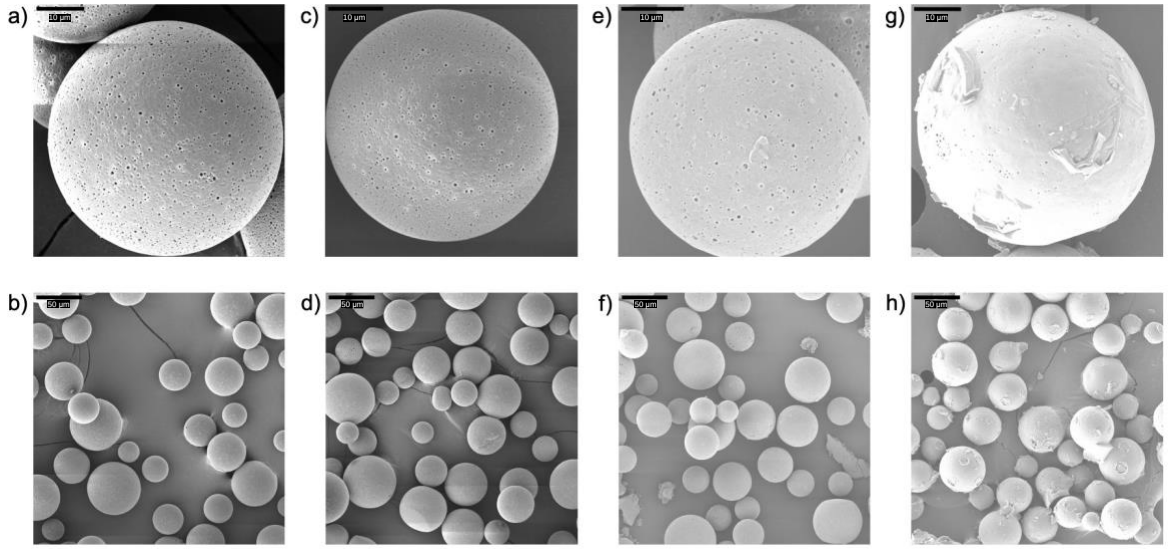

***Figure S2-8**. A porous network is created, maintained, and healed. a,b) Scanning electron micrographs of PLGA microspheres prepared as described. c,d) Scanning electron micrographs of PLGA microspheres prepared without the inclusion of trehalose in the inner-water phase. e,f) Scanning electron micrographs of PLGA microspheres following incubation at room temperature for 48 h rotating at 30 rpm. g,h) Scanning electron micrographs of PLGA microspheres following incubation at room temperature for 48 h rotating at 30 rpm and at 43 °C for 42 h rotating at 30 rpm.*

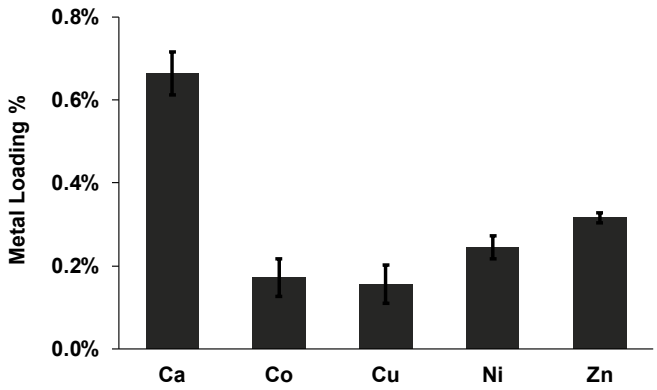

***Figure S2-9**. Divalent metal cations are remotely loaded into PLGA microspheres via simple mixing. Weight-by-weight loading as measured by ICP.*

Chapter 3: Optimizing Zinc-HisTag Coordination Remote Loading of Proteins in PLGA Microspheres

3.1. Abstract

Metal-HisTag coordination remote loading (MHCRL) of HisTag proteins in PLGA microspheres was previously developed to help overcome challenges to discovery and preclinical development of controlled release formulations. While proof-of-concept MHCRL was promising, several areas of potential improvement have been identified, including (1) reducing thermal stress on the proteins, (2) decreasing the complexity and duration of the procedure, (3) increasing the loading capacity, (4) increasing the penetration depth of protein, and (5) improving the release profile. Directly encapsulating $ZnCO_3$ to provide a source of Zn^{2+} for HisTag coordination, rather than remotely loading Zn^{2+} and binding the cation with dextran sulfate, increased the Zn content in the microspheres ~6-fold. Microspheres with directly encapsulated $ZnCO_3$ ($_{DE}ZnCO_3$) more efficiently encapsulated HSA at protein loading solutions concentrations $\geq$ 100 μg/mL than remotely loaded Zn^{2+} microspheres ($_{RL}Zn^{2+}$). HisTag green fluorescent protein was more deeply encapsulated in $_{DE}ZnCO_3$ microspheres than in $_{RL}Zn^{2+}$ microspheres. To reduce the loading and healing temperatures, tributyl acetylcitrate was included in the PLGA matrix and was found to be an effective plasticizer in terms of decreasing the glass transition temperature, but also led to a decrease in protein encapsulation efficiency. With or without plasticizer, the loading stage was reducible to 2 hours at 4°C and the healing stage to 6 hours at 37°C while maintaining strong encapsulation efficiency for $_{DE}ZnCO_3$ microspheres, potentially owed to the use of shorter and higher solubility PLGA chains compared to those used

in previous, non-MHCRL, studies. This resulted in significant improvements in protein stability. Immunoreactive protein was slowly released for months following a modest burst release, showing improved release kinetics as compared to previous MHCRL formulations. Plasticization was found to decrease the initial burst release. The improved remote loading microspheres and shorter, low-temperature encapsulation procedure developed here could be a valuable asset to drug discovery scientists who seek to study the controlled release of a delicate and/or costly biologic candidate.

3.2. Introduction

Metal-HisTag coordination remote loading (MHCRL) was developed in order to provide a universal remote loading platform that requires very small quantities of protein.[1] Proteins and other biologics have allowed us to treat previously untreated or undertreated diseases. Due to poor bioavailability by non-invasive routes, though, these game-changing drug products must most often be injected, which is inconvenient for patients and leads to poor patient compliance.[2] To reduce the frequency of injection, controlled release formulations have been developed, with poly(lactic-co-glycolic acid) (PLGA) being an industry standard due to its versatility, biodegradability, strong safety profile, and tunable performance. PLGA has been used to encapsulate and slowly release a wide variety of therapeutics, including peptides, proteins, antibodies, vaccine antigens, and nucleic acids in formulations including nanospheres, microspheres, implants, and thin films.[3-10]

One challenge of encapsulating biologics within PLGA microspheres is the harsh conditions of directly encapsulating the molecule, which lead to instability and aggregation of proteins.[11] This process can expose the molecule to stressors including micronization, organic/aqueous interfaces, air/water interfaces, high shear stress, organic solvents, and high temperatures.[8,12-18] Another issue that is particularly challenging during drug discovery and early

development is that the standard batch formulation process requires large amounts of the drug molecule, which can be cost-prohibitive or simply infeasible at these stages.[19,20]

To avoid these stressors and reduce the mass of protein required during formulation, aqueous remote loading and self-healing encapsulation has been developed with our group being pioneers in the space.[11,13,21-23] Here, briefly, porous and drug-free microspheres are produced and then exposed to an aqueous solution containing a biomacromolecule of interest, which loads into the microspheres and becomes encapsulated after modest heating, which closes the pores of the microspheres. One shortcoming, however, of current remote loading preformed microsphere formulations is that they rely on an inherent property of the protein of interest (i.e., charge or binding affinity for a particular moiety) and, thus, are not universally applicable to any recombinant protein.[11]

MHCRL was developed to create a more universally applicable remote loading approach to easily encapsulate and control the release of small quantities of proteins in PLGA. In previous work, porous, drug-free self-healing PLGA microspheres with high molecular weight dextran sulfate (HDS) and remotely loaded and immobilized divalent transition metal ions were placed in the presence of proteins with or without HisTags to bind the protein in the pores of the polymer before healing the surface pores.[1] This mechanism relies on the coordination bond formed between histidine and divalent transition metal cations above pH 6. This same mechanism is used in immobilized metal affinity chromatography, a commonly utilized method of isolating and purifying recombinant proteins.[24-27] It was shown that MHCRL was able to efficiently microencapsulate micrograms of multiple HisTag proteins and slowly release them while minimizing losses of protein immunoreactivity and/or bioactivity over weeks-to-months.

Here, we aim to build on and improve this work. Specifically, we identified five areas of focus to improve the platform and make it more applicable for its intended purpose of preclinical drug discovery and development: (1) reduce the thermal stress on the proteins, (2) decrease the complexity and duration of the protocol, (3) increase the protein loading capacity of the microspheres, (4) increase the penetration depth of the encapsulated protein, and (5) improve the release profile of the encapsulation protein. In this effort, $ZnCO_3$ was introduced as an excipient to help control the acidity of the microclimate within PLGA delivery systems in addition to serving as a porosigen.[28-30] Aside from these functions, $ZnCO_3$ can provide a reservoir of Zn^{2+} ions for HisTags to bind. Other excipients introduced to meet these goals include two plasticizers, tributyl acetylcitrate (TBAC) and triethyl citrate (TEC). These agents were introduced in the preformed microspheres to increase the polymer chain mobility, decreasing the T_g of the polymer phase, which would allow for faster healing of microspheres at lower temperatures. TBAC has been used to plasticize PLGA microspheres previously[31,32] and has been shown to have a very favorable toxicity profile.[33,34] Meanwhile, TEC has also been used in the release medium of PLGA microspheres to increase polymer permeability[35] and is used as a food and cosmetic additive.

3.3. Experimental Methods

3.3.1. Materials

Resomer RG 504 PLGA (50:50, ester-terminated, molecular weight 38,000-54,000 Da), magnesium carbonate, trehalose, 88% hydrolyzed poly(vinyl alcohol) (PVA), and high molecular weight (>500,000 Da) dextran sulfate (HDS) were purchased from Sigma Aldrich. Zinc acetate and zinc carbonate basic were purchased from Sigma Aldrich. Poly-histidine tagged (HisTag) Human Serum Albumin (HSA) was purchased from Arco Biosystems and untagged (NoTag) HSA was purchased from Raybiotech. HisTag insulin-like growth factor 1 (IGF-1) was

purchased from Signalway Antibodies and NoTag IGF-1 was purchased from Sino Biological. HisTag green fluorescent protein (GFP) was purchased from Sino Biological. All HisTag proteins contained tags of six histidine residues. Tags were at the N-terminus for GFP and IGF-1, whereas the Tag for HSA was at the C-terminus. Bovine serum albumin (BSA) was purchased from Sigma Aldrich and blocker casein in PBS was purchased from ThermoFisher. Tributyl acetylcitrate (TBAC) and triethyl citrate (TEC) were purchased from Sigma Aldrich. All other common reagents and solvents were purchased from Sigma Aldrich, except where otherwise specified.

3.3.2. Preparation of MHCRL PLGA microspheres

3.3.2.1. Remotely loaded Zn^{2+} in HDS/$MgCO_3$ microspheres

Porous PLGA microspheres with HDS as a metal immobilizer, $MgCO_3$ as a pH-modulator and porosigen,[28-30] and trehalose as a porosigen were prepared by double water-oil-water (w/o/w) emulsion and solvent evaporation. The first emulsion was created by homogenizing a suspension of 1 mL of 250 mg/mL dissolved PLGA and 6% w/w fine particulate $MgCO_3$ in methylene chloride (continuous phase) with an inner water phase (disperse phase) of 200 μL of 4% w/v HDS and 3% w/v trehalose in a glass cell culture tube at 18,000 rpm for 60 s over an ice bath, using a Tempest IQ^2. The second emulsion was created by adding 2 mL of 5% PVA to the primary emulsion and vortexing for 60 s. The w/o/w double emulsion was added to 100 mL of 0.5% PVA and stirred for 3 h at room temperature in a 150 mL beaker to allow for hardening and evaporation of methylene chloride. The 20-63 μm fraction of microspheres was collected using sieves and the microspheres were washed with excess double-distilled water and lyophilized. For future HisTag coordination, Zn^{2+} was then remotely loaded into the HDS/PLGA microspheres by incubating the microspheres in at least 1 mL of 500 mM zinc acetate salt solution (or water as a control) per 1 mg of microspheres for 24 h rotating at 30 rpm at room

temperature. Microspheres were washed extensively with double-distilled water under vacuum on a 0.2 μm nylon filter and lyophilized. Microspheres that were incubated in water, rather than 500 mM zinc acetate, are referred to as Zn^{2+}-free HDS/PLGA. The remotely loaded Zn^{2+} microspheres thus prepared are referred to $_{RL}Zn^{2+}$ microspheres. The $_{DE}ZnCO_3$ microspheres described below did not undergo this procedure.

3.3.2.2. Inclusion of plasticizers

To create 2.5% or 5% w/w TBAC- or TEC-plasticized microspheres, 6.5 μL or 13.4 μL TBAC, respectively, was added to the 250 mg PLGA in 1 mL methylene chloride continuous phase before emulsification. To create 2.5% or 5% w/w TEC-plasticized microspheres, 6 μL or 12.3 μL TEC, respectively, was added to the 250 mg PLGA in 1 mL methylene chloride continuous phase before emulsification.

3.3.2.3. Direct encapsulation of $ZnCO_3$ in place of remote Zn^{2+} loading and $MgCO_3$

To create direct encapsulation $ZnCO_3$ HDS/PLGA microspheres ($_{DE}ZnCO_3$ microspheres), $ZnCO_3$ replaced $MgCO_3$ in the 250 mg PLGA in 1 mL methylene chloride continuous phase before emulsification. These microspheres were not remotely loaded with Zn^{2+} from zinc acetate as described above.

3.3.3. Determination of dry and hydrated T_g with differential scanning calorimetry

Thermographs were collected with the TA Instruments (USA) nano series differential scanning calorimeter (DSC). Approximately 0.5-1 mg of microspheres were weighed into the provided aluminum pans. For hydrated samples, 20 μL ddH_2O was added, incubated at room temperature for 24 h, and the pans were sealed with aluminum hermetic lids. Data were collected on the second heating from 5-75 ºC at a scan rate of 3 ºC /min using a heat-cool-heat cycle. Empty reference pans were also used and the T_g was determined by TA TRIOS software analysis.

3.3.4. Assessment of microsphere morphology by scanning electron microscopy

The surface morphology of microspheres was examined via a Tescan MIRA3 FEG electron microscope (SEM). Microspheres were mounted onto a brass stub via double-sided adhesive tape and sputtered with gold for 60 s at 40 W under vacuum. Images were taken at an excitation voltage of 2 kV or 5 kV as indicated. Prior to imaging, microspheres were incubated in protein-free sodium acetate, sodium chloride loading solution for the specified duration at the specified temperature rotating at 30 rpm, then washed with double-distilled water and lyophilized.

3.3.5. Remote loading and encapsulation of and proteins

3.3.5.1. Standard Procedures

Remote loading HisTag and NoTag protein solutions were prepared by buffer exchange with Amicon ultra centrifugal filter units (for HSA) or by diluting lyophilized powders in loading solution (for GFP and IGF-1). Proteins were remotely loaded into the Zn-loaded microspheres by incubating 1 mg of microspheres in 100 μL of HisTag or NoTag protein of the indicated concentration in pH 8 phosphate buffered saline, or 50 mM sodium acetate, 300 mM sodium chloride, pH 8 solution where indicated. Remote loading and self-healing consisted of a loading stage followed by a healing stage at increased temperature. During both stages, microspheres and protein loading solutions were rotated at 30 rpm. The durations and temperatures of these stages were adjusted as described below.

3.3.5.2. Determination of Zn loading

The amount of Zn^{2+} remotely loaded into $_{RL}Zn^{2+}$ microspheres was determined by dissolving several mg of microspheres in acetone, centrifuging for 5 min at 8,000 rpm, and removing the supernatant for three cycles. The pellet was then reconstituted in water and analyzed using a Perkin-Elmer Nexion 2000 ICP-MS using appropriate standards and scandium

as an internal standard. To determine the amount of Zn directly encapsulated in $_{DE}ZnCO_3$ microspheres, the same procedures were followed, although 10% nitric acid was used in place of water to reconstitute the $ZnCO_3$. Loading percentage was calculated as:

$$\frac{\text{mass of Zn in micropsheres}}{\text{total mass of microspheres}} \times 100\%$$

3.3.5.3. Determination of immunoreactive protein by ELISA

HSA and IGF-1 ELISA kits were purchased from Raybiotech and performed according to kit instructions to determine immunoreactive protein concentrations. In all ELISAs, NoTag and HisTag proteins used for remote loading encapsulation were also included as reference standards.

3.3.5.4. Determination of total protein by Coomassie Plus protein assay

Total protein content for NoTag and HisTag HSA in loading solutions was measured by Coomassie Plus protein assay using a 1:1 sample-to-reagent ratio. BSA standards were used, with the NoTag and HisTag proteins included as reference standards, and absorbance was read at 595 nm in accordance with the protocol.

3.3.5.5. Estimation of encapsulation efficiency

Encapsulation efficiency of the available protein was estimated by ELISA and Coomassie Plus protein assay by comparing the final concentrations of protein in the loading solution to a control loading solution, which underwent the same conditions without microspheres as follows:

$$EE_{avail} = \frac{C_C - C_{MS}}{C_C} \times 100\%$$

Where C_C and C_{MS} are the concentration of protein in control loading solution and the concentration of protein in the loading solution with microspheres quantified by either Coomassie Plus protein assay (for total protein) or ELISA (for immunoreactive or “active” protein), respectively.

Actual active encapsulation efficiency of active protein was calculated as:

$$EE_{actual} = \frac{C_C - C_{MS}}{C_i} \times 100\%$$

Where C_C, C_{MS}, and C_i are the concentration of protein in control loading solution, concentration of protein in the loading solution with microspheres, and the original concentration of protein in the loading solution quantified by ELISA, respectively. Actual total encapsulation efficiency was calculated similarly with concentrations of protein quantified by Coomassie Plus protein assay used in place of those measured by ELISA.

3.3.5.6. Determination of spatial loading with confocal imaging

Following remote loading of HisTag GFP from 50 mM sodium acetate, 300mM sodium chloride, pH 8 loading solution into ${}_{DE}ZnCO_3$ and ${}_{RL}Zn^{2+}$ microspheres, and Zn^{2+}-free HDS/PLGA microspheres using a 48h room temperature loading stage followed by a 42h, 43°C healing stage, microspheres were suspended in water and imaged. A Leica SP8 confocal laser scanning microscope (Leica Microsystems, Wetzlar, Germany) was equipped with a four-laser system and an inverted microscope. HisTag GFP was excited at 487 nm by an Ar laser and the emission at 508 nm was captured. All measurements were conducted using a HC PL APO CS2 40X water immersion objective lens with numerical aperture of 1.1. The detection gain was set at 100, and the pinhole was 330 µm. The power of the Ar laser was set to 30% of its full power. The image size was 512 x 512 pixels, and the images were scanned by 8-bit plane mode at a scan speed of 400 Hz.

3.3.5.7. Optimization of protein loading stage

The duration of the room temperature loading stage was varied from 48 h down to 0.5 h. The healing stage was held constant at 42 h at 37°C. Using a 100µg/mL HisTag HSA pH 8 PBS loading solution (pH was increased with NaOH), the available total protein encapsulation

efficiency was measured by Coomassie Plus protein assay as described above. The temperature of the loading stage was also decreased to 4°C and the duration varied from 2 h to 12 h, with the healing stage being held constant at 42 h at 37°C before determination of total protein encapsulation efficiency by Coomassie Plus protein assay.

3.3.5.8. Optimization of microsphere healing stage

Using a 2h, 4°C loading stage, the duration of the 37°C healing stage was varied from 42 h down to 2 h. Using a 100μg/mL HisTag HSA pH 8 PBS loading solution, the available total protein encapsulation efficiency was measured by Coomassie Plus protein assay as described above.

3.3.5.9. Evaluation of release kinetics

HSA release was conducted by incubating 10 mg microspheres in 0.15 mL phosphate buffered saline (PBS) + 0.02% Tween 80 + 1% casein, pH 7.4. IGF-1 release was conducted by incubating 1 mg microspheres in 0.4 mL PBS + 0.02% Tween 80 + 1% BSA, pH 7.4. Media was completely replaced at each timepoint after centrifuging for 5 min at 8,000 rpm and removing the supernatant. All samples were incubated at 37 ºC with shaking. Casein was used as a blocking agent in place of BSA for HSA release to avoid interference in the HSA ELISA. All samples for release studies were prepared by encapsulating protein with a 2h, 4°C loading stage followed by a 6h, 37°C healing stage in pH 8 PBS loading solution.

3.3.5.10. Effect of pH on remote loading encapsulation efficiency

Using both HisTag HSA (100 μg/mL) and HisTag IGF-1 (50 μg/mL), the pH of PBS loading solution was adjusted to 4, 5, 6, 7, or 8 and microspheres underwent a 2h, 4°C loading stage followed by a 6h, 37°C healing stage. The available total protein encapsulation efficiency was measured by Coomassie Plus protein assay as described above. Unencapsulation controls were included at each pH.

3.4. Results and Discussion

To build off the proof-of-concept work completed previously,[1] we identified five goals: (1) reduce the thermal stress on the proteins, (2) decrease the complexity and duration of the protocol, (3) increase the loading capacity of the microspheres, (4) increase the penetration depth of the encapsulated protein, and (5) improve the release profile of the encapsulation protein. As described below, we sought to accomplish these goals by investigating: (a) plasticization of the microspheres, (b) changing the way the transition metal is introduced in the microspheres (and at the same time switching the basic additive), and (c) adjusting loading/healing conditions (time, temperature, protein concentration, and pH).

3.4.1. Plasticization of microspheres

The first of these goals is an extension of one of the purposes of remote loading in general: to encapsulate delicate proteins without exposing them to stressors which cause denaturation and aggregation. One of the most significant sources of stress present in the MHCRL protocol previously described[1] is the duration and temperature of the healing stage (42 h at 43°C), when the temperature of the microspheres and protein loading solution must be raised above the T_g of polymer phase to induce self-healing pore-closure, which encapsules the protein within the microspheres. Stress from this heating stage has been shown to damage proteins previously.[1,13]

The second of these goals was set with the end-user in mind. This platform is meant to be able to be utilized by non-formulation scientists during the drug discovery and early development process. Shortening the duration of the protocol from the ~six-day protocol described previously and reducing the complexity of the protocol would make it a more useful tool in this sense.[1] Decreasing the duration of the loading and/or healing stages helps towards this goal. One method of reducing the necessary duration and temperature of the healing stage is

to reduce the T_g of the polymer phase by incorporating plasticizers into the continuous phase of the double-emulsion formulation.[13]

Here, we incorporated TBAC or TEC at 2.5% or 5% w/w. To determine the extent that these agents were able to lower the T_g of the microspheres, DSC was used to measure the dry and hydrated T_g. The inclusion of 2.5% and 5% TBAC resulted in a decrease in the dry T_g from 47.3 °C to 43.0 °C and 38.4 °C, respectively, and a decrease in the hydrated T_g from 31.6 °C to 28.1 °C and 25.0 °C, respectively (**Figure 3-1**). Inclusion of 2.5% and 5% TEC, on the other hand, was far less effective at lowering the T_g (dry: 46.8 °C and 46.5 °C, respectively; hydrated: 31.3 °C and 31.0 °C, respectively). This led us to further investigate the 2.5% and 5% TBAC formulation, along with the unplasticized formulation.

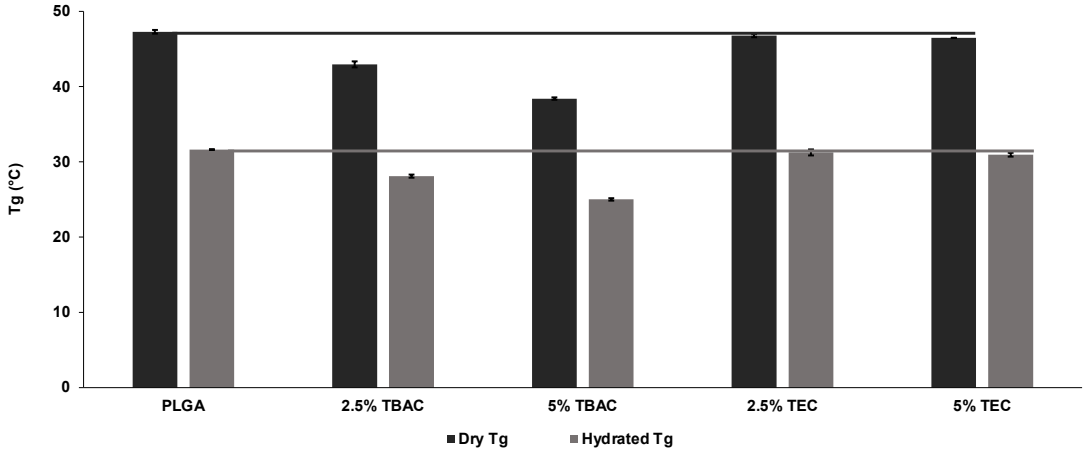

***Figure 3-1**. Inclusion of TBAC results in a dose-dependent decrease in both dry and hydrated T_g of HDS/PLGA microspheres with negligible effect of TEC. Hydrated microspheres were incubated in ddH_2O for 24 h before analysis. Horizontal lines indicate T_g of unplasticized microspheres for reference. Values represent mean ± SD (n=3).*

3.4.2. Direct encapsulation of $ZnCO_3$

The next potential change to the formulation was motivated by the second, third, fourth, and fifth goals. Rather than creating microspheres free of metal cations and remotely loading Zn^{2+}, we replaced the 6% w/w $MgCO_3$ in the continuous phase of the microspheres with 6% w/w $ZnCO_3$. This helps towards the second goal of decreasing the complexity and duration of the protocol by obviating the remote loading of Zn^{2+}, removing a 24h incubation period and a

lyophilization step. Incorporating $ZnCO_3$ in PLGA has been shown to release Zn^{2+} during remote encapsulation of proteins.[36]

The third goal of increasing the loading capacity of the microspheres was motivated by the fact that a decrease in encapsulation efficiency was seen with an increase in protein loading solution concentration in previous studies.[1] It was hypothesized that increasing the amount of Zn^{2+} available to the HisTags for coordination bonding would help address Zn^{2+} availability. Directly encapsulating $ZnCO_3$ in the HDS/PLGA microspheres ($_{DE}ZnCO_3$ microspheres) resulting in a nearly 6-fold increase in the Zn^{2+} content (2.42% ± 0.14%) as compared to remotely loaded Zn^{2+} HDS/PLGA microspheres ($_{RL}Zn^{2+}$ microspheres) (0.42% ± 0.12%) (**Figure 3-2**).

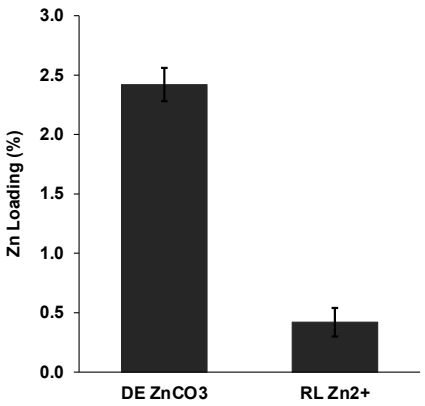

***Figure 3-2**. Effect of Zn incorporation method on metal loading. $ZnCO_3$ was either directly encapsulated in HDS/PLGA microspheres ($_{DE}ZnCO_3$) or remotely loading HDS/PLGA microspheres ($_{RL}Zn^{2+}$). Values represent mean ± SD (n=3).*

3.4.3. Encapsulation of HSA at increased loading solution concentration

To probe whether $_{DE}ZnCO_3$ microspheres were better able to efficiently encapsulate HisTag proteins at increased protein loading solution concentration, a 400μg/mL HisTag HSA loading solution was used. $_{DE}ZnCO_3$ microspheres significantly outperformed $_{RL}Zn^{2+}$ microspheres here ($p < 0.10$) (**Figure 3-3**) (**Table 3-1**). As discussed, this was hypothesized due to the large increase in the amount of Zn^{2+} present in the microspheres.

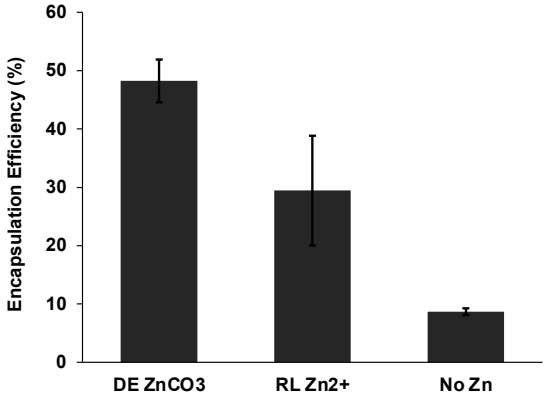

***Figure 3-3**. Effect of Zn incorporation on remote encapsulation of HisTag HSA from MHCRL PLGA microspheres. Available protein encapsulation efficiency of HisTag HSA from 400 μg/mL protein loading solution. Forty μg protein and 1 mg of microspheres in 100 μL sodium acetate, sodium chloride pH 8 loading solution. Total EE_{avail} by total protein assay. Values represent mean ± SD (n=3).*

***Table 3-1**. Summary of remote self-healing encapsulation by Zn^{2+}-HisTag protein binding. One mg microspheres, 100 μL loading solution was used unless noted otherwise. Values represent mean ± SD (n=3).*

HisTag Protein	Zn^{2+} source	Loading/ Healing duration, temp	Active Protein Loaded (μg)	Total Protein Loaded (μg)	Active Available EE (%) [1]	Total Available EE (%) [1]	Actual Active EE (%) [1]	Actual Total EE (%) [1]
HSA (400 μg/mL)	Direct $ZnCO_3$	48h, RT / 42h, 43°C	--	19.1 ± 1.5	--	48.2 ± 3.7	--	47.8 ± 3.7
HSA (400 μg/mL)	Remote Zn^{2+}	48h, RT / 42h, 43°C	--	11.6 ± 3.7	--	29.4 ± 9.4	--	29.0 ± 9.3
GFP (50 μg/mL)	Direct $ZnCO_3$	48h, RT / 42h, 43°C	--	4.3 ± 0.2	--	89.0 ± 3.0	--	86.8 ± 2.9
GFP (50 μg/mL)	Remote Zn^{2+}	48h, RT / 42h, 43°C	--	3.1 ± 1.1	--	64.6 ± 18.5	--	63.0 ± 18.0
IGF-1 (50 μg/mL)	Direct $ZnCO_3$	2h, 4°C / 6h, 37°C	3.6 ± 0.1	4.0 ± 0.0	79.7 ± 1.5	83.9 ± 1.0	72.4 ± 1.3	80.6 ± 1.0
IGF-1 (50 μg/mL)	Remote Zn^{2+}	48h, RT / 42h, 43°C	2.4 ± 0.7	--	81.0 ± 23.4	--	47.5 ± 17.3	--
HSA (100 μg/mL)[2]	Direct $ZnCO_3$	2h, 4°C / 6h, 37°C	84.9 ± 1.3	86.7 ± 2.3	92.2 ± 1.4	88.3 ± 2.3	84.9 ± 1.3	86.7 ± 2.3

[1] EE = Encapsulation Efficiency.
[2] 10 mg microspheres, 1 mL loading solution

3.4.4. Encapsulation of HisTag GFP

With respect to the fourth goal of increasing the penetration depth of the encapsulation protein, there was concern that the remotely loaded Zn^{2+} may be more concentrated within pores near the surface of the microspheres, resulting in remotely loaded protein also being localized

there. This could have negative effects on the loading capacity and efficiency, as well as the release profile of the proteins. It was hypothesized that directly encapsulating $ZnCO_3$ would result in Zn being more evenly distributed throughout the microspheres, which should result in remotely loaded protein being encapsulated deeper within the microspheres. To test this, HisTag GFP was used as the protein drug in a 50 μg/mL loading solution. It was found that the encapsulation efficiency into $_{DE}ZnCO_3$ microspheres was significantly greater ($p < 0.10$) than into $_{RL}Zn^{2+}$ microspheres (**Figure 3-4a**). Next, to visualize the spatial distribution of the encapsulated GFP within the microspheres, the microspheres were imaged under confocal microscopy. As shown, the GFP in the $_{DE}ZnCO_3$ microspheres appears to be encapsulated much more deeply within the microspheres as compared to the GFP in the $_{RL}Zn^{2+}$ microspheres, which appears to be mostly located near the surface of the microspheres (**Figure 3-4b**).

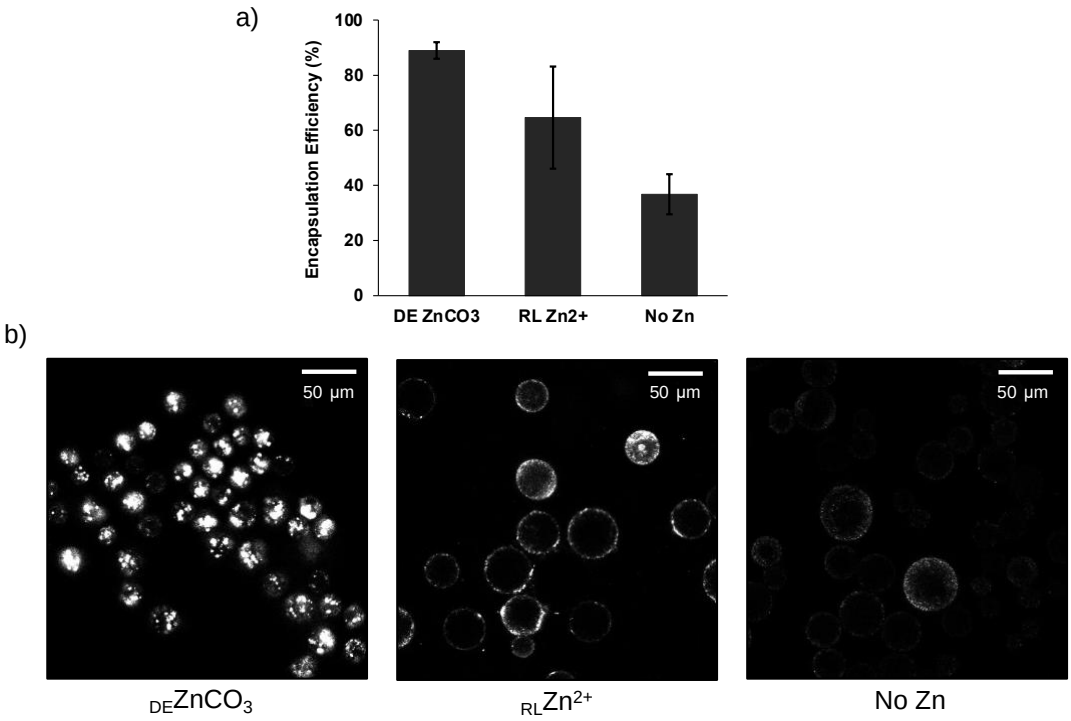

***Figure 3-4**. HisTag GFP is deeply and efficiently encapsulated in $_{DE}ZnCO_3$ microspheres by remote loading relative to $_{RL}Zn^{2+}$ microspheres, and Zn^{2+}-free HDS/PLGA microspheres. a) Available protein encapsulation efficiency of HisTag GFP from 50 μg/mL protein loading solution into $_{DE}ZnCO_3$ microspheres, $_{RL}Zn^{2+}$ microspheres, and Zn^{2+}-free HDS/PLGA microspheres. Five μg protein and 1 mg of microspheres in 100 μL PBS pH 8 loading solution. EE_{avail} by total protein assay. b) Confocal microscopic images of HisTag GFP loading into $_{DE}ZnCO_3$ microspheres, $_{RL}Zn^{2+}$ microspheres, and Zn^{2+}-free HDS/PLGA microspheres. Total EE_{avail} by total protein assay. Values represent mean ± SD (n=3).*

3.4.5. Optimization of loading stage and healing stage times

Following these results, we explored if TBAC, at 2.5% and 5% w/w, could be used to plasticize the $_{DE}ZnCO_3$ microspheres as it had the $_{RL}Zn^{2+}$ microspheres. The results, in terms of dry and hydrated T_g (**Figure S3-11**) were similar as compared to the unplasticized and 2.5% and 5% TBAC $MgCO_3$-containing microspheres (**Figure 3-1**), with the T_g's of the $_{DE}ZnCO_3$ microspheres being 1.5-3 C° lower.

As described above, the main purpose of including plasticizers was to shorten the duration and/or decrease the temperature of the healing stage of the remote loading and self-encapsulation process. It would also be beneficial to decrease the duration and/or lower the temperature of the loading stage. These changes would make the protocol gentler on the proteins by decreasing the thermal stress and would make the protocol more convenient for the user. To begin, we focused on optimizing the loading stage varying duration of this stage from 48 h down to 0.5 h and measured the encapsulation efficiency of HisTag HSA from a 100μg/mL protein loading solution into unplasticized, 2.5% TBAC, and 5% TBAC $_{DE}ZnCO_3$ microspheres. At nearly all durations, the unplasticized formulation was superior to the 2.5% TBAC formulation, which was superior to the 5% TBAC formulation (**Figure 3-5a**). Also, with the exception of the 5% TBAC formulation at durations above 12 h, the increase in duration of the loading stage above 0.5 h did not result in an increase in encapsulation efficiency.

One possible explanation for the decrease in encapsulation efficiency observed with an increase in TBAC content could be that the microspheres were becoming plasticized such that the pores were healing during the room temperature loading stage before protein was able to load into the microspheres. Indeed, the T_g of the 5% TBAC $_{DE}ZnCO_3$ microspheres was measured to be near room temperature, and SEM micrographs suggest an accelerated rate of pore-closure (**Figure S3-12**). This increased plasticization could also explain the increase in encapsulation

efficiency into the 5% TBAC microspheres observed at longer loading stage durations; new pores may have been able to form, allowing protein to load into the microspheres.

To address this issue, the temperature of the loading stage was decreased to 4°C and the experiment was repeated, with loading stage durations ranging from 2 h to 12 h. Again, an increase in TBAC content was associated with a decrease in encapsulation efficiency and no significant changes ($p > 0.10$) in the encapsulation efficiencies within formulations with increasing loading stage duration were seen (**Figure 3-5b**). Also, for the unplasticized formulation, the change in loading stage temperature from room temperature to 4°C did not yield a significant change ($p > 0.10$) in encapsulation efficiency at any duration. The lower temperature, though, should be gentler on the protein.

Next, using a 2h, 4°C loading stage, we focused on optimizing the duration of the 37°C healing stage by varying the duration of it from 1 h to 42 h, again using a 100μg/mL HisTag HSA protein loading solution. An increase in this duration past six hours was not associated with a significant increase ($p > 0.10$) in encapsulation efficiency (**Figure 3-5c**), suggesting that this stage, too, can be decreased in duration in the interest of protein stability and convenience without sacrificing encapsulation efficiency.

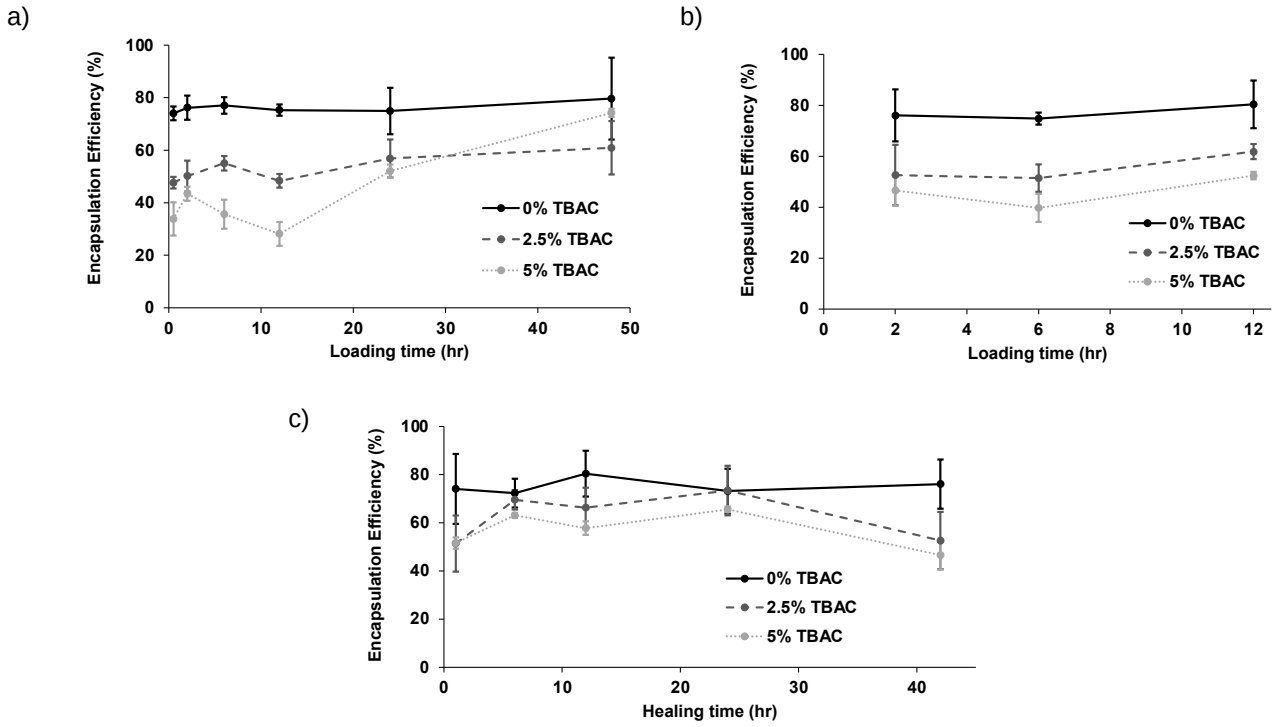

Figure 3-5*. Optimization of loading stage and healing stage durations. Available protein encapsulation efficiency of HisTag HSA from 100 μg/mL protein loading solution into unplasticized, 2.5% TBAC, and 5% TBAC* $_{DE}ZnCO_3$ *microspheres. Ten μg protein and 1 mg of microspheres in 100 μL PBS pH 8 loading solution. a) Room temperature loading stage times were varied as indicated, followed by a 42hr, 37°C healing stage. b) 4°C loading stage times were varied as indicated, followed by a 42hr, 37°C healing stage. c) 2h 4°C loading stage was followed by a 37°C healing stage of the indicated duration. In all cases, Total* EE_{avail} *was by total protein assay. Values represent mean ± SD (n=3).*

3.4.6. Comparison of encapsulation efficiencies at increased loading solution concentrations

As described before, one purpose of directly encapsulating $ZnCO_3$ was to increase the loading capacity and efficiency of the microspheres at increased concentrations. To probe this improvement following the loading and healing stage optimization experiments, $_{DE}ZnCO_3$ microspheres underwent a 2h, 4°C loading stage and a 6h, 37°C healing stage and the encapsulation efficiencies from HisTag HSA loading solutions of various concentrations were measured. Remote loading Zn^{2+} underwent a 48h, room temperature loading stage and a 42h, 43°C healing stage per the previously described protocol[1] and the encapsulation efficiencies from HisTag HSA loading solutions of various concentrations were measured. While the $_{RL}Zn^{2+}$ protocol slightly outperformed the $_{DE}ZnCO_3$ protocol at a protein loading solution concentration

of 50 μg/mL, the $_{DE}ZnCO_3$ protocol showed greater encapsulation efficiencies and loading percentages at greater loading solution concentrations ranging from ~250 μg/mL to ~750 μg/mL HisTag HSA as compared to the $_{RL}Zn^{2+}$ protocol (**Figure 3-6**). Additionally, using the two-sample F-test for the equality of variances, the variances in encapsulation efficiencies between replicates at given conditions with loading solution concentrations greater than 500 μg/mL for the $_{DE}ZnCO_3$ protocol were shown to be significantly smaller ($p < 0.10$) than the for the $_{RL}Zn^{2+}$ protocol, and trend that is consistent across other data presented here. This could be very helpful during drug discovery and development, when a level of precise control is desired.

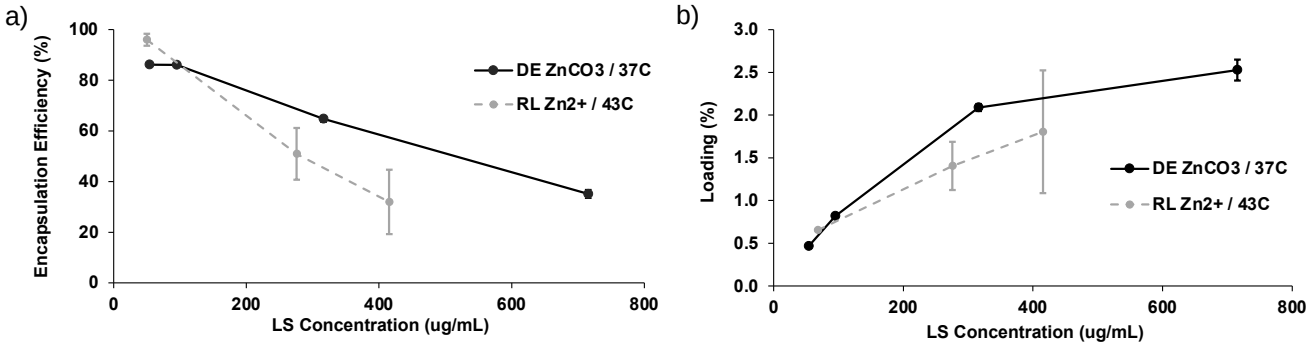

***Figure 3-6**. Effect of loading solution (LS) concentration on (a) total available protein encapsulation efficiency and (b) protein loading of HisTag HSA for two different protocols. The protein was loaded from 100 μL protein loading solution at the indicated concentration into 1 mg $_{DE}ZnCO_3$ microspheres and $_{RL}Zn^{2+}$ microspheres. $_{DE}ZnCO_3$ microspheres underwent a 2h, 4°C loading stage followed by a 6h, 37°C healing stage using PBS pH 8 loading solution. $_{RL}Zn^{2+}$ microspheres underwent a 48h, room temperature loading stage followed by a 42h, 43°C healing stage using sodium acetate, sodium chloride pH 8 loading solution. Total EE_{avail} and loading was by total protein assay. Values represent mean ± SD (n=3). 50 μg/mL LS Concentration $_{RL}Zn^{2+}$ / 43C data (left-most • in each plot) reproduced from Albert, et al.[1]*

3.4.7. Effect of loading protocol optimization on IGF-1 encapsulation efficiency

While $_{DE}ZnCO_3$ microspheres have been shown to more efficiently encapsulate HisTag GFP from a protein loading solution of 50 μg/mL (**Figure 3-4a**) and from HisTag HSA loading solutions of ≥ 100 μg/mL (**Figure 3-6**), we wanted to test the new $_{DE}ZnCO_3$ protocol with a pharmaceutically relevant protein: IGF-1. $_{DE}ZnCO_3$ microspheres underwent a 2h, 4°C loading stage and a 6h, 37°C healing stage, while $_{RL}Zn^{2+}$ microspheres underwent a 48h, room temperature loading stage and a 42h, 43°C healing stage per the previously described protocol[1]

and the active encapsulation efficiencies from a 50 μg/mL protein loading solution were measured. At this relatively low loading solution concentration, there was no significant difference ($p > 0.10$) in active encapsulation efficiencies between the two protocols, although the variance of the $_{DE}ZnCO_3$ formulation was again far smaller than that of the $_{RL}Zn^{2+}$ formulation (**Figure 3-7**). Active protein loading was 0.36 ± 0.01% and 0.24 ± 0.07% for $_{DE}ZnCO_3$ and $_{RL}Zn^{2+}$ microspheres, respectively. Crucially, the actual active encapsulation efficiency for $_{DE}ZnCO_3$ microspheres was 72.4 ± 1.3% compared to 47.5 ± 17.3% for $_{RL}Zn^{2+}$ microspheres (**Table 3-1**). This was owed to the increase in protein stability under the optimized loading and healing protocol with shorter time and lower temperature.

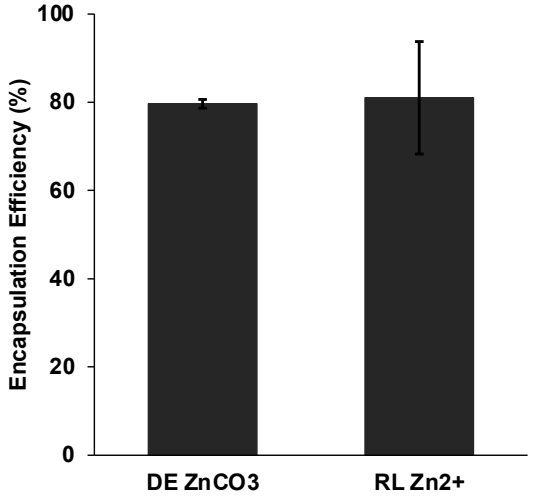

Figure 3-7*. Effect of Zn incorporation method on active available protein encapsulation efficiency of HisTag IGF-1. The protein was loaded from 100 μL 50 μg/mL protein solution and 1 mg $_{DE}ZnCO_3$ microspheres or $_{RL}Zn^{2+}$ microspheres. $_{DE}ZnCO_3$ microspheres underwent a 2h, 4°C loading stage followed by a 6h, 37°C healing stage using PBS pH 8 loading solution. $_{RL}Zn^{2+}$ microspheres underwent a 48h, room temperature loading stage followed by a 42h, 43°C healing stage using sodium acetate, sodium chloride pH 8 loading solution. Active EE_{avail} was by ELISA. Values represent mean ± SD (n=3). $_{RL}Zn^{2+}$ data reproduced from Albert, et al. 2022.*

3.4.8. Effect of pH on encapsulation efficiency

To further probe the Zn^{2+}-HisTag coordination mechanism and to explore how durable this remote loading platform can be across a range of pH's, the pH of the loading solution was varied from the standard 8 down to 4 and the encapsulation efficiencies of NoTag and HisTag HSA and IGF-1 into $_{DE}ZnCO_3$ microspheres were monitored using a 2h, 4°C loading stage and a

6h, 37°C healing stage. It was hypothesized that the encapsulation efficiency for the HisTag proteins would be highest above pH 6, where histidine begins to deprotonate and is able to form coordination bonds with metal cations, and that below pH 6, HisTag proteins would have similar encapsulation efficiencies to NoTag proteins, as the protonated histidine should offer little-to-no increased binding activity. With HSA, HisTag protein did have significantly higher ($p < 0.10$) encapsulation efficiencies than NoTag protein at pH > 6 (**Figure 3-8a**), while the encapsulation efficiencies were nearly identical at pH ≤ 5. At pH 4, though, the encapsulation efficiencies of both the HisTag and NoTag HSA was found to be higher than at any other pH. One possible explanation for this is that the isoelectric point of HSA is reported to be 4.7.[37] Thus, at pH 4, HSA carries a net positive charge, which may aid the protein to bind to the negatively charged HDS present in the microspheres. Another possible explanation is that HSA is known to undergo a conformational change at this pH,[38] which could increase its binding affinity for Zn^{2+} and/or HDS. As the HisTag and NoTag HSA were similarly affected, HisTag-metal coordination does not seem to be playing a role in this phenomenon. With IGF-1, the hypothesized trend was confirmed; HisTag IGF-1 was encapsulated most efficiently at pH ≥ 6 and least efficiently at pH < 6 (**Figure 3-8b**). Further, HisTag IGF-1 is encapsulated significantly more efficiently ($p < 0.10$) than NoTag IGF-1 at pH ≥ 6, while the encapsulation efficiencies at pH < 6 are remarkably similar.

Another significant finding suggested by these results is that the pH of the loading solution can be decreased from 8 to 7 or 6 while maintaining relatively high encapsulation efficiency. This could prove useful for proteins that may retain activity better at pH < 8, allowing this platform to be more generalizable and robust.

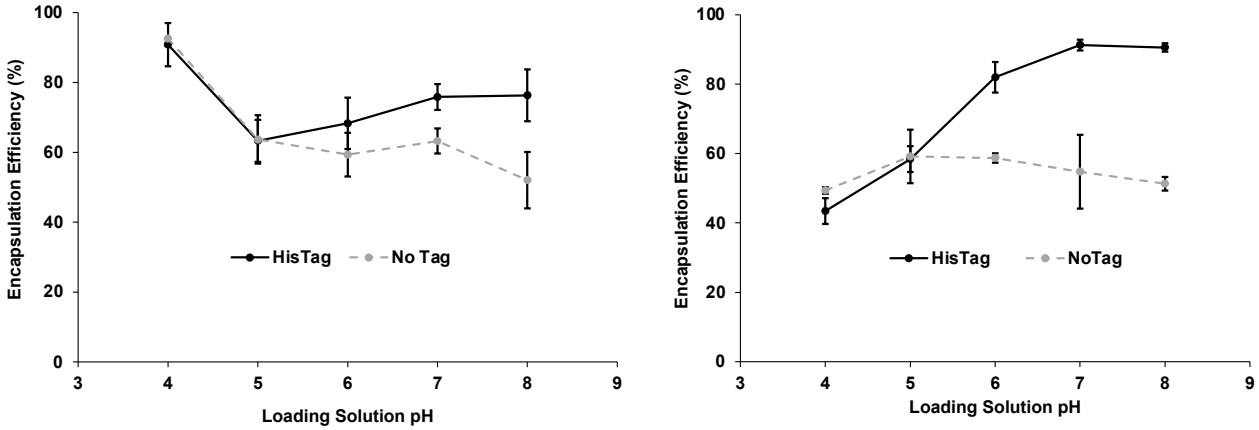

Figure 3-8*. Effect of loading solution pH on available total protein encapsulation efficiency of a) HisTag HSA and b) HisTag IGF-1 into* $_{DE}ZnCO_3$ *microspheres. One mg microspheres in 100 µL PBS loading solution underwent a 2h, 4°C loading stage followed by a 6h, 37°C healing stage. a) Loading solution of 100 µg/mL HisTag HSA. b) Loading solution of 50 µg/mL HisTag IGF-1. Total* EE_{avail} *by total protein assay. Values represent mean ± SD (n=3).*

3.4.9. Evaluation of release kinetics from $_{DE}ZnCO_3$ microspheres

One of the goals of directly encapsulating $ZnCO_3$ within HDS/PLGA microspheres was to improve the release profile as compared to $_{RL}Zn^{2+}$microspheres. From the confocal images of HisTag GFP, proteins likely are encapsulated more deeply within $_{DE}ZnCO_3$ microspheres (**Figure 3-4b**), which will hopefully limit the burst release and lead to more steady release of protein.

To test this, the release of immunoreactive HisTag HSA and HisTag IGF-1 from $_{DE}ZnCO_3$ microspheres was monitored via ELISA (**Figure 3-9**). HisTag proteins were remotely loaded and encapsulated from a pH 8 loading solution using a 2h, 4°C loading stage and a 6h, 37°C healing stage. The active loading and encapsulation efficiency of HisTag HSA and HisTag IGF-1 were 0.85 ± 0.01% and 92.2 ± 1.4%, and 0.36 ± 0.01% and 79.7 ± 1.5%, respectively. In both cases, modest burst release remained, followed by approximately two months of steady, continuous release. While these profiles are more desirable than what was previously seen with $_{RL}Zn^{2+}$ microspheres, the initial burst can still be improved upon (see below).

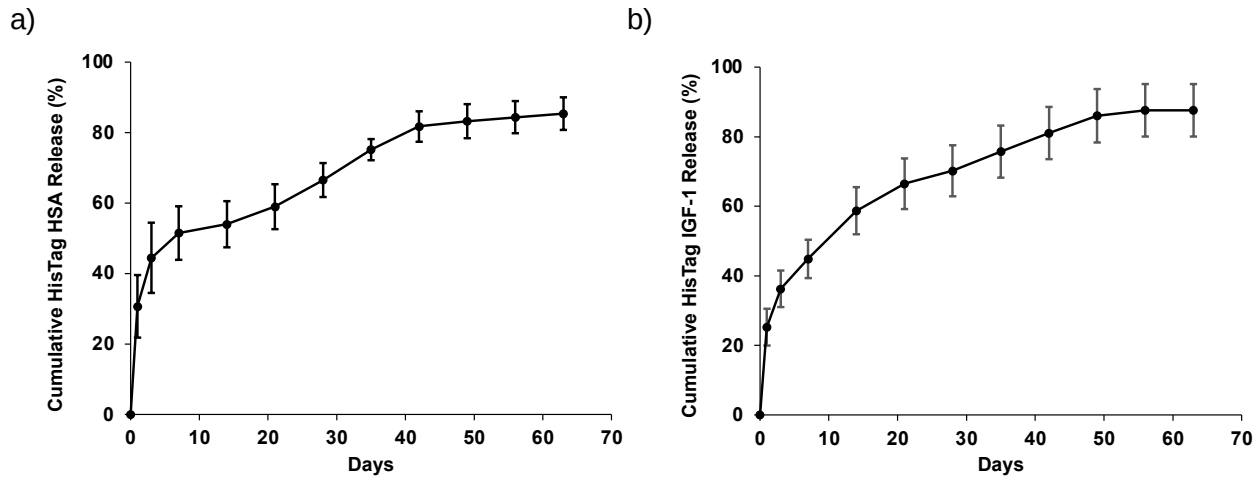

Figure 3-9*. Release of immunoreactive HisTag protein from $_{DE}ZnCO_3$ microspheres. a) Release of immunoreactive HisTag HSA from 10 mg $_{DE}ZnCO_3$ microspheres in 150 μL PBS + 0.02% Tween 80 + 1% casein, pH 7.4 at 37 °C. Loading was conducted using 100 μg protein and 10 mg of microspheres in 1 mL PBS pH 8 loading solution. b) Release of immunoreactive HisTag IGF-1 from 1 mg $_{DE}ZnCO_3$ microspheres in 400 μL PBS + 0.02% Tween 80 + 1% BSA, pH 7.4 at 37 °C. Loading was conducted using 5 μg protein and 1 mg of microspheres in 100 μL PBS pH 8 loading solution. Values represent mean ± SD (n=3).*

3.4.10. Effect of plasticization on initial burst release of HisTag HSA

To address the initial burst (~20-30% in **Figure 3-9**), which may be high for certain applications, the effect of TBAC plasticization on the release of HisTag HSA from $_{DE}ZnCO_3$ microspheres was measured. Initial burst release is initiated by the hydration of microspheres, which solubilizes drug and excipients located on the surface or in percolating pores connected to the surface of the microspheres. These dissolved species can then easily diffuse out of the microspheres through interconnected pores, or from the surface, of microspheres. The hypothesis was that the increase in plasticizer content would lower the T_g of the microspheres, allowing the polymer chains to be more mobile and close pores more completely and more quickly as the influx of water creates new pores, and that this decrease is surface porosity would correspond to a decrease in initial burst, as encapsulated protein would be less freely able to diffuse out of the microspheres.

Here, HisTag HSA was remotely loaded and encapsulated into unplasticized $_{DE}ZnCO_3$ microspheres and 2.5% and 5% TBAC $_{DE}ZnCO_3$ microspheres using a 2h, 4°C loading stage and

a 6h, 37°C healing stage and release was measured with ELISA. These three formulations had loading and encapsulation efficiencies of 0.62 ± 0.05% and 74 ± 6%, 0.46 ± 0.06% and 54% ± 7%, and 0.33 ± 0.12% and 40% ± 14%, respectively.

Through one, three, and seven days, increase in TBAC content was associated with a decrease in released protein (**Figure 3-10**). This supports the hypothesis that plasticization can limit the initial burst, potentially by increasing pore-closure during the healing stage, although further studies would be needed to gain a more complete picture of this concept and its utility. Preliminary studies do suggest that surface pores of plasticized microspheres heal rather quickly (**Figure S3-12**). The initial burst can also be affected by the osmotic pressure within microspheres, which is largely driven by excipients.

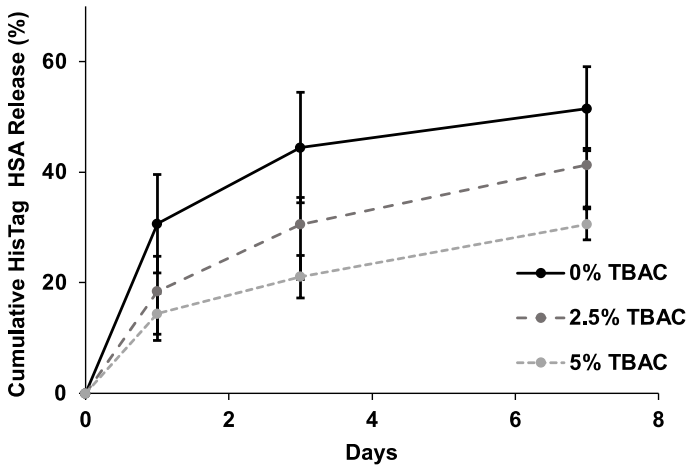

***Figure 3-10**. Plasticization of $_{DE}ZnCO_3$ PLGA microspheres slows release of HisTag HSA. Release of immunoreactive HisTag HSA from 1 mg TBAC-plasticized or $_{DE}ZnCO_3$ microspheres in 400 μL PBS + 0.02% Tween 80 + 1% casein, pH 7.4 at 37 °C. Loading was conducted using 10 μg protein and 1 mg of microspheres in 100 μL PBS pH 8 loading solution. Values represent mean ± SD (n=3).*

3.5. Conclusion

This work builds off the proof-of-concept of using metal-HisTag coordination to remotely and efficiently encapsulate diverse proteins in PLGA microspheres for controlled release. Replacing $MgCO_3$ with $ZnCO_3$ by direct encapsulation in the reformed microspheres with HDS removed the need for the remote loading of Zn^{2+}, resulted in higher Zn^{2+} loading. This

improvement also led to deeper encapsulation of HisTag proteins and higher encapsulation efficiencies at increased protein loading solution concentrations as compared to the previously described formulation. TBAC was found to be an effective plasticizer in terms of lowering the T_g of the microspheres and evidence suggests that it speeds pore-healing, but plasticized microspheres show generally lower encapsulation efficiencies as compared to unplasticized microspheres at short loading times. It was found that the loading and healing stages can be dramatically reduced in temperature and/or duration without resulting in substantial decreases in encapsulation efficiency, drastically improving protein stability through the encapsulation process. This result may be caused by shorter and higher solubility PLGA chains compared to those used in previous, non-MHCRL, studies.[13] It was found that the pH of the protein loading solution can be decreased slightly without substantially decreasing encapsulation efficiency, providing more flexibility to basic pH-labile proteins. Finally, while an appreciable initial burst release still exists with $_{DE}ZnCO_3$ microspheres, plasticization was shown to slow release within the first week. In all, this work makes progress toward the five goals of (1) reducing thermal stress on the proteins, (2) decreasing the complexity and duration of the protocol, (3) increasing the loading capacity of the microspheres, (4) increasing the penetration depth of the encapsulation protein, and (5) improving the release profile of the encapsulation protein, though further work can be done here. This improved protocol could be a valuable asset to drug discovery and development scientists who seek to study the controlled release of a delicate biologic candidate using very small quantities of the protein.

3.6. References

1. Albert J, Chang RS, Garcia GA, Schwendeman SP. Metal-HisTag coordination for remote loading of very small quantities of biomacromolecules into PLGA microspheres. *Bioengineering & Translational Medicine*. 2022-02-17 2022;doi:10.1002/btm2.10272
2. Qi F, Wu J, Li H, Ma G. Recent research and development of PLGA/PLA microspheres/nanoparticles: A review in scientific and industrial aspects.

3. Tomic I, Vidis-Millward A, Mueller-Zsigmondy M, Cardot JM. Setting accelerated dissolution test for PLGA microspheres containing peptide, investigation of critical parameters affecting drug release rate and mechanism. *Int J Pharm*. May 2016;505(1-2):42-51. doi:10.1016/j.ijpharm.2016.03.048
4. Jiang W, Gupta RK, Deshpande MC, Schwendeman SP. Biodegradable poly(lactic-co-glycolic acid) microparticles for injectable delivery of vaccine antigens. *Adv Drug Deliv Rev*. Jan 2005;57(3):391-410. doi:10.1016/j.addr.2004.09.003
5. Alonso MJ, Gupta RK, Min C, Siber GR, Langer R. Biodegradable microspheres as controlled-release tetanus toxoid delivery systems. *Vaccine*. Mar 1994;12(4):299-306. doi:10.1016/0264-410x(94)90092-2
6. Aguado MT, Lambert PH. Controlled-release vaccines--biodegradable polylactide/polyglycolide (PL/PG) microspheres as antigen vehicles. *Immunobiology*. Feb 1992;184(2-3):113-25. doi:10.1016/S0171-2985(11)80470-5
7. Waeckerle-Men Y, Gander B, Groettrup M. Delivery of tumor antigens to dendritic cells using biodegradable microspheres. *Methods Mol Med*. 2005;109:35-46. doi:10.1385/1-59259-862-5:035
8. Schwendeman SP. Recent advances in the stabilization of proteins encapsulated in injectable PLGA delivery systems. *Crit Rev Ther Drug Carrier Syst*. 2002;19(1):73-98. doi:10.1615/critrevtherdrugcarriersyst.v19.i1.20
9. Wischke C, Schwendeman SP. Principles of encapsulating hydrophobic drugs in PLA/PLGA microparticles. *Int J Pharm*. Dec 8 2008;364(2):298-327. doi:10.1016/j.ijpharm.2008.04.042
10. Schwendeman SP, Shah RB, Bailey BA, Schwendeman AS. Injectable controlled release depots for large molecules. *Journal of Controlled Release*. 2014-09-01 2014;190:240-253. doi:10.1016/j.jconrel.2014.05.057
11. Shah RB, Schwendeman SP. A biomimetic approach to active self-microencapsulation of proteins in PLGA. *J Control Release*. Dec 2014;196:60-70. doi:10.1016/j.jconrel.2014.08.029
12. Wu F, Jin T. Polymer-based sustained-release dosage forms for protein drugs, challenges, and recent advances. *AAPS PharmSciTech*. 2008;9(4):1218-29. doi:10.1208/s12249-008-9148-3
13. Reinhold SE, Desai KG, Zhang L, Olsen KF, Schwendeman SP. Self-healing microencapsulation of biomacromolecules without organic solvents. *Angew Chem Int Ed Engl*. Oct 2012;51(43):10800-3. doi:10.1002/anie.201206387
14. Cohen S, Bernstein H. *Microparticulate systems for the delivery of proteins and vaccines*. Drugs and the pharmaceutical sciences,. Marcel Dekker; 1996:ix, 525 p.
15. Ando S, Putnam D, Pack DW, Langer R. PLGA microspheres containing plasmid DNA: preservation of supercoiled DNA via cryopreparation and carbohydrate stabilization. *J Pharm Sci*. Jan 1999;88(1):126-30. doi:10.1021/js9801687
16. Han FY, Thurecht KJ, Whittaker AK, Smith MT. Bioerodable PLGA-Based Microparticles for Producing Sustained-Release Drug Formulations and Strategies for Improving Drug Loading. *Front Pharmacol*. 2016;7:185. doi:10.3389/fphar.2016.00185
17. Giovagnoli S, Blasi P, Ricci M, Rossi C. Biodegradable microspheres as carriers for native superoxide dismutase and catalase delivery. *AAPS PharmSciTech*. Oct 2004;5(4):e51. doi:10.1208/pt050451

18. Schwendeman SP, Cardamone M, Brandon MR, Klibanov A, Langer R. The stability of proteins and their delivery from biodegradable polymer microspheres. In: Cohen S, Bernstein H, eds. *Microparticulate Systems for the Delivery of Proteins and Vaccines*. Marcel Dekker; 1996:1-49.
19. Strohl WR, Knight DM. Discovery and development of biopharmaceuticals: current issues. *Curr Opin Biotechnol*. Dec 2009;20(6):668-72. doi:10.1016/j.copbio.2009.10.012
20. Murray J, Brown L, Langer R. Controlled release of microquantities of macromolecules. *Cancer Drug Deliv*. 1984;1(2):119-23. doi:10.1089/cdd.1984.1.119
21. Wang J, Wang BM, Schwendeman SP. Characterization of the initial burst release of a model peptide from poly(D,L-lactide-co-glycolide) microspheres. *J Control Release*. Aug 21 2002;82(2-3):289-307. doi:10.1016/s0168-3659(02)00137-2
22. Schwendeman SP, inventor; Methods for Encapsulation of Biomacromolecules in Polymers. patent application PCT/U2005/017140. 15 December 2005 2005.
23. Schwendeman SP, Reinhold SE, Kang J, inventors; The Regents of the University of Michigan, assignee. Methods for Encapsulation of Biomacromolecules in Polymers. USA patent US 8017155 B2. 2011 Sept 13 2011.
24. Porath J, Carlsson J, Olsson I, Belfrage G. Metal chelate affinity chromatography, a new approach to protein fractionation. *Nature*. Dec 1975;258(5536):598-9. doi:10.1038/258598a0
25. Liao SM, Du QS, Meng JZ, Pang ZW, Huang RB. The multiple roles of histidine in protein interactions. *Chem Cent J*. Mar 2013;7(1):44. doi:10.1186/1752-153X-7-44
26. Block H, Maertens B, Spriestersbach A, et al. Immobilized-metal affinity chromatography (IMAC): a review. *Methods Enzymol*. 2009;463:439-73. doi:10.1016/S0076-6879(09)63027-5
27. Giacometti J, Josic D. Protein and Peptide Separations. *Liquid Chromatography: Applications*. Elsevier Inc.; 2013:149-175:chap 3.
28. Zhu G, Schwendeman SP. Stabilization of proteins encapsulated in cylindrical poly(lactide-co-glycolide) implants: mechanism of stabilization by basic additives. *Pharm Res*. Mar 2000;17(3):351-7. doi:10.1023/a:1007513425337
29. Bernstein H, Zhang Y, Khan M, Tracy MA, inventors; Alkermes Controlled Therapeutics Inc, assignee. Modulated release from biocompatible polymers. patent US5656297A. 1994.
30. Zhu G, Mallery SR, Schwendeman SP. Stabilization of proteins encapsulated in injectable poly (lactide- co-glycolide). *Nature Biotechnology*. 2000-01-01 2000;18(1):52-57. doi:10.1038/71916
31. Hazekawa M, Kojima H, Haraguchi T, Yoshida M, Uchida T. Effect of Self-healing Encapsulation on the Initial Burst Release from PLGA Microspheres Containing a Long-Acting Prostacyclin Agonist, ONO-1301. *Chemical and Pharmaceutical Bulletin*. 2017-01-01 2017;65(7):653-659. doi:10.1248/cpb.c17-00025
32. Desai KG, Schwendeman SP. Active self-healing encapsulation of vaccine antigens in PLGA microspheres. *J Control Release*. Jan 2013;165(1):62-74. doi:10.1016/j.jconrel.2012.10.012
33. Finkelstein M, Gold H. Toxicology of the citric acid esters: tributyl citrate, acetyl tributyl citrate, triethyl citrate, and acetyl triethyl citrate. *Toxicol Appl Pharmacol*. May 1959;1(3):283-98. doi:10.1016/0041-008x(59)90113-9

34. Final Report on the Safety Assessment of Acetyl Triethyl Citrate, Acetyl Tributyl Citrate, Acetyl Trihexyl Citrate, and Acetyl Trioctyl Citrate. *International Journal of Toxicology*. 2002-10-01 2002;21(2_suppl):1-17. doi:10.1080/10915810290096504
35. Doty AC, Zhang Y, Weinstein DG, et al. Mechanistic analysis of triamcinolone acetonide release from PLGA microspheres as a function of varying in vitro release conditions. *Eur J Pharm Biopharm*. Apr 2017;113:24-33. doi:10.1016/j.ejpb.2016.11.008
36. Pisupati K. *Stability and Structural Analysis of hGH and Infliximab for Controlled Release Depots and Biosimilars*. University of Michigan; 2016.
37. Vlasova I, Saletsky A. Study of the denaturation of human serum albumin by sodium dodecyl sulfate using the intrinsic fluorescence of albumin. Article. *Journal of Applied Spectroscopy*. JUL 2009 2009;76(4):536-541. doi:10.1007/s10812-009-9227-6
38. Peters TJ. Serum Albumin. *Advances in Protein Chemistry*. 1985:161-245.

3.7. Supplementary Information

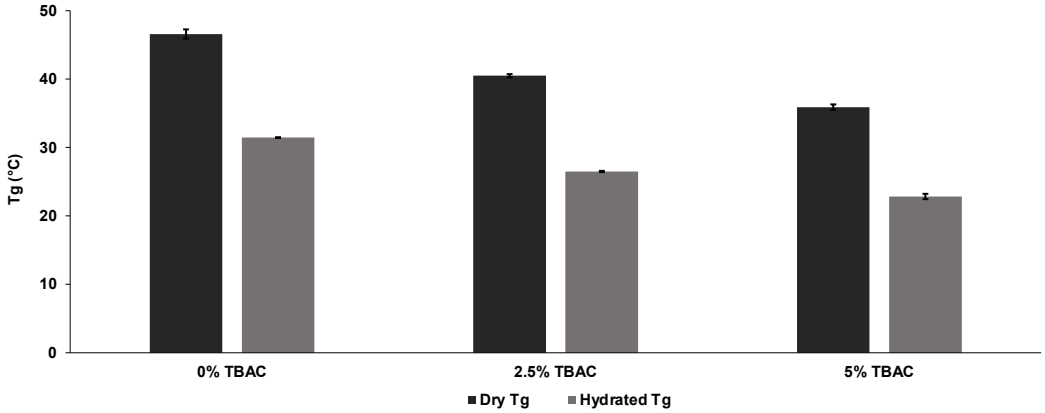

***Figure S3-11**. Inclusion of TBAC results in a dose-dependent decrease in both dry and hydrated T_g of $_{DE}ZnCO_3$ microspheres. Determined by DSC. Hydrated microspheres were incubated in ddH_2O for 24 h. Values represent mean ± SD (n=3).*

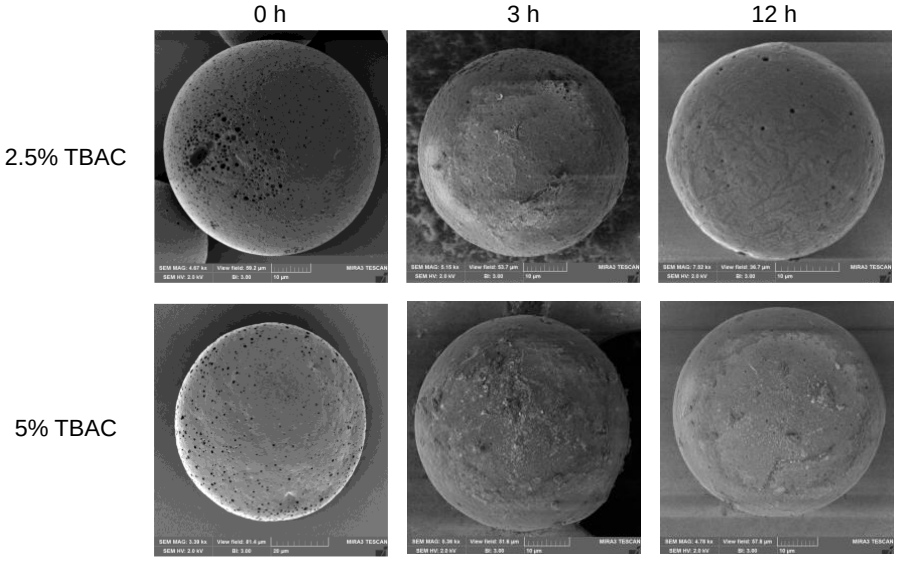

***Figure S3-12**. Plasticized microspheres undergo quick pore-healing. Scanning electron images of 2.5% and 5% TBAC $_{DE}ZnCO_3$ microspheres after 0 h, 3 h, and 12 h of incubation in protein-free PBS pH 8 at 37°C.*

Chapter 4: Characterization of the Erosion and Excipient Release from Rapid Self-Encapsulating PLGA Microspheres

4.1. Abstract

Metal-HisTag coordination remote loading (MHCRL) of HisTag proteins is a promising method to fill the translational need of a universal PLGA microsphere remote loading platform. Previous studies have shown the ability to efficiently encapsulate and slowly release immune and bioactive HisTag protein from very small quantities of MHCRL PLGA microspheres, which contain divalent metal ions (Zn^{2+}, Mg^{2+}) as freely bound to high molecular weight dextran sulfate (HDS) and/or as poorly soluble carbonate bases. However, little is known regarding the encapsulation and release of excipients used during MHCRL. This work aimed to characterize the properties and behavior of MHCRL formulations with a focus on the role played by excipients. Using a variety of techniques, HDS was shown to function as a porosigen and encourage water uptake. While HDS was not shown to significantly affect the Zn^{2+} loading of directly encapsulated $ZnCO_3$ microspheres, it was shown to play a critical role in the remote loading of various divalent transition metal cations. Replacing $MgCO_3$ with $ZnCO_3$ was shown to speed both erosion and degradation significantly, potentially owed to the superior pH-modulating ability of $MgCO_3$. HDS was shown to exhibit a high burst release followed by a multi-week plateau and seemingly erosion-dependent release, while Zn^{2+} release appears erosion-driven. Release of HisTag human serum albumin (HSA) from HDS-free $ZnCO_3$ microspheres showed higher burst and faster release than HDS-containing formulations have

shown previously. Hence, these findings inform future development of self-healing PLGA microsphere formulations for MHCRL or other remote loading platforms.

4.2. Introduction

Controlled release formulations have allowed for reduced frequency of injection of many therapeutics, including biologics which must be injected.[1] Such advancements have led to increased patient satisfaction and compliance, and improved patient outcomes.[2] Due to its versatility, biocompatibility and biodegradability, and tunable performance, poly(lactic-co-glycolic acid) (PLGA) has become one of the most commonly used vehicles for controlled release of a wide array of therapeutics and an industry favorite, with at least 19 controlled release PLGA formulations having been FDA-approved.[1,3,4] While PLGA can be formulated into several different structures, including implants and thin films, injectable microspheres have become a popular formulation geometry.

Unfortunately, the process of encapsulating proteins within PLGA microspheres can expose molecules to stressors including micronization, organic/aqueous interfaces, air/water interfaces, high shear stress, organic solvents, and high temperatures, which can lead to instability and aggregation of proteins.[3,5-12] For this reason, and to reduce the batch size of the encapsulation process, which can require prohibitively large amounts of protein during discovery and development, remote loading and self-encapsulation has been developed largely by the Schwendeman Lab.[8]

In remote loading and self-encapsulation, porous, drug-free microspheres are produced and exposed to an aqueous solution of protein or peptide, which diffuses into the microsphere. Then, modest heating is used to induce the closure of the pores of the microspheres. To date, though, remote loading preformed microsphere formulations rely on an inherent property of the protein of interest (i.e. charge or binding affinity for a particular moiety).[12,13] In an attempt to

create a more universally applicable remote loading platform, metal-HisTag coordination remote loading (MHCRL) was developed.[14] Here, the affinity between poly-histidine tags, which can easily be expressed on recombinant proteins, and divalent metal cations, which can be immobilized within PLGA microspheres, is exploited to induce efficient self-encapsulation and immunoreactive and bioactive release of protein over weeks-to-months. The work presented here builds off of the demonstration of proof-of-concept of MHCRL and significant optimization and development of the platform.

In the initial MHCRL formulation, high molecular weight dextran sulfate (HDS) was included in the inner-water phase of the microsphere formulation to serve as a metal trapping agent and immobilizer. In these protocols, microspheres were formulated without any transition metal or transition metal cation. Rather, metal cations were remotely loaded into the microspheres before being lyophilized and then remotely loaded with HisTag proteins. As such, HDS served as a trapping agent for the remote loading of metal cations and as a metal immobilizer to allow for drug loading. This is analogous to the function of the chelating agent that immobilizes metal ions within immobilized metal affinity chromatography (IMAC) columns.[15-17] In attempts to optimize MHCRL, $ZnCO_3$ was directly included in the continuous polymer phase of the microsphere formulation in place of $MgCO_3$, rather than Zn^{2+} being remotely loaded after microsphere formulation (Chapter 3). This change raises the question of the need for, and role of, HDS in the formulation.

Dextran sulfate is a sulfated, anionic, highly soluble, branched polysaccharide, and is a glycosaminoglycan (GAG) analog. It is widely used in materials, food, and drug products, and it is biocompatible and biodegradable.[18] Dextran sulfate sodium has been used as an antiviral, anticoagulant, hypocholesterolemic, and extensively as a drug carrier or as part of a drug

carrier.[19] The dextran sulfate used here is of high molecular weight (>500 kDa) and is a sodium salt. This material has also been explored as a trapping agent for remote loading and self-encapsulation platforms, as it can bind to many proteins that have affinity for GAGs.[12] Dextran sulfate has been shown to prevent aggregation of proteins, specifically at acidic pH like that found within PLGA microspheres.[20]

Release of protein (and large excipients) from PLGA microspheres is typically largely governed by two processes: aqueous diffusion of the molecule (presuming it is too large to diffuse through the polymer at substantial levels) and erosion of the polymer.[21,22] The initial burst occurs as water enters the microsphere, solubilizing protein at or near the surface of the microspheres, allowing them to be quickly released. Large molecules, like proteins, that are encapsulated more deeply within the microspheres are typically released as the polymer erodes. This process depends on the rate of hydrolysis of the polymer chains, which is promoted by water and the available soluble acidic products of the hydrolysis, itself. Basic salts, like $MgCO_3$ and $ZnCO_3$, have been included in PLGA microspheres in part to mitigate this phenomenon. Once in dissociated, basic salts can combine with the acidic byproducts of PLGA degradation, moderating the drop in pH, and slowing degradation.[23] Eventually, the chains reach a critical molecular weight, below which polymer fragments are soluble and can diffuse away, eroding the microsphere and creating a network of large pores through which large molecules can diffuse.[24]

The inclusion of excipients can affect a wide variety of attributes of PLGA microspheres, including porosity, water uptake, internal pH, degradation and erosion, and protein stability, all of which can affect the encapsulation efficiency, release profile, and efficacy of the microsphere formulation. For these reasons, effects of excipients including $MgCO_3$, $ZnCO_3$, and HDS on the

properties and behaviors of the PLGA microsphere formulations previously used in MHCRL are investigated here.

4.3. Experimental Methods

4.3.1. Materials

Resomer RG 504 PLGA (50:50, ester-terminated, molecular weight 38,000-54,000 Da), magnesium carbonate, trehalose, 88% hydrolyzed poly(vinyl alcohol) (PVA), and high molecular weight (>500,000 Da) dextran sulfate sodium (HDS) were purchased from Sigma Aldrich. Zinc, copper, cobalt, nickel, and calcium acetate salts were purchased from Sigma Aldrich. Zinc carbonate basic were purchased from Sigma Aldrich. Poly-histidine tagged (HisTag) Human Serum Albumin (HSA) was purchased from Arco Biosystems and untagged (NoTag) HSA was purchased from Raybiotech. HisTag insulin-like growth factor 1 (IGF-1) was purchased from Signalway Antibodies and NoTag IGF-1 was purchased from Sino Biological. All HisTag proteins contained tags of six histidine residues. Tags were at the N-terminus for IGF-1. Tags were at the C-terminus for HSA. Bovine serum albumin (BSA) was purchased from Sigma Aldrich and blocker casein in PBS was purchased from ThermoFisher. 1,9 dimethylmethylene blue, glycine, glacial acetic acid, and Tris base were purchased from Sigma Aldrich. All other common reagents and solvents were purchased from Sigma Aldrich, unless otherwise specified.

4.3.2. Preparation of microspheres

Porous PLGA microspheres with HDS as a metal immobilizer, $MgCO_3$ as a pH-modulator and porosigen,[5,12] and trehalose as a porosigen were prepared by double water-oil-water (w/o/w) emulsion and solvent evaporation. The first emulsion was created by homogenizing a suspension of 1 mL of 250 mg/mL dissolved PLGA and 6% w/w fine particulate $MgCO_3$ in methylene chloride with an inner water phase of 200 μL of 4% w/v HDS and 3% w/v

trehalose in a glass cell culture tube at 18,000 rpm for 60 s over an ice bath, using the Tempest IQ^2. The second emulsion was created by adding 2 mL of 5% PVA to the primary emulsion and vortexing for 60 s. The w/o/w double emulsion was added to 100 mL of 0.5% PVA and stirred for 3 h at room temperature in a 150 mL beaker to allow for hardening and evaporation of methylene chloride. The 20-63 μm fraction of microspheres was collected using sieves and the microspheres were washed with excess double-distilled water and lyophilized.

4.3.2.1. Inclusion of $ZnCO_3$

To create direct encapsulation $ZnCO_3$ microspheres ($_{DE}ZnCO_3$/HDS/PLGA) replaced $MgCO_3$ in the 250 mg PLGA in 1 mL methylene chloride continuous phase before emulsification. These microspheres were not remotely loaded with Zn^{2+} from zinc acetate as described below.

4.3.2.2. Exclusion of dextran sulfate

To create HDS-free $_{DE}ZnCO_3$/PLGA microspheres, HDS was excluded from the inner water phase during microsphere formulation. Instead, an inner water phase of 3% w/v trehalose was used. $ZnCO_3$ was included as described above.

4.3.3. Determination of microsphere porosity

The porosity of remotely loaded Zn^{2+} HDS/PLGA ($_{RL}Zn^{2+}$/HDS/PLGA), $_{DE}ZnCO_3$/HDS/PLGA, and $_{DE}ZnCO_3$/PLGA microspheres, prepared as described above, was determined by mercury intrusion porosimetry (AutoPore V Series, Micromeritics). Between 100 and 200 mg of microspheres were used for analysis, which was performed over low and high pressure ranging from 0.5 psia to 61,000 psia with a fill rate of 0.5 s and equilibration of 10 s at each pressure. Bulk density of samples was calculated by the instrument at atmospheric pressure.

4.3.4. Quantification of dextran sulfate

The amount of dextran sulfate encapsulated in microspheres was determined by dissolving several mg of microspheres in acetone, centrifuging for 5 min at 8,000 rpm, and removing the supernatant for three cycles. The pellet was then reconstituted in water and analyzed using a dimethylmethylene blue (DMMB) assay with dextran sulfate sodium standards.[25] DMMB Reagent was produced by mixing 16 mg 1,9 dimethylmethylene blue, 3.04 g glycine, 1.6 g NaCl, and 95 mL of 0.1M acetic acid in 1 L ddH_2O. The solution was adjusted to pH 3 and filtered under vacuum using a 0.2μm filter.

4.3.5. Determination of water uptake

The water uptake into various formulations of microspheres was measured by first incubating ~10 mg microspheres in 1 mL PBS for 10 days, with media replacement at 1, 3, and 7 days. Microspheres were then collected on pre-weighed nylon membrane filters and washed with 2 mL ddH_2O. Microspheres were dried under vacuum for ~5 s to remove surface water, and the wet weight was recorded. Microspheres were then dried under vacuum at room temperature for 4 days, and the dry weight was recorded. Interparticle water was calculated by briefly dispersing dry microspheres in PBS at 4°C (water uptake is assumed to be negligible at these conditions) and the wet and dry weights were recorded as described. Interparticle water was calculated as:

$$W_{int} = \frac{\left(W_{wet}^0 - W_{dry}^0\right)}{W_{dry}^0},$$

where W_{wet}^0 and W_{dry}^0 are the weights of wet microspheres and dry microspheres, respectively, after immediate collection at t_0. The water uptake of microspheres was then calculated as:

$$W_{ms} = \frac{\left(W_{wet} - W_{dry} - \left(W_{dry} W_{int}\right)\right)}{W_{dry}},$$

where W_{wet} and W_{dry} are the wet and dry microsphere weights after incubation and drying.

4.3.6. Remote loading and encapsulation of metals and proteins

4.3.6.1. Standard procedures

For $_{RL}Zn^{2+}$/HDS/PLGA microspheres, Zn^{2+} (or another divalent metal) was remotely loaded by incubating microspheres in at least 1 mL of 500 mM zinc (or other metal) acetate salt solution (or water as a control) per 1 mg of microspheres for 24 h rotating at 30 rpm at room temperature. Microspheres were washed with double-distilled water under vacuum on a 0.2 μm nylon filter and lyophilized. $_{DE}ZnCO_3$ microspheres did not undergo this procedure.

Remote loading HisTag and NoTag protein solutions were prepared by buffer exchange with Amicon ultra centrifugal filter units (for HSA) or by diluting lyophilized powders in loading solution (for IGF-1). Proteins were remotely loaded into the Zn-containing microspheres by incubating 1 mg of microspheres in 100 μL of HisTag or NoTag protein of the indicated concentration in pH 8 phosphate buffered saline (PBS). Remote loading and self-healing consisted of a 2h, 4°C loading stage followed by a 6h, 37°C healing stage. During both stages, microspheres and protein loading solutions were rotated at 30 rpm.

4.3.6.2. Determination of metal cation loading

The amount of divalent metal cation remotely loaded into microspheres was determined by dissolving several mg of microspheres in acetone, centrifuging for 5 min at 8,000 rpm, and removing the supernatant for three cycles. The pellet was then reconstituted in water and analyzed using a Perkin-Elmer Nexion 2000 ICP-MS using appropriate standards and scandium as an internal standard. To determine the amount of Zn encapsulated in $_{DE}ZnCO3$ microspheres, the same procedures were followed, and 10% nitric acid was used to dissolve the $ZnCO_3$. Loading percentage was calculated as:

$$\frac{\text{mass of Zn in micropsheres}}{\text{total mass of microspheres}} \times 100$$

4.3.6.3. Determination of erosion of microspheres

To measure the erosion of various microsphere formulations, ~5 mg of pre-weighed microspheres were incubated in PBS + 0.02% Tween 80, pH 7.4 in 1.5mL eppendorf tubes, unless otherwise specified. All samples were incubated at 37ºC with shaking. Media was completely replaced at each timepoint after centrifuging for 5 min at 8,000 rpm and removing the supernatant. Once a sample had been incubated for the designated amount of time, the supernatant was removed, the microspheres were dried at room temperature under vacuum for 96 h, and the dried microspheres were weighed. Normalized mass loss percentage was calculated as:

$$\left(1 - \frac{\text{final microsphere mass}}{\text{initial microsphere mass}}\right) \times 100$$

4.3.6.4. Determination of degradation of microspheres

To measure the degradation of various microsphere formulations, ~5 mg of microspheres were incubated in PBS + 0.02% Tween 80, pH 7.4 in 1.5mL eppendorf tubes, unless otherwise specified. All samples were incubated at 37ºC with shaking. Media was completely replaced at each timepoint after centrifuging for 5 min at 8,000 rpm and removing the supernatant. Once a sample had been incubated for the designated amount of time, the supernatant was removed, and the microspheres were dried at room temperature under vacuum for 96 h. Dried microspheres were then dissolved in tetrahydrofuran (THF). The obtained polymer solutions were then subjected to gel permeation chromatography using two styragel columns (HR 1 and HR 0.5 columns, Waters, US) with a Waters 1525 HPLC system and THF as the elution medium at a flow rate of 1 mL/min. Poly(styrene) standards of known molecular weights were used for

calibration, and the weight-average molecular weight of polymer samples was calculated. Normalized molecular weight loss percentage was calculated as:

$$\left(1 - \frac{\text{final microsphere molecular weight}}{\text{initial microsphere molecular weight}}\right) \times 100$$

4.3.6.5. Determination of immunoreactive protein by ELISA

HSA and IGF-1 ELISA kits were purchased from Raybiotech and performed according to kit instructions to determine immunoreactive protein concentrations. In all ELISAs, NoTag and HisTag proteins used for remote loading encapsulation were also included as reference standards.

4.3.6.6. Estimation of encapsulation efficiency

Encapsulation efficiency of the available protein was estimated by ELISA and Coomassie Plus protein assay by comparing the final concentrations of protein in the loading solution to a control loading solution, which underwent the same conditions without microspheres as follows:

$$EE_{avail} = \frac{C_C - C_{MS}}{C_C} \times 100\%$$

Where C_C and C_{MS} are the concentration of protein in control loading solution and the concentration of protein in the loading solution with microspheres quantified ELISA.

4.3.6.7. Evaluation of release kinetics

HSA release was conducted by incubating 1 mg microspheres in 0.4 mL PBS + 0.02% Tween 80 + 1% casein, pH 7.4. Media was completely replaced at each timepoint after centrifuging for 5 min at 8,000 rpm and removing the supernatant. All samples were incubated at 37 ºC with shaking. Casein was used as a blocking agent (as opposed to BSA) to avoid interference in the HSA ELISA. Release was quantified using ELISA as described.

Zn^{2+} and HDS release was conducted by incubating ~5 mg microspheres in 1 mL PBS + 0.02% Tween 80, pH 7.4. Media was completely replaced at each timepoint after centrifuging for

5 min at 8,000 rpm and removing the supernatant. All samples were incubated at 37 ºC with shaking. Zn^{2+} release was measured using ICP-MS as described. HDS release was measured using DMMB assay as described.

4.4. Results and Discussion

In an effort to better understand the roles and effects of various excipients used in this project, the characteristics and performance of microspheres containing or lacking HDS, $MgCO_3$, and $ZnCO_3$ were analyzed. First, the porosity, water uptake, and metal encapsulation ability of $ZnCO_3$/HDS/PLGA, HDS-free/$ZnCO_3$/PLGA, and $MgCO_3$/HDS/PLGA microspheres were measured. Next, the erosion and degradation kinetics of these formulations and the release kinetics of HDS and Zn^{2+} from these formulations were determined. Finally, the role of HDS in the remote encapsulation and release of HisTag proteins was studied.

4.4.1. Effect of excipients on porosity

To probe the effects of HDS, $ZnCO_3$, and $MgCO_3$ on physical attributes of the microspheres, mercury porosimetry was used to measure the porosity of the microspheres. Remote loading, as a mechanism, relies on microspheres containing an interconnected pore network into which drug molecules can diffuse before being encapsulated via self-healing of the microsphere surface pores. Porosity has been shown to be a critical parameter affecting drug loading as well as release.[26,27]

It was hypothesized that the replacement of $MgCO_3$ with $ZnCO_3$ would result in a decrease in porosity due to the decreased solubility of $ZnCO_3$ as compared to $MgCO_3$, which should result in decreased leaching and pore-formation during formulation. Further, it was hypothesized that the exclusion of dextran sulfate would result in decreased porosity. The dextran sulfate used in these formulations is a sodium salt. The inclusion of solutes, especially salts, in the inner water phase of PLGA microspheres formulated via the double-emulsion

solvent evaporation method has been shown to increase porosity. All formulations studied here contained the same trehalose content; the inner-water phase of the HDS-free microspheres contained fewer solutes than the inner-water phase of HDS-containing microspheres.

As for the difference in porosity between $ZnCO_3$-containing microspheres and $MgCO_3$-containing microspheres, while the average porosity for the $ZnCO_3$/HDS/PLGA microspheres (43.5 ± 8.3%) was lower than that of the $MgCO_3$/HDS/PLGA microspheres (54.0 ± 5.2%), the difference was not found to be significant (**Figure 4-1**). The second hypothesis was supported by the data. $ZnCO_3$/PLGA microspheres lacking dextran sulfate sodium in the inner-water phase had significantly lower porosity (32.6 ± 1.7%) than $ZnCO_3$/HDS/PLGA microspheres.

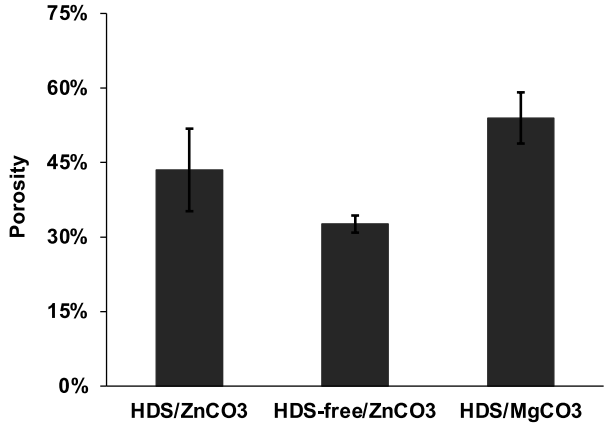

Figure 4-1*. Porosity of various formulations of microspheres are measured by mercury porosimetry. 100-200 mg of microspheres were used and intrusion of mercury under pressure from 0.5 to 61,000 psia was measured. $ZnCO_3$/HDS-free porosity significantly lower than $ZnCO_3$/HDS porosity; $p < 0.10$.*

4.4.2. Effect of excipients on water uptake

The next physical characteristic measured was water uptake. The propensity for PLGA microspheres to absorb water and swell can depend on several factors, including the end-group of the polymer chains (ester end-capped PLGA does not significantly absorb water prior to hydrolysis), and osmotic pressure created by water-soluble species within the microspheres. Water uptake can have myriad effects on the behavior of PLGA microspheres. Water acts as a plasticizer, lowering the glass transition temperature (T_g) of the polymer.[28] Increased water

uptake could also lead to faster release due to hastened degradation and, therefore, erosion of the PLGA. Water can also increase the mobility of encapsulated proteins, increasing their propensity to aggregate and/or denature.

It was hypothesized that microspheres containing $MgCO_3$ would have greater water uptake than microspheres containing $ZnCO_3$, as $MgCO_3$ is more soluble than $ZnCO_3$, and therefore should exert more osmotic pressure. Further, it was hypothesized that microspheres including HDS would have greater water uptake than microspheres lacking HDS. Aside from the sodium included in the dextran sulfate, which should exert osmotic pressure, dextran sulfate itself is highly water soluble and should exert osmotic pressure.

Each of these hypotheses were supported by the data. $ZnCO_3$/HDS/PLGA microspheres had significantly lower water uptake (22.6 ± 1.7%) than $MgCO_3$/HDS/PLGA microspheres (29.3 ± 5.4%) (**Figure 4-2**). Further, HDS-free $ZnCO_3$/PLGA (17.7 ± 3.7%) microspheres had significantly lower water uptake than $ZnCO_3$/HDS/PLGA microspheres. The relative order of these values is plausibly explained above and could have effects on the erosion, degradation, and release from microspheres as described.

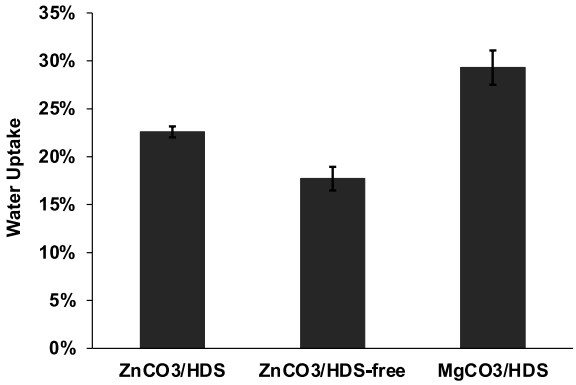

Figure 4-2*. Water uptake into $ZnCO_3$/HDS/PLGA, $ZnCO_3$/HDS-free/PLGA, and $MgCO_3$/HDS/PLGA microspheres after 10 days is measured by comparing the wet mass and dried mass of microspheres and accounting for interparticle water. All water uptake values significantly different; $p < .10$.*

4.4.3. Effect of HDS on encapsulation of metals

4.4.3.1. Effect of HDS on remote loading of metal cations

In remotely loaded Zn^{2+} HDS/PLGA microspheres ($_{RL}Zn^{2+}$/HDS/PLGA), HDS was included as a trapping agent and immobilizer for the remote loading of metal ions, due to its high molecular weight (and slow dissolution rate) and negative charge. To probe whether HDS was necessary in order to remotely load and encapsulate divalent transition metal ions, microspheres containing and lacking HDS were exposed to aqueous solutions of 500 mM metal acetate salts for 24 h, washed with water, and lyophilized, and metal ion content was determined with ICP-MS. It was found that microspheres lacking HDS in their inner-water phase encapsulated significantly less divalent transition metal cations (0.03 ± 0% for each metal) than microspheres containing HDS in their inner-water phase (0.19 ± 0.05%, 0.17 ± 0.02%, 0.27 ± 0.04%, and 0.42 ± 0.12% for cobalt, copper, nickel, and zinc, respectively) (**Figure 4-3**). This supports the idea that HDS is serving its intended purpose as a metal trapping and immobilizer and should not be excluded from the $_{RL}Zn^{2+}$/HDS/PLGA formulation.

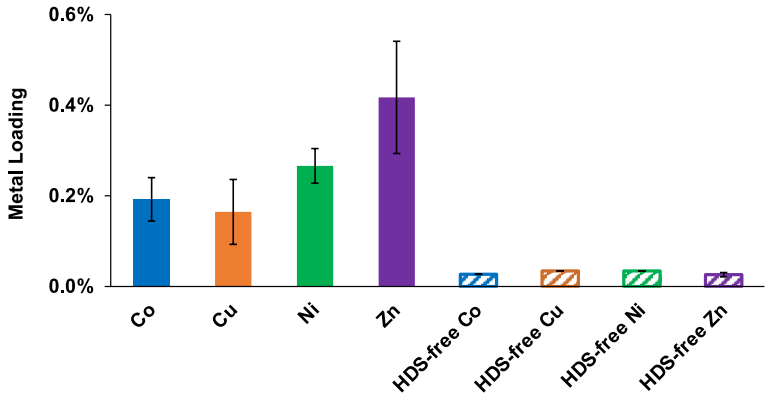

***Figure 4-3**. The inclusion of HDS in the inner-water phase significantly increases the remote loading of divalent transition metal cations into PLGA microspheres. Microspheres were exposed to at least 1 mL 500mM metal acetate solution per 1 mg microspheres for 24 h at room temperature and analyzed via ICP-MS. All within-metal differences significant; $p < 0.05$.*

4.4.3.2. Effect of HDS on direct encapsulation of $ZnCO_3$

With the direct encapsulation of $ZnCO_3$, the role of, and need for, HDS was questioned. To probe whether the inclusion of HDS in the inner-water phase had any effect on the loading of

directly encapsulated $ZnCO_3$, HDS-free/$ZnCO_3$/PLGA were formulated, and ICP-MS was used to measure the Zn^{2+} content as described. Microspheres containing or lacking HDS were not found to have significantly different Zn^{2+} content (2.42 ± 0.14% and 2.34 ± 0.14%, respectively) (**Figure 4-4**). This suggests that HDS plays little if any role in the loading of directly encapsulated $ZnCO_3$ when $ZnCO_3$ is including in the continuous phase of a double-emulsion formulation. This was expected as $ZnCO_3$ is sparingly soluble in water, and thus should largely remain in the continuous phase of the emulsion, largely unaffected by excipients included in the inner water phase. Further studies, discussed below, will be needed to elucidate what effect, if any, the inclusion or exclusion of HDS has on HisTag protein encapsulation and the release profile of encapsulated protein and Zn^{2+} from microspheres with directly encapsulated $ZnCO_3$.

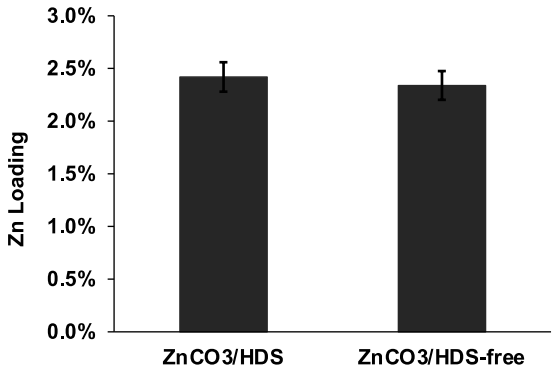

Figure 4-4*. Inclusion or exclusion of HDS in the inner-water phase does not have a significant effect on the loading of $ZnCO_3$ into PLGA microspheres. 6% w/w $ZnCO_3$ was included in the continuous phase of the double-emulsion solvent evaporation formulation. Microspheres were dissolved in and washed with acetone and pellets were reconstituted in 10% nitric acid to solubilize $ZnCO_3$.*

4.4.4. Effect of excipients on erosion of microspheres

The erosion profile of a polymer microsphere can be a rate-determining parameter with respect to the release kinetics of the payload. As such, determining the erosion profiles of the three formulations discussed here was of interest. Approximately 5 mg of microspheres were incubated in PBS + 0.02% Tween 80 for pre-determined durations with full media replacement at each timepoint. After washing and drying the microspheres, the dry weights were compared to the initial weights and the Normalized mass loss was calculated as described.

HDS was not shown to affect the erosion profile of $ZnCO_3$-containing microspheres, as the profiles HDS/$ZnCO_3$ and HDS-free/$ZnCO_3$ microspheres were nearly identical (**Figure 4-5**). This was predictable as, while HDS may encourage increased water uptake into the pores of the microspheres, it will have little-to-no effect within the polymer phase of microspheres, especially for ester end-capped PLGAs, like the one used throughout this work.

It was hypothesized that HDS/$MgCO_3$ microspheres would show slower erosion and degradation as compared to HDS/$ZnCO_3$ microspheres. The hydrolysis of PLGA chains produces water-soluble acidic monomers and oligomers, which decrease the pH of their surrounding environment. Within microspheres, these water-soluble acids partition between the aqueous phase and the polymer phase.[29] Once solubilized, bases, like $MgCO_3$ and $ZnCO_3$, can react with the acids in the aqueous pores, depleting the acid content in the polymer phase, as well. This modulates the pH within the polymer phase, preventing it from dropping to the degree that it would otherwise, mitigating auto-catalysis of future hydrolysis and thereby slowing degradation and erosion. $MgCO_3$ is more soluble than $ZnCO_3$, making it a more effective binding partner for the water-soluble acids and a better pH-modulator and degradation- and erosion-dampener.[30-32] Fitting with this hypothesis, the initial stage of slow weight loss lasted ~1 week longer for HDS/$MgCO_3$ microspheres than for HDS/$ZnCO_3$ (and HDS-free/$ZnCO_3$) microspheres (**Figure 4-5**). Further, the second phase of faster weight loss, being delayed ~1 week, lasted until ~Week 7. At each timepoint from Week 3 to Week 6, the formulation containing $MgCO_3$ showed significantly lower erosion than the formulations containing $ZnCO_3$.

In all cases, erosion can be broken into two phases: an initial stage of slow weight loss (induction phase) (lasting ~2-4 weeks), followed by a stage of faster weight loss, which continues until the microspheres have effectively eroded entirely (by ~6-7 weeks).

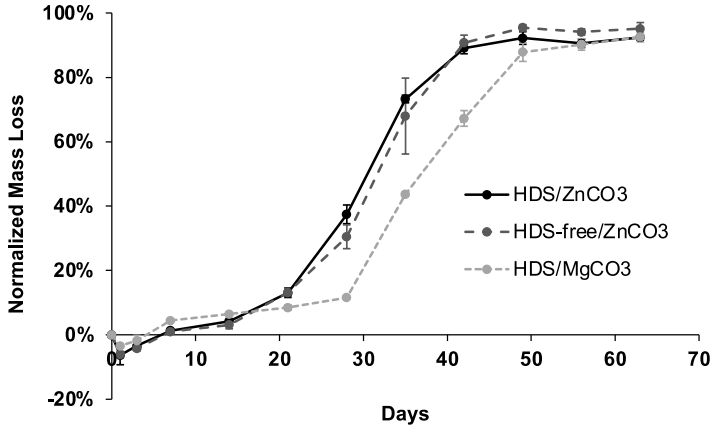

Figure 4-5*. Erosion of $MgCO_3$-containing microspheres is slower than $ZnCO_3$-containing microspheres as measured by normalized mass loss. Approximately 5 mg of pre-weighed microspheres were incubated in PBS + 0.02% Tween 80 at 37°C for predetermined durations before being dried and re-weighed.*

4.4.5. Effect of excipients on degradation of microspheres

Having analyzed the erosion profiles of the three formulations, the next logical data to scrutinize was the degradation profiles. The same samples that were used for erosion calculations were analyzed using GPC to determine the molecular weight, and the normalized molecular weight was calculated as described. Given the erosion curves (**Figure 4-5**), it was hypothesized that the degradation profiles of HDS/$ZnCO_3$ microspheres and HDS-free/$ZnCO_3$ microspheres would not be significantly different. As shown, these two curves are practically indistinguishable (**Figure 4-6**); the inclusion or exclusion of HDS from the inner water phase of $ZnCO_3$/PLGA microspheres does not seem to affect the degradation behavior of the PLGA at all. As stated, this was expected as ester end-capped PLGAs, like the one used here, do not initially take up water. Thus, whatever increase in water content is caused by HDS will not dramatically affect the polymer phase.

As with erosion, HDS/$MgCO_3$ microspheres showed significantly slower degradation. At all timepoints from Week 1 to Week 4, the normalized molecular weight loss for HDS/$MgCO_3$ microspheres was significantly lower than the other formulations (**Figure 4-6**). Once again, this

is likely due to the superior pH-modulating activity of $MgCO_3$ vs. $ZnCO_3$, largely owed to its greater solubility.

The erosion kinetics (**Figure 4-5**) show that $ZnCO_3$-containing microspheres have induction times of ~21 days, while $MgCO_3$-containing microspheres have an induction time of ~28 days. These correspond to critical molecular weights of ~9 kDa for $ZnCO_3$-containing microspheres and ~12 kDa for $MgCO_3$-containing microspheres, though more frequent timepoints would need to be taken around these critical points in order to achieve better resolution.

In all cases, the molecular weight of the PLGA drops to less than 5% of the initial molecular weight when just ~40% of the microspheres' initial weight has eroded (Week 4 and Week 5 for $ZnCO_3$-containing and $MgCO_3$-containing microspheres, respectively).

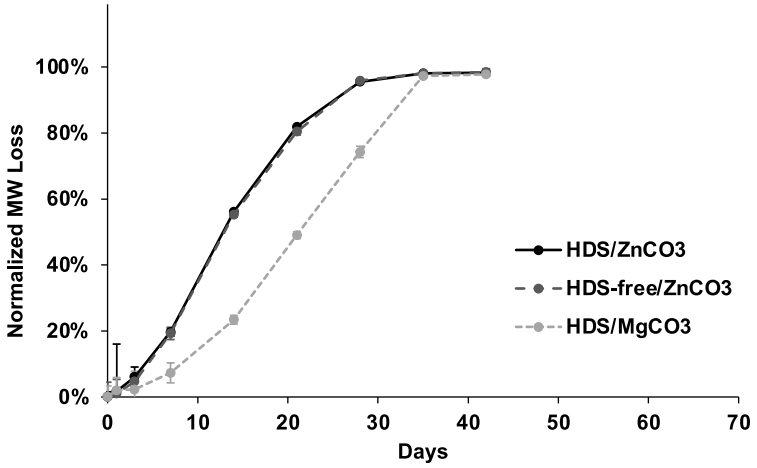

***Figure 4-6**. Degradation of $MgCO_3$-containing microspheres is slower than $ZnCO_3$-containing microspheres as measured by normalized molecular weight loss. Approximately 5 mg of pre-weighed microspheres were incubated in PBS + 0.02% Tween 80 at 37°C for predetermined durations before being dried, dissolved in THF, and analyzed via GPC with polystyrene standards.*

4.4.6. Effect of buffer on erosion and degradation

Notably, the rate of erosion as measured in PBS + 0.02% Tween 80 (**Figure 4-5**) seems to outpace the rate of protein release seen from $ZnCO_3$-containing formulations. As stated previously, the rate of hydrolysis of PLGA chains (and consequently the rate of degradation and

erosion) is affected by pH. In fact, the rate of hydrolysis of polymer chains tends to be higher in the interior of microspheres than at the surface, where buffering species in the surrounding environment modulate the pH.[33] For purposes of ELISA quantification, protein release studies were conducted in blocking buffers of either 1% casein or 1% BSA w/v, which is known to serve as a buffer in physiological conditions.[34] Thus, we endeavored to measure the effect of the inclusion of 1% BSA in the media on the erosion and degradation of the three formulations discussed.

After 28 days of incubation, $ZnCO_3$ microspheres in PBS + 0.02% Tween + 1% BSA showed significantly higher amounts of normalized mass retained (**Figure 4-7a**) and normalized molecular weight (**Figure 4-7b**). Meanwhile, $MgCO_3$-containing microspheres showed less drastic decreases in normalized mass retained and insignificant changes in normalized molecular weight. Taken together, these data suggest that the inclusion of BSA in the media mitigates the rate of degradation and erosion in $ZnCO_3$-containing PLGA microspheres, likely due to pH-modulating effects. The lesser effect on $MgCO_3$-containing microspheres could be due to the fact that $MgCO_3$ is able to buffer the pH sufficiently (as discussed above), and the addition of BSA does little to improve this.

These results also underscore the importance of *in vivo – in vitro* correlation (IVIVC) with respect to the behavior of PLGA microspheres. Much work has, and continues to be, done by our lab to elucidate the factors that affect PLGA microsphere degradation, erosion, and release *in vivo* in order to create reliable *in vitro* assays. The concentration of proteins within extracellular fluids like plasma is 60-80 mg/mL, with at least half of mass coming from albumins.[35] It may be important to include 0.5-1% w/v albumin, or a similar species, in the release media of PLGA microspheres in order to achieve better IVIVC.

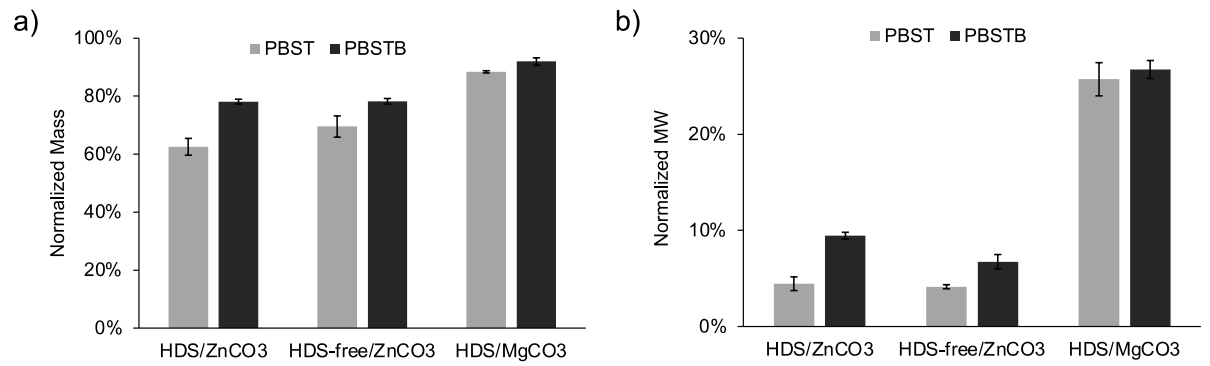

Figure 4-7*. Inclusion of BSA in media slows erosion and degradation of some microsphere formulations. a) Microspheres in PBS + 0.02% Tween 80 + 1% BSA retain significantly more mass than microspheres in PBS + 0.02% Tween 80 after 28 days. b) $ZnCO_3$-containing microspheres in PBS + 0.02% Tween 80 + 1% BSA have significantly higher molecular weights than $ZnCO_3$-containing microspheres in PBS + 0.02% Tween 80 after 28 days. Approximately 5 mg of pre-weighed microspheres were incubated in the indicated buffer at 37°C for 28 days before being dried, re-weighed, dissolved in THF, and analyzed via GPC with polystyrene standards. All within-formulation differences, except HDS/$MgCO_3$ molecular weight, significant; $p < 0.05$.*

4.4.7. Release kinetics of excipients

Having well characterized the erosion and degradation kinetics of these three formulations and several factors affecting, or not affecting, them, we then turned to the release profiles of two excipients: HDS and Zn^{2+}. Both of these excipients, especially Zn^{2+}, could have an effect on drug release, as both, especially Zn^{2+}, could be involved in binding and trapping drug within the microspheres.

4.4.7.1. Release of kinetics of HDS

To monitor the release of HDS, ~5 mg of $MgCO_3$/HDS and $ZnCO_3$/HDS microspheres were incubated in 1 mL PBS + 0.02% Tween and timepoints were taken at predetermined timepoints with complete media replacement and HDS was quantified with a DMMB assay, as described.

Through three weeks, the release of HDS from the two formulations were similar (**Figure 4-8**). Both formulations showed very large initial burst releases of HDS in Day 1 and Day 3, resulting in ~47% of HDS being released. In both cases, this was followed by a plateau, where little-to-no HDS released occurred. For $ZnCO_3$-containing microspheres, this plateau ended at three weeks, while it ended at four weeks for $MgCO_3$-containing microspheres. From then, HDS

is released with near zero-order kinetics for 2-3 weeks. In the context of the degradation profiles of these formulations (**Figure 4-6**), the second phase of HDS release begins when the normalized molecular weight loss reaches at least ~85%, which occurs after Week 3 for $ZnCO_3$-containing microspheres and after Week 4 for $MgCO_3$-containing microspheres. These curves also track with the erosion curves, with the second phase of HDS release coinciding with the end of the induction phase for the two formulations. This suggests that, following the initial burst of HDS in the first three days, HDS is trapped within the polymer matrix of the microspheres until the polymer chains reach a critical molecular weight or until the HDS is freed via erosion.

The release profile of HDS can also provide insights to some of the release mechanisms of HisTag proteins from these microsphere formulations. For instance, the initial burst of protein release was presumably attributed to incomplete or shallow encapsulation of protein within the microspheres. Here, though, HDS, which is directly encapsulated within the microspheres, also shows large initial burst. This suggests that the cause of the initial burst of protein is not related to the remote loading and encapsulation mechanism, but due to the microsphere formulation itself. Potential causes of large initial burst have been shown to include microsphere porosity and incomplete pore-healing as well as high solute content, which can increase osmotic pressure. Each of these factors could be at play with these formulations. Between trehalose, dextran sulfate, and the carbonate compounds included in the formulations, there are high solute levels. The potential effect of pore closure on burst release was examined in Section 3.4.11.

Further, the plateau in HDS release from Day 3 to Week 3 shows that protein release is not coupled with HDS release, as large amounts of protein release has been shown to occur in that span. This suggests that released protein is not bound to HDS.

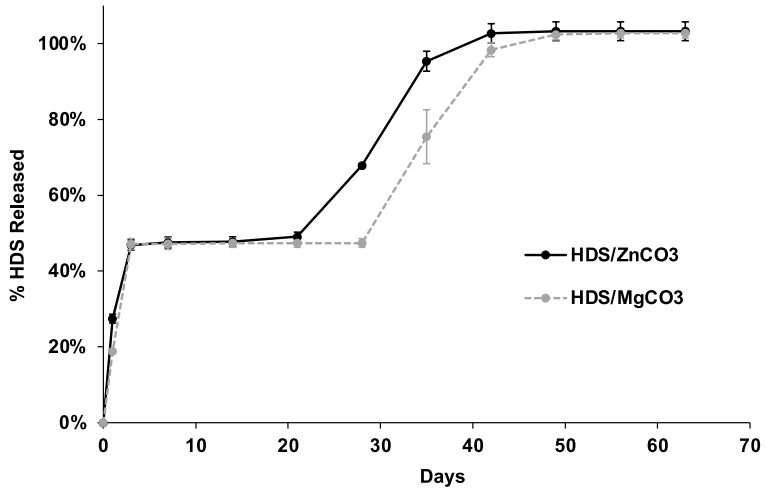

Figure 4-8*. Release of HDS from $ZnCO_3$/HDS and $MgCO_3$/HDS microspheres is monitored. Approximately 5 mg microspheres were incubated in PBS + 0.02% Tween 80 at 37°C and the release media was analyzed using DMMB assay.*

4.4.7.2. Release kinetics of Zn^{2+}

Next, to monitor the release of Zn^{2+}, ~5 mg of $ZnCO_3$/HDS, $ZnCO_3$/HDS-free, and $MgCO_3$/HDS microspheres were incubated in 1 mL PBS + 0.02% Tween and timepoints were taken at predetermined timepoints with complete media replacement and Zn^{2+} was quantified with an ICP-MS, as described.

Unlike water-soluble HDS (**Figure 4-8**), Zn^{2+}, including in the poorly-soluble $ZnCO_3$ salt form, does not show a burst release from any of the formulations (**Figure 4-9**). Rather, the release of Zn^{2+} more closely resembles a slightly expedited version of the erosion profiles for the three formulations. Specifically, little-to-no Zn^{2+} is released in the first two weeks for the $ZnCO_3$-containing microspheres and in the first three weeks for the $MgCO_3$-containing microspheres. After these points, Zn^{2+} is released with near zero-order kinetics over the next 2-4 weeks. This phase of Zn^{2+} release begins one week before the second phase of erosion begins for each of the formulations, and Zn^{2+} reaches approximately complete release one week before the formulation reaches approximately complete erosion. As with the erosion profiles, $MgCO_3$-containing microspheres showed slower Zn^{2+} release than $ZnCO_3$-containing microspheres. In

this case, as opposed to the erosion profiles, the inclusion or exclusion of HDS seems to slow the release of Zn^{2+} between Week 3 and Week 5. As $ZnCO_3$ dissolves in response to acid production from PLGA, the cation becomes ionically anchored to the immobilized HDS, ~50% of which is still present within the microspheres at this point (**Figure 4-8**).

This near-mirroring of Zn^{2+} release with mass loss kinetics suggests that Zn^{2+} release is erosion-driven. While $ZnCO_3$ is rather insoluble at neutral pH, its solubility is greatly increased at low pH, like those values found within PLGA microspheres as soluble oligomers and monomers of lactic and glycolic acid decrease the pH.

Similarly to HDS release, the differences between this release profile and the release profiles of HisTag proteins (specifically the fact that very little Zn^{2+} is released in the first 2-3 weeks) may suggest that released HisTag protein is not bound to Zn^{2+}. HisTag proteins, however, were not included in these samples and, when HisTag protein is present, the majority of Zn^{2+} is likely associated with species other than HisTag protein due to their relative abundances.

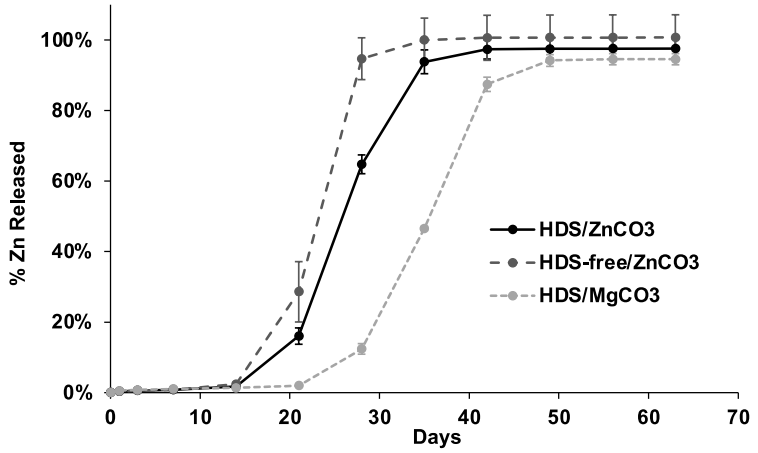

***Figure 4-9**. Release of Zn^{2+} from $ZnCO_3$/HDS, $ZnCO_3$/HDS-free, and $MgCO_3$/HDS microspheres is monitored. Approximately 5 mg microspheres were incubated in PBS + 0.02% Tween 80 at 37°C and the release media was analyzed using ICP-MS.*

4.4.8. Effect of HDS on remote loading and release of HisTag proteins

4.4.8.1. Remote loading and encapsulation

With the effects of excipients on various physical characteristics and behaviors of the microsphere formulations having been examined, we next studied the effects of the inclusion of HDS in the inner-water phase on the remote loading and encapsulation of HisTag HSA and HisTag IGF-1. Remote loading was conducted by incubating 1 mg of microspheres in 100 µL of protein loading solution (100µg/mL for HisTag HSA and 50µg/mL for HisTag IGF-1) for 2 h at 4ºC followed by 6 h at 37ºC and loading solutions were compared to microsphere-free controls via ELISA as described.

For HisTag HSA, no significant difference in encapsulation efficiency between the HDS-containing and HDS-free $ZnCO_3$ microspheres was seen (**Figure 4-10a**) (

Table 4-1). For IGF-1, HDS-containing microspheres showed significantly higher encapsulation efficiency (83.9 ± 1.0%) than the HDS-free $ZnCO_3$ microspheres (73.9 ± 2.8%) (**Figure 4-10b**). Together, these results suggest that including HDS in the inner-water phase may result in modest increases in encapsulation efficiency, though this may depend on the affinity of the particular protein for dextran sulfate. These data do not suggest that HDS substantially affects the HisTag-Zn^{2+} binding that drives the remote loading of this platform.

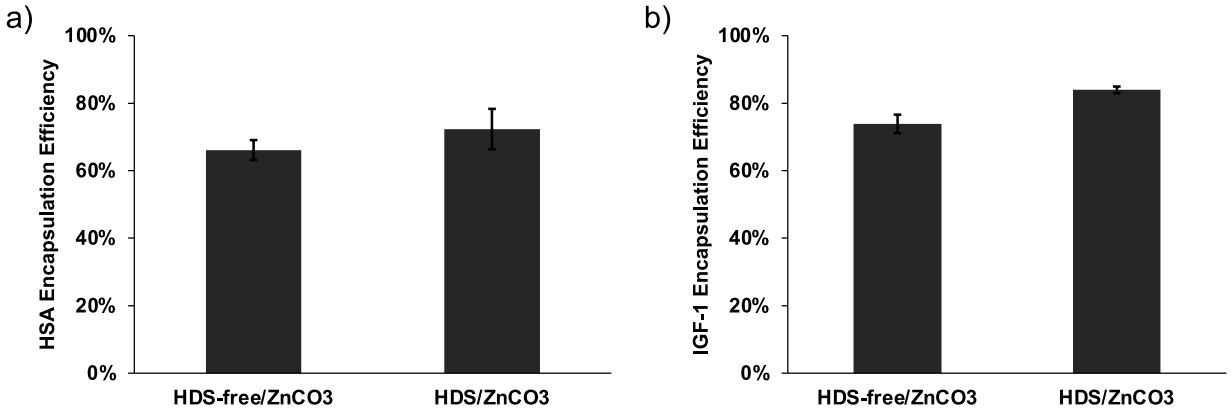

Figure 4-10*. HisTag proteins are remotely encapsulated in HDS-containing and HDS-free $ZnCO_3$ microspheres. a) Total available protein encapsulation efficiency of HisTag HSA in HDS-containing and HDS-free $ZnCO_3$ microspheres by remote loading from 100 µg/mL protein loading solution. EE_{avail} by total protein assay. b) Total available protein encapsulation efficiency of HisTag IGF-1 in HDS-containing and HDS-free $ZnCO_3$ microspheres by remote loading from 50 µg/mL protein loading solution. EE_{avail} by total protein assay. HDS-containing EE_{avail} significantly greater; $p < 0.05$.*

***Table 4-1**. Summary of remote self-healing encapsulation by Zn^{2+}-HisTag protein binding (EE = Encapsulation Efficiency).*

Protein	HDS	Active Protein Loaded (µg)	Total Protein Loaded (µg)	Active Available EE (%)	Total Available EE (%)	Actual Active EE (%)	Actual Total EE (%)
HSA (100 µg/mL)	(-)	5.5 ± 0.5	6.4 ± 0.3	64.4 ± 6.2	66.1 ± 3.0	54.8 ± 5.2	63.8 ± 2.9
HSA (100 µg/mL)	(+)	--	6.9 ± 0.6	--	72.3 ± 6.0	--	68.7 ± 5.7
IGF-1 (50 µg/mL)	(-)	--	3.48 ± 0.1	--	73.9 ± 2.8	--	69.6 ± 2.6
IGF-1 (50 µg/mL)	(+)	3.6 ± 0.1	4.0 ± 0.0	79.7 ± 1.5	83.9 ± 1.0	72.4 ± 1.3	80.6 ± 1.0

4.4.8.2. Release kinetics of HisTag HSA

To measure the release of HisTag HSA from HDS-free $ZnCO_3$ microspheres, 1 mg of microspheres that were loaded as described in Section 4.4.8.1 were incubated in 0.4 mL PBS + 0.02% Tween + 1 % casein as a blocking agent, and samples were analyzed using ELISA as described.

The release profile showed a significant burst release in the first three days and had ceased releasing immunoreactive HSA after three weeks (**Figure 4-11a**). The burst and speed of release are considerably larger and faster than what has been seen previously with HDS- and $ZnCO_3$-containing Zn^{2+}-HisTag coordination remote loading formulations (**Figure 4-11b**). This may suggest that the Zn-HisTag protein complex associates with immobilized HDS during encapsulation, prolonging the duration of release.

While experiments have shown that the inclusion of HDS in the inner-water phase of the formulation has minimal, if any, effect on the erosion (**Figure 4-5**) and degradation (**Figure 4-6**) of the microspheres, HDS was shown to exhibit a large burst release, itself (**Figure 4-8**). One possible mechanism driving the higher burst release of protein seen in the HDS-free formulation

is that the osmotic pressure in the microspheres needs to be relieved, and HDS is not available to help do this, resulting in large release of protein.

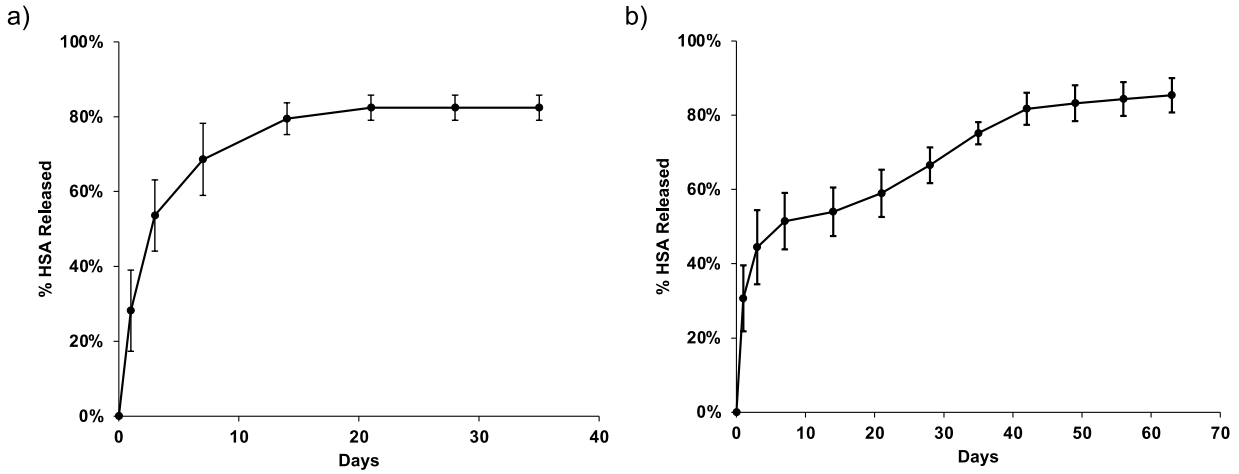

***Figure 4-11**. Release kinetics of HisTag HSA from $ZnCO_3$/HDS-free PLGA microspheres (a) compared with that from $ZnCO_3$/HDS PLGA microspheres (replotted from Figure 3.10a) (b). One mg microspheres were incubated in PBS + 0.02% Tween 80 + 1% casein at 37°C and the release media was analyzed using ELISA.*

4.5. Conclusion

With previous work having shown proof-of-concept of metal-HisTag coordination remote loading as a viable universal remote loading platform requiring very small quantities of protein[14] and having improved upon this formulation in several ways (Chapter 3), this work serves to better characterize the properties and behavior of these microsphere formulations with a focus on the role played by excipients. Dextran sulfate sodium was shown to function as a porosigen, encourage water uptake, slightly extend Zn^{2+} release, and strongly affect protein release. $MgCO_3$ was also shown to promote greater water uptake than $ZnCO_3$. While HDS was not shown to significantly affect the Zn^{2+} loading of directly encapsulated $ZnCO_3$ microspheres, it was shown to play a critical role in the remote loading of various divalent transition metal cations. Though HDS was not shown to significantly impact the erosion or degradation profiles of the microspheres, replacing $MgCO_3$ with $ZnCO_3$ accelerated erosion and degradation significantly, which suggests that the superior pH-controlling ability of $MgCO_3$ plays a large

role. This fits with the physical effects of $MgCO_3$ described above. Due to its greater solubility, $MgCO_3$ results in greater osmotic pressure and porosity, and $MgCO_3$ is also better able to combine with soluble acidic byproducts of PLGA, preventing autocatalysis of further hydrolysis.

In terms of release of excipients, HDS was shown to exhibit a high burst release followed by a multi-week plateau and seemingly degradation-dependent approximately first-order release, with $MgCO_3$-containing particles having a longer plateau period. This high burst release suggests that the high burst of protein release seen in these formulations may be due to the microsphere formulation, itself, rather than incomplete or shallow encapsulation of remotely loaded protein. Zn^{2+} release profiles were very similar to the erosion profiles, with release from $MgCO_3$-containing microspheres being delayed as compared to $ZnCO_3$-containing microspheres. For $ZnCO_3$-containing microspheres, HDS did seem to slow the release of Zn^{2+} by at least one week. It should be noted these experiments were conducted without loaded protein, though the low levels of protein loading may not substantially affect the behavior of the excipients. Finally, with respect to the effects of HDS on remote loading and release of HisTag proteins, HDS may encourage increased encapsulation, though this may vary depending on the innate affinity of proteins for dextran sulfate. In a key finding, release of HisTag HSA from HDS-free $ZnCO_3$ microspheres showed higher burst and faster release than $MgCO_3$/HDS and $ZnCO_3$/HDS microspheres have shown previously.

In all, the release of encapsulated protein does not seem to be coupled to the release of Zn^{2+}. The findings presented here will help inform future development of these or similar PLGA microsphere formulations. The metal-HisTag coordination remote loading microsphere formulations described here and previously are complex platforms, and elucidating underlying mechanisms and behavior should yield dividends in future development.

4.6. References

1. Qi F, Wu J, Li H, Ma G. Recent research and development of PLGA/PLA microspheres/nanoparticles: A review in scientific and industrial aspects.
2. Schwendeman SP, Shah RB, Bailey BA, Schwendeman AS. Injectable controlled release depots for large molecules. *Journal of Controlled Release*. 2014-09-01 2014;190:240-253. doi:10.1016/j.jconrel.2014.05.057
3. Han FY, Thurecht KJ, Whittaker AK, Smith MT. Bioerodable PLGA-Based Microparticles for Producing Sustained-Release Drug Formulations and Strategies for Improving Drug Loading. *Front Pharmacol*. 2016;7:185. doi:10.3389/fphar.2016.00185
4. Park K, Skidmore S, Hadar J, et al. Injectable, long-acting PLGA formulations: Analyzing PLGA and understanding microparticle formation. *J Control Release*. 06 2019;304:125-134. doi:10.1016/j.jconrel.2019.05.003
5. Wu F, Jin T. Polymer-based sustained-release dosage forms for protein drugs, challenges, and recent advances. *AAPS PharmSciTech*. 2008;9(4):1218-29. doi:10.1208/s12249-008-9148-3
6. Schwendeman SP. Recent advances in the stabilization of proteins encapsulated in injectable PLGA delivery systems. *Crit Rev Ther Drug Carrier Syst*. 2002;19(1):73-98. doi:10.1615/critrevtherdrugcarriersyst.v19.i1.20
7. van de Weert M, Hoechstetter J, Hennink WE, Crommelin DJ. The effect of a water/organic solvent interface on the structural stability of lysozyme. *J Control Release*. Sep 2000;68(3):351-9. doi:10.1016/s0168-3659(00)00277-7
8. Reinhold SE, Desai KG, Zhang L, Olsen KF, Schwendeman SP. Self-healing microencapsulation of biomacromolecules without organic solvents. *Angew Chem Int Ed Engl*. Oct 2012;51(43):10800-3. doi:10.1002/anie.201206387
9. Cohen S, Bernstein H. *Microparticulate systems for the delivery of proteins and vaccines*. Drugs and the pharmaceutical sciences,. Marcel Dekker; 1996:ix, 525 p.
10. Ando S, Putnam D, Pack DW, Langer R. PLGA microspheres containing plasmid DNA: preservation of supercoiled DNA via cryopreparation and carbohydrate stabilization. *J Pharm Sci*. Jan 1999;88(1):126-30. doi:10.1021/js9801687
11. Giovagnoli S, Blasi P, Ricci M, Rossi C. Biodegradable microspheres as carriers for native superoxide dismutase and catalase delivery. *AAPS PharmSciTech*. Oct 2004;5(4):e51. doi:10.1208/pt050451
12. Shah RB, Schwendeman SP. A biomimetic approach to active self-microencapsulation of proteins in PLGA. *J Control Release*. Dec 2014;196:60-70. doi:10.1016/j.jconrel.2014.08.029
13. Giles M. *Aqueous Remote Loading of Peptides in PLGA Microspheres*. University of Michigan; 2017. hdl.handle.net/2027.42/144200
14. Albert J, Chang RS, Garcia GA, Schwendeman SP. Metal-HisTag coordination for remote loading of very small quantities of biomacromolecules into PLGA microspheres. *Bioengineering & Translational Medicine*. 2022-02-17 2022;doi:10.1002/btm2.10272
15. Block H, Maertens B, Spriestersbach A, et al. Immobilized-metal affinity chromatography (IMAC): a review. *Methods Enzymol*. 2009;463:439-73. doi:10.1016/S0076-6879(09)63027-5
16. Schmitt J, Hess H, Stunnenberg HG. Affinity purification of histidine-tagged proteins. *Molecular Biology Reports*. 1993-10-01 1993;18(3):223-230. doi:10.1007/bf01674434

17. Spriestersbach A, Kubicek J, Schafer F, Block H, Maertens B. Purification of His-Tagged Proteins. *Methods Enzymol*. 2015;559:1-15. doi:10.1016/bs.mie.2014.11.003
18. Yucel Falco C, Falkman P, Risbo J, Cardenas M, Medronho B. Chitosan-dextran sulfate hydrogels as a potential carrier for probiotics. *Carbohydr Polym*. Sep 15 2017;172:175-183. doi:10.1016/j.carbpol.2017.04.047
19. Noureldein MH, Dia BA, Nabbouh AI, Eid AA. Promising anti-diabetic effect of dextran sulfate sodium: Is it its clinical come back? *Diabetes Res Clin Pract*. Jan 2020;159:107661. doi:10.1016/j.diabres.2019.03.016
20. Chung K, Kim J, Cho BK, Ko BJ, Hwang BY, Kim BG. How does dextran sulfate prevent heat induced aggregation of protein? The mechanism and its limitation as aggregation inhibitor. *Biochim Biophys Acta*. Feb 2007;1774(2):249-57. doi:10.1016/j.bbapap.2006.11.015
21. Fredenberg S, Wahlgren M, Reslow M, Axelsson A. The mechanisms of drug release in poly(lactic-co-glycolic acid)-based drug delivery systems--a review. *Int J Pharm*. Aug 30 2011;415(1-2):34-52. doi:10.1016/j.ijpharm.2011.05.049
22. Wang J, Wang BM, Schwendeman SP. Characterization of the initial burst release of a model peptide from poly(D,L-lactide-co-glycolide) microspheres. *J Control Release*. Aug 21 2002;82(2-3):289-307. doi:10.1016/s0168-3659(02)00137-2
23. Sandor M, Riechel A, Kaplan I, Mathiowitz E. Effect of lecithin and MgCO3 as additives on the enzymatic activity of carbonic anhydrase encapsulated in poly(lactide-co-glycolide) (PLGA) microspheres. *Biochim Biophys Acta*. Feb 15 2002;1570(1):63-74. doi:10.1016/s0304-4165(02)00153-8
24. Doty AC, Zhang Y, Weinstein DG, et al. Mechanistic analysis of triamcinolone acetonide release from PLGA microspheres as a function of varying in vitro release conditions. *Eur J Pharm Biopharm*. Apr 2017;113:24-33. doi:10.1016/j.ejpb.2016.11.008
25. Coulson-Thomas VJ, Caterson B, Kao WW. Transplantation of human umbilical mesenchymal stem cells cures the corneal defects of mucopolysaccharidosis VII mice. *Stem Cells*. Oct 2013;31(10):2116-26. doi:10.1002/stem.1481
26. Yang YY, Chia HH, Chung TS. Effect of preparation temperature on the characteristics and release profiles of PLGA microspheres containing protein fabricated by double-emulsion solvent extraction/evaporation method. *J Control Release*. Oct 3 2000;69(1):81-96. doi:10.1016/s0168-3659(00)00291-1
27. Freiberg S, Zhu XX. Polymer microspheres for controlled drug release. *Int J Pharm*. Sep 10 2004;282(1-2):1-18. doi:10.1016/j.ijpharm.2004.04.013
28. Hancock BC, Zografi G. The relationship between the glass transition temperature and the water content of amorphous pharmaceutical solids. *Pharm Res*. Apr 1994;11(4):471-7. doi:10.1023/a:1018941810744
29. Ding AG, Shenderova A, Schwendeman SP. Prediction of microclimate pH in poly(lactic-co-glycolic acid) films. *J Am Chem Soc*. Apr 26 2006;128(16):5384-90. doi:10.1021/ja055287k
30. Zhu G, Schwendeman SP. Stabilization of proteins encapsulated in cylindrical poly(lactide-co-glycolide) implants: mechanism of stabilization by basic additives. *Pharm Res*. Mar 2000;17(3):351-7. doi:10.1023/a:1007513425337
31. Yoo JY, Kim JM, Seo KS, Jeong YK, Lee HB, Khang G. Characterization of degradation behavior for PLGA in various pH condition by simple liquid chromatography method. *Biomed Mater Eng*. 2005;15(4):279-88.

32. Zolnik BS, Burgess DJ. Effect of acidic pH on PLGA microsphere degradation and release. *J Control Release*. Oct 8 2007;122(3):338-44. doi:10.1016/j.jconrel.2007.05.034
33. Li S, McCarthy S. Further investigations on the hydrolytic degradation of poly (DL-lactide). *Biomaterials*. Jan 1999;20(1):35-44. doi:10.1016/s0142-9612(97)00226-3
34. Gounden V, Vashisht R, Jialal I. Hypoalbuminemia. *StatPearls*. 2021.
35. Leeman M, Choi J, Hansson S, Storm MU, Nilsson L. Proteins and antibodies in serum, plasma, and whole blood-size characterization using asymmetrical flow field-flow fractionation (AF4). *Anal Bioanal Chem*. Aug 2018;410(20):4867-4873. doi:10.1007/s00216-018-1127-2

Chapter 5: Conclusions, Significance, and Future Directions

5.1. Conclusions and Significance

As described, there is a pre-clinical translational need for a universal and highly efficient PLGA microsphere remote loading and self-encapsulation platform for biomacromolecules. Controlled release from PLGA microspheres offers many advantages for biologic formulations, however, the encapsulation process is unacceptably harsh for many delicate biomacromolecules. For over a decade, the Schwendeman Lab has been actively developing remote loading methods, by which proteins, peptides, and vaccine antigens can be encapsulated within preformed blank, porous PLGA microspheres by simple mixing and modest heating.[1-10] One significant limitation of current active remote loading methods, though, is lack of universality; proteins must have innate affinity for the trapping agent used. The platform presented in the preceding chapters offers a solution to this. Metal-HisTag Coordination Remote Loading (MHCRL) aims to be a platform that is universally applicable to any recombinant protein or peptide. By taking advantage of the coordination bonds formed between histidine and divalent transition metals, HisTag proteins and peptides can be efficiently and gently encapsulated in PLGA microspheres and released over weeks-to-months while retaining activity. This platform would allow non-formulation scientists to easily and cost-effectively test early stage drug candidates with a controlled release formulation in *in vitro* and *in vivo* pre-clinical studies.[11] This would help inform decisions regarding whether or not to pursue further development of a potential clinical controlled release formulation. Due to the immunogenicity of HisTags, this platform does not lend itself to clinical use.

In Chapter 2, the basic principles of MHCRL were probed. The combination of HisTags on proteins and Zn^{2+} within PLGA microspheres was shown to increase encapsulation efficiencies. Multiple proteins, of widely varying pI, were loaded at high encapsulation efficiency using very small quantities of PLGA and protein. Immunoreactive and bioactive protein was slowly and continuously released. Also, experiments using a variety of metals as well as a strong chelating agent were shown to support the hypothesis that metal-HisTag coordination was driving the increase in encapsulation efficiency.

In Chapter 3, five areas of potential improvement on the novel platform were identified and systematically addressed. The replacement of remotely loaded Zn^{2+} with directly encapsulated $ZnCO_3$ offered several benefits. Further, the durations and temperatures of the loading and healing stages were shown to be lowerable without sacrificing significant encapsulation efficiency. This means conditions can be even gentler for the molecules of interest and that encapsulation can be completed in just one workday. The use of plasticizers was shown to decrease encapsulation efficiency, though it may also result in a decrease in initial burst release, a potentially important improvement.

In Chapter 4, the degradation, erosion, excipient release, and other physical properties were characterized for various MHCRL formulations. $MgCO_3$ was shown to slow degradation and erosion, likely through its pH-modulation capacity. HDS was not shown to significantly affect these behaviors, and was shown to have a large burst release, potentially providing insight as to the cause of the burst release of encapsulated protein. HDS plays an important role in immobilizing remotely-loaded Zn^{2+} within the microspheres and seems to greatly prolong the duration of release of protein.

In all, MHCRL has achieved its goals of (1) being virtually universal for any recombinant peptide or protein, (2) being highly efficient, (3) using very small quantities of the protein or peptide, (4) slowly and continuously releasing active protein, and (5) being capable of being performed by scientists without training in microencapsulation and without specialized mixing or drying equipment. This platform, or ones that build off it, could offer immense value to scientists investigating new biologic candidates that have controlled release applications, but which would be cost- or resource-prohibitive to formulate using traditional encapsulation techniques. This platform has been successfully used to encapsulate just 5 μg of protein, as opposed to the several milligrams that would likely be needed for traditional batch methods. Extending remote loading and self-encapsulation at this scale and to any recombinant protein or peptide could be a very useful tool in aiding the progression of biologic candidates from drug discover and pre-clinical development to clinical therapeutics that improve patients' lives.

5.2. Future Directions

The most significant limitation of this technique is that it requires the protein to have a HisTag, at least during the remote loading process. HisTags have been shown to be substantially immunogenic,[12,13] which could limit the utility of this platform in *in vivo* studies, if the immune response interferes with the ability to usefully measure the pharmacokinetics and pharmacodynamics of the candidate. Indeed, *in vivo* experiments would be the next step for this platform. Further studies on the bioactivity of various released HisTag proteins would also be helpful to examine the effect of the HisTag on the EC_{50} of the proteins, as the addition of the HisTag could alter the binding kinetics and efficacy of the molecule. It is possible this can be mitigated by the option of expressing the HisTag at either the C-terminus or N-terminus.[14] Cleavable HisTags are often used in molecular biology and it is conceivable that a

physiologically cleavable HisTag could be utilized.[15] Finally, the length of the HisTag could be varied in an attempt to optimize it for the most efficient encapsulation.

Protein loading will also need to be increased in order to expand utility for systemic delivery or for local delivery of much less potent proteins (e.g., monoclonal antibodies). While progress was made toward this goal, further improvement will likely be needed. Third, the initial burst release of protein requires attention. The use of plasticizers to potentially increase pore-closure and limit burst release is promising, but other methods of increasing pore-closure, including lengthening the healing stage, should be explored. Methods of decreasing the osmotic pressure within the microspheres, including decreasing the content of water-soluble excipients, should also be explored. Fourth, further studies to determine whether released protein is bound to Zn^{2+} and/or HDS would be useful. Finally, HisTags are not the only widely applicable affinity tags. It is not difficult to imagine replacing the HisTag-metal ion pair with a maltose binding protein (MBP)-maltose pair or a glutathione S-transferase (GST)-glutathione pair.[16,17] These and other affinity tag-ligand pairs will be important to examine in the future. Across all self-encapsulation platforms, this work has shown that remote loading and self-encapsulation is possible with as short as an eight-hour procedure. This could pay large dividends in pre-clinical and clinical development of controlled release biologics in terms of ease of use, speed of development, and protein stability.

5.3. References

1. Shah RB, Schwendeman SP. A biomimetic approach to active self-microencapsulation of proteins in PLGA. *J Control Release*. Dec 2014;196:60-70. doi:10.1016/j.jconrel.2014.08.029
2. Reinhold SE, Desai KG, Zhang L, Olsen KF, Schwendeman SP. Self-healing microencapsulation of biomacromolecules without organic solvents. *Angew Chem Int Ed Engl*. Oct 2012;51(43):10800-3. doi:10.1002/anie.201206387
3. Reinhold SE, Schwendeman SP. Effect of polymer porosity on aqueous self-healing encapsulation of proteins in PLGA microspheres. *Macromol Biosci*. Dec 2013;13(12):1700-10. doi:10.1002/mabi.201300323

4. Giles M. *Aqueous Remote Loading of Peptides in PLGA Microspheres*. University of Michigan; 2017. hdl.handle.net/2027.42/144200
5. Desai KG, Schwendeman SP. Active self-healing encapsulation of vaccine antigens in PLGA microspheres. *J Control Release*. Jan 2013;165(1):62-74. doi:10.1016/j.jconrel.2012.10.012
6. Bailey BA, Desai KH, Ochyl LJ, Ciotti SM, Moon JJ, Schwendeman SP. Self-encapsulating Poly(lactic-co-glycolic acid) (PLGA) Microspheres for Intranasal Vaccine Delivery. *Mol Pharm*. 09 2017;14(9):3228-3237. doi:10.1021/acs.molpharmaceut.7b00586
7. Bailey BA, Ochyl LJ, Schwendeman SP, Moon JJ. Toward a Single-Dose Vaccination Strategy with Self-Encapsulating PLGA Microspheres. *Adv Healthc Mater*. Jun 2017;6(12)doi:10.1002/adhm.201601418
8. Mazzara JM, Balagna MA, Thouless MD, Schwendeman SP. Healing kinetics of microneedle-formed pores in PLGA films. *J Control Release*. Oct 2013;171(2):172-7. doi:10.1016/j.jconrel.2013.06.035
9. Huang J, Mazzara JM, Schwendeman SP, Thouless MD. Self-healing of pores in PLGAs. *J Control Release*. May 2015;206:20-9. doi:10.1016/j.jconrel.2015.02.025
10. Mazzara JM, Ochyl LJ, Hong JKY, Moon JJ, Prausnitz MR, Schwendeman SP. Self-healing encapsulation and controlled release of vaccine antigens from PLGA microparticles delivered by microneedle patches. *Bioeng Transl Med*. Jan 2019;4(1):116-128. doi:10.1002/btm2.10103
11. Kwong E, Higgins J, Templeton AC. Strategies for bringing drug delivery tools into discovery. *Int J Pharm*. Jun 2011;412(1-2):1-7. doi:10.1016/j.ijpharm.2011.03.024
12. Watson DS, Platt VM, Cao L, Venditto VJ, Szoka FC, Jr. Antibody response to polyhistidine-tagged peptide and protein antigens attached to liposomes via lipid-linked nitrilotriacetic acid in mice. *Clin Vaccine Immunol*. Feb 2011;18(2):289-97. doi:10.1128/CVI.00425-10
13. Khan F, Legler PM, Mease RM, Duncan EH, Bergmann-Leitner ES, Angov E. Histidine affinity tags affect MSP1(42) structural stability and immunodominance in mice. *Biotechnol J*. Jan 2012;7(1):133-47. doi:10.1002/biot.201100331
14. Block H, Maertens B, Spriestersbach A, et al. Immobilized-metal affinity chromatography (IMAC): a review. *Methods Enzymol*. 2009;463:439-73. doi:10.1016/S0076-6879(09)63027-5
15. Booth WT, Schlachter CR, Pote S, et al. Impact of an N-terminal Polyhistidine Tag on Protein Thermal Stability. *ACS Omega*. 2018-01-31 2018;3(1):760-768. doi:10.1021/acsomega.7b01598
16. Nemergut M, Skrabana R, Berta M, Pluckthun A, Sedlak E. Purification of MBP fusion proteins using engineered DARPin affinity matrix. *Int J Biol Macromol*. Sep 30 2021;187:105-112. doi:10.1016/j.ijbiomac.2021.07.117
17. Schafer F, Seip N, Maertens B, Block H, Kubicek J. Purification of GST-Tagged Proteins. *Methods Enzymol*. 2015;559:127-39. doi:10.1016/bs.mie.2014.11.005

Appendix A: Norrin as a Use Case

A.1. Introduction

The intended use case for metal-HisTag coordination remote loading (MHCRL) is a delicate, costly biologic candidate for which pre-clinical *in vitro* and *in vivo* controlled release formulations and data is desired. In these cases, traditional microencapsulation strategies are either too harsh on the protein or too costly, or both. Norrin, is a protein that meets these conditions.

Macular edema, resulting from diabetic retinopathy, retinal vein occlusion, wet age-related macular degeneration, or other pathogeneses is the leading cause of visual loss in modernized countries worldwide.[1] A hallmark of these diseases is neovascularization and leakage in the retina, which is often triggered by vascular endothelial growth factor (VEGF). As such, the current treatments involve anti-VEGF therapy. Unfortunately, about half of patients do not respond to anti-VEGF treatment.[2] Also, while anti-VEGF therapy addresses the cause of the damaged blood-retinal barrier (BRB), it does nothing to actively restore the integrity of the BRB.

Norrin is an endogenous protein which signals through the frizzled 4 (FZD4) receptor and activation of β-catenin that is needed for normal angiogenesis and formation of the blood-retinal barrier.[3] Research from collaborators has demonstrated that addition of norrin to endothelial cells restores the endothelial barrier after VEGF treatment.[4] Thus, exogenous norrin could plausibly be used as a paradigm-shifting therapeutic for macular edema, by regenerating the blood-retinal barrier after pathological barrier loss.

The eye, the posterior segment of the eye in particular, can be a difficult tissue to target due to the various barriers surrounding it. Thus, the most commonly used delivery method is intravitreal injection, which has the benefit of maximizing and localizing drug concentration in the back of the eye. Due to clearance mechanisms, however, dosing is required as frequently as every four weeks, creating significant burdens for both clinicians and patients, and adherence to dosing regimens is frequently lacking.[5] Moreover, injections are not risk-free; each injection introduces risk of endophthalmitis, uveitis, vitreous hemorrhage, and other complications.[6] Thus, there is a need for a longer-acting injectable therapies, which poly(lactic-co-glycolic acid) (PLGA) microspheres can provide.

Our lab has previously attempted to encapsulate norrin within PLGA microspheres, but encountered difficulties with protein stability. Similar issues were found when attempted to formulate norrin-containing millicylinder implants. This technique avoids the mechanical shear, high temperatures, and interfaces of microsphere formulation, but requires exposing the protein to an organic solvent. Thus, norrin is a potential use case for MHCRL.

A.2. Experimental Methods

A.2.1. Materials

Resomer RG 504 PLGA (50:50, ester-terminated, molecular weight 38,000-54,000 Da), magnesium carbonate, trehalose, 88% hydrolyzed poly(vinyl alcohol) (PVA), and high molecular weight (>500,000 Da) dextran sulfate (HDS) were purchased from Sigma Aldrich. Zinc acetate and zinc carbonate basic were purchased from Sigma Aldrich. Poly-histidine tagged (HisTag) norrin was purchased from LSBio and untagged (NoTag) norrin was purchased from R&D Systems. Bovine serum albumin (BSA) was purchased from Sigma Aldrich. All other common reagents and solvents were purchased from Sigma Aldrich, except where otherwise specified.

A.2.2. Preparation of microspheres

Porous PLGA microspheres with HDS as a metal immobilizer, $MgCO_3$ as a pH-modulator and porosigen,[7,8] and trehalose as a porosigen were prepared by double water-oil-water (w/o/w) emulsion and solvent evaporation. The first emulsion was created by homogenizing a suspension of 1 mL of 250 mg/mL dissolved PLGA and 6% w/w fine particulate $MgCO_3$ in methylene chloride (continuous phase) with an inner water phase of 200 μL of 4% w/v HDS and 3% w/v trehalose in a glass cell culture tube at 18,000 rpm for 60 s over an ice bath, using a Tempest IQ^2. The second emulsion was created by adding 2 mL of 5% PVA to the primary emulsion and vortexing for 60 s. The w/o/w double emulsion was added to 100 mL of 0.5% PVA and stirred for 3 h at room temperature in a 150 mL beaker to allow for hardening and evaporation of methylene chloride. The 20-63 μm fraction of microspheres was collected using sieves and the microspheres were washed with excess double-distilled water and lyophilized.

A.2.2.1. Inclusion of $ZnCO_3$

To create direct encapsulation $ZnCO_3$ microspheres, $ZnCO_3$ replaced $MgCO_3$ in the 250 mg PLGA in 1 mL methylene chloride continuous phase before emulsification. These microspheres were not remotely loaded with Zn^{2+} as described below.

A.2.3. Remote loading of and encapsulation of metals and proteins

A.2.3.1. Standard Procedures

For remotely loaded Zn^{2+} microspheres, Zn^{2+} was remotely loaded into the PLGA microspheres by incubating the microspheres in at least 1 mL of 500 mM zinc acetate salt solution (or water as a control) per 1 mg of microspheres for 24 h rotating at 30 rpm at room temperature. Microspheres were washed with double-distilled water under vacuum on a 0.2 μm nylon filter and lyophilized. Direct encapsulation $ZnCO_3$ microspheres did not undergo this procedure.

Remote loading HisTag and NoTag protein solutions were prepared by diluting lyophilized powders in loading solution. Proteins were remotely loaded into the Zn-loaded microspheres by incubating 1 mg of microspheres in 100 μL of 50μg/mL HisTag or NoTag protein in pH 8 phosphate buffered saline. Remote loading and self-healing consisted of a either a 48h, room temperature loading stage and a 42h 43°C healing stage for remotely loaded Zn^{2+} formulations, or a 2h, 4°C loading stage followed by a 6h, 37°C healing stage for direct encapsulation $ZnCO_3$ formulations. During both stages, microspheres and protein loading solutions were rotated at 30 rpm.

A.2.3.2. Determination of immunoreactive protein by ELISA

Norrin ELISA kits were purchased from Raybiotech and performed according to kit instructions to determine immunoreactive protein concentrations. In all ELISAs, NoTag and HisTag proteins used for remote loading encapsulation were also included as reference standards.

A.2.3.3. Determination of total protein by Coomassie Plus protein assay

Total protein content for NoTag and HisTag Norrin in loading solutions was measured by Coomassie Plus protein assay using a 1:1 sample-to-reagent ratio. BSA standards were used, with the NoTag and HisTag proteins included as reference standards, and absorbance was read at 595 nm in accordance with the protocol.

A.2.3.4. Estimation of encapsulation efficiency

Encapsulation efficiency of the available protein was estimated by ELISA and Coomassie Plus protein assay by comparing the final concentrations of protein in the loading solution to a control loading solution, which underwent the same conditions without microspheres as follows:

$$EE_{avail} = \frac{C_C - C_{MS}}{C_C} \times 100\%$$

Where C_C and C_{MS} are the concentration of protein in control loading solution and the concentration of protein in the loading solution with microspheres quantified by either Coomassie Plus protein assay (for total protein) or ELISA (for immunoreactive protein), respectively.

A.2.3.5. Evaluation of release kinetics

Norrin release was conducted by incubating 1 mg microspheres in 0.5 mL phosphate buffered saline (PBS) + 0.02% Tween 80 + 1% BSA, pH 7.4. Media was completely replaced at each timepoint after centrifuging for 5 min at 8,000 rpm and removing the supernatant. All samples were incubated at 37 ºC with shaking.

A.3. Results and Discussion

A.3.1. Encapsulation of Norrin

Remote loading and encapsulation of HisTag and NoTag norrin was measured using the original formulation and protocol described in Chapter 2 and the formulation and protocol developed in Chapter 3. HisTag norrin was efficiently encapsulated into both remote loaded Zn^{2+} ($_{RL}Zn^{2+}$) microspheres (83 ± 1%) and direct encapsulation $ZnCO_3$ ($_{DE}ZnCO_3$) microspheres (94 ± 9%) (**Figure A-1**). These data once again support the hypothesis the combination of Zn^{2+} and HisTags improve remote loading encapsulation efficiency. Controls without HisTag, without Zn^{2+}, and without HisTag and Zn^{2+} were higher for norrin than for the previously studied proteins. This could be due to ionic interactions between the norrin and the HDS encapsulated within the microspheres. Norrin has an isoelectric point of 10.3 and carries a net positive charge at pH 8, the pH of the loading solution.[9] This would allow for ionic interactions with HDS, which is anionic.

For this protein, there was no significant difference between in encapsulation efficiency of HisTag protein into $_{RL}Zn^{2+}$ and $_{DE}ZnCO_3$ microspheres. In previous work, the most substantial

advantages in encapsulation efficiency into $_{DE}ZnCO_3$ microspheres was seen at protein loading solution concentrations greater than the 50 μg/mL used here.

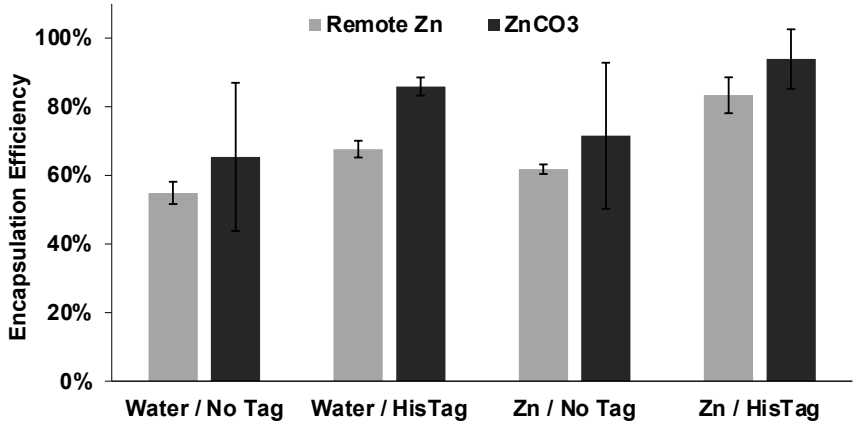

***Figure A-1**. HisTag and NoTag norrin is encapsulated in Zn^{2+}-containing and Zn^{2+}-free PLGA microspheres by remote loading. Total protein encapsulation efficiency of norrin from 50μg/mL protein loading solution. Five μg protein and 1 mg of microspheres in 100 μL PBS, pH 8 loading solution. EE_{avail} by total protein assay.*

A.3.2. Release of Norrin

The release of immunoreactive HisTag norrin from $_{RL}Zn^{2+}$ and $_{DE}ZnCO_3$ microspheres was then measured. In both cases, after modest burst release (<20% and <10% in the first three days for $_{RL}Zn^{2+}$ and $_{DE}ZnCO_3$, respectively), immunoreactive protein ceased to be detected in the release media within two weeks (**Figure A-2**). This differs from release seen with other proteins previously. One possibility is the norrin, either while encapsulated within the microspheres or in solution in the release media, loses immunoreactivity. Norrin has been reported to have a half-life of 72 hours in solution, and preliminary studies showed that norrin stored in release media at 37 ºC with mild agitation (release conditions) lost immunoreactivity at least this quickly. While protein stability can be prolonged by encapsulation in PLGA matrices, it seems that the loss of immunoreactivity by norrin either in the microspheres or after being released occurs too quickly to be quantified by the methods used here. Using shorter, perhaps daily, timepoints and analyzing the media immediately could prove useful, assuming the protein is not degraded while in the microspheres.

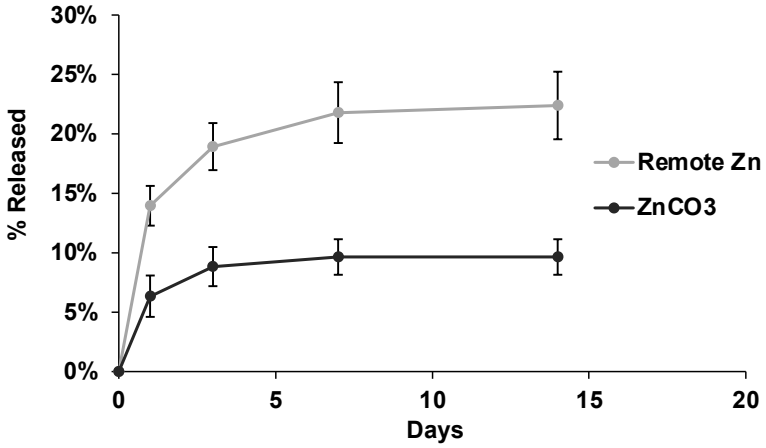

***Figure A-2**. Release of immunoreactive HisTag norrin from Zn^{2+}-containing PLGA microspheres in 0.5 mL PBS + 0.02% Tween 80 + 1% BSA, pH 7.4 at 37 °C. Five μg protein and 1 mg of microspheres in 100 μL loading solution for self-healing encapsulation.*

A.4. References

1. Antonetti DA, Barber AJ, Hollinger LA, Wolpert EB, Gardner TW. Vascular endothelial growth factor induces rapid phosphorylation of tight junction proteins occludin and zonula occluden 1. A potential mechanism for vascular permeability in diabetic retinopathy and tumors. *J Biol Chem*. Aug 13 1999;274(33):23463-7.
2. Yang S, Zhao J, Sun X. Resistance to anti-VEGF therapy in neovascular age-related macular degeneration: a comprehensive review. *Drug Des Devel Ther*. 2016;10:1857-67. doi:10.2147/DDDT.S97653
3. Ke J, Harikumar KG, Erice C, et al. Structure and function of Norrin in assembly and activation of a Frizzled 4-Lrp5/6 complex. *Genes Dev*. Nov 1 2013;27(21):2305-19. doi:10.1101/gad.228544.113
4. Díaz-Coránguez M, Lin C-M, Liebner S, Antonetti DA. Norrin restores blood-retinal barrier properties after vascular endothelial growth factor–induced permeability. *Journal of Biological Chemistry*. 2020-04-01 2020;295(14):4647-4660. doi:10.1074/jbc.ra119.011273
5. Finger RP, Wiedemann P, Blumhagen F, Pohl K, Holz FG. Treatment patterns, visual acuity and quality-of-life outcomes of the WAVE study - a noninterventional study of ranibizumab treatment for neovascular age-related macular degeneration in Germany. *Acta Ophthalmol*. Sep 2013;91(6):540-6. doi:10.1111/j.1755-3768.2012.02493.x
6. Day S, Acquah K, Mruthyunjaya P, Grossman DS, Lee PP, Sloan FA. Ocular complications after anti-vascular endothelial growth factor therapy in Medicare patients with age-related macular degeneration. *Am J Ophthalmol*. Aug 2011;152(2):266-72. doi:10.1016/j.ajo.2011.01.053
7. Shah RB, Schwendeman SP. A biomimetic approach to active self-microencapsulation of proteins in PLGA. *J Control Release*. Dec 2014;196:60-70. doi:10.1016/j.jconrel.2014.08.029
8. Wu F, Jin T. Polymer-based sustained-release dosage forms for protein drugs, challenges, and recent advances. *AAPS PharmSciTech*. 2008;9(4):1218-29. doi:10.1208/s12249-008-9148-3

9. Perez-Vilar J, Hill RL. Norrie disease protein (norrin) forms disulfide-linked oligomers associated with the extracellular matrix. *J Biol Chem*. Dec 26 1997;272(52):33410-5. doi:10.1074/jbc.272.52.33410